PL-TR-94-2132

DETAILED COMPONENT DESIGN FOR A COMPACT ENVIRONMENTAL ANOMALY SENSOR (CEASE)

John O. McGarity
Alan C. Huber
John A. Pantazis
David Sperry

Hugh Anderson
Douglas Potter

AMPTEK, INC.
6 De Angelo Drive
Bedford, MA 01730

25 March 1994

Scientific Report No. 3

PHILLIPS LABORATORY
Directorate of Geophysics
AIR FORCE MATERIEL COMMAND
HANSCOM AFB, MA 01731-3010

This technical report has been reviewed and is approved for publication.

for PAUL S. SEVERANCE
Contract Manager

DAVID A. HARDY
Branch Chief

WILLIAM SWIDER
Deputy Division Director

This report has been reviewed by the ESC Public Affairs Office (PA) and is releasable to the National Technical Information Service (NTIS).

Qualified requestors may obtain additional copies from the Defense Technical Information Center (DTIC). All others should apply to the National Technical Information Service (NTIS).

If you address has changed, or if you wish to be removed from the mailing list, or if the addressee is no longer employed by your organization, please notify PL/TSI, 29 Randolph Road, Hanscom AFB, MA 01731-3010. This will assist us in maintaining a current mailing list.

Do not return copies of this report unless contractual obligations or notices on a specific document requires that it be returned.

REPORT DOCUMENTATION PAGE

Form Approved
OMB No. 0704-0188

1. AGENCY USE ONLY *(Leave blank)*	2. REPORT DATE	3. REPORT TYPE AND DATES COVERED
	25 Mar 1994	Scientific No. 3

4. TITLE AND SUBTITLE

Detailed Component Design for a Compact Environmental Anomaly Sensor (CEASE)

5. FUNDING NUMBERS

PE 63410F
PR 2823 TA 01 WU AC

Contract F19628-90-C-0159

6. AUTHOR(S)

John O. McGarity
Alan C. Huber
John A. Pantazis
David J. Sperry
Hugh Anderson
Douglas Potter

7. PERFORMING ORGANIZATION NAME(S) AND ADDRESS(ES)

AMPTEK, Inc.
6 De Angelo Drive
Bedford, MA 01730

8. PERFORMING ORGANIZATION REPORT NUMBER

9. SPONSORING/MONITORING AGENCY NAME(S) AND ADDRESS(ES)

Phillips Laboratory
29 Randolph Road
Hanscom AFB, MA 01731-3010

Contract Manager: Capt Paul Severance/GPSG

10. SPONSORING/MONITORING AGENCY REPORT NUMBER

PL-TR-94-2132

11. SUPPLEMENTARY NOTES

12a. DISTRIBUTION/AVAILABILITY STATEMENT

Approved for public release.
Distribution unlimited.

12b. DISTRIBUTION CODE

13. ABSTRACT *(Maximum 200 words)*

The outer space environment experienced by a modern, electronically sophisticated spacecraft can be very hostile due to interactions between its complex, sensitive electronics systems and the naturally occurring energetic particle population indigenous to the solar system. The Compact Environmental Anomaly Sensor (CEASE) is being developed as a small, low-power device to monitor space "weather" and provide autonomous warnings of conditions that may cause operational anomalies in a host spacecraft. CEASE uses a two-element solid-state telescope and two radiation dosimeters to sample critical energetic particle fluxes and uses a sophisticated real-time processing program that can forecast hazardous environmental conditions before they effect the spacecraft. The spacecraft, in turn, can re-prioritize its operations, inhibit any anomaly sensitive operations such as attitude adjustments, or take any other prudent action suggested by the potential of erratic conditions. The CEASE instrument is forecast to be packaged as a 4 inch cube weighing 2 pounds and dissipating a maximum of 2 watts.

14. SUBJECT TERMS

Compact Environmental Anomaly Sensor, CEASE, Surface Charging, Deep Dielectric Charging, Single Event Upsets, Radiation Dose Effects.

15. NUMBER OF PAGES

74

16. PRICE CODE

17. SECURITY CLASSIFICATION OF REPORT	18. SECURITY CLASSIFICATION OF THIS PAGE	19. SECURITY CLASSIFICATION OF ABSTRACT	20. LIMITATION OF ABSTRACT
Unclassified	Unclassified	Unclassified	SAR

CONTENTS

Tables

Figures

1. Introduction

The instrument CEASE (Compact Environmental Anomaly Sensor) is designed to detect conditions that may cause anomalies, that is, occurrences that may adversely affect spacecraft operation. It will do so before these conditions become so severe that anomalies actually occur, and will provide warnings or flags on which spacecraft may act to protect themselves. These anomalies are:

Body charging occurs when the spacecraft chassis accumulates electrical charge and the whole space frame must rise to a significant potential (with respect to the surrounding plasma) in order to null the net current to it. This charging occurs even when the whole spacecraft surface is conducting and electrically connected. Body charging is caused by spacecraft emitting charge, such as in a particle beam, or when they are bombarded by kilovolt electrons such as the auroral electron flux or the hot plasma in GEO. The charging can become significant in the absence of neutralizing currents such as cooler plasma or photoelectrons ejected by sunlight.

Differential charging occurs under the same conditions as body charging if the spacecraft exterior has sections of electrically isolated conductors. As different portions of the surface experience different currents, these separate sections may reach different equilibrium potentials.

Surface dielectric charging occurs when somewhat penetrating particles bombard exposed dielectrics and stop in them. If the rate of charge buildup exceeds leakage through the dielectric, the resulting charge density may produce a very strong electric field that eventually breaks down the dielectric. Leakage depends upon the dielectric material; hence, charging may be cumulative over minutes up to many hours. Leakage increases as conductivity is enhanced by the effect of the bombarding particles. Consequently, protons are not very effective in causing dielectric charging because they readily increase dielectric conductivity. In addition, sunlight may help discharge very shallow deposits of charge. The result of these factors is that surface charging occurs when the electron flux exceeds a threshold value and sums to a fluence that exceeds a threshold.

Deep dielectric charging is produced in the same way as surface dielectric charging except that the causative electrons have enough energy to penetrate some distance into the dielectric. In some cases they may reach dielectrics that are behind conductors. An example of a buried dielectric is the insulator within a coaxial cable. Obviously, the energy boundary that divides surface and deep charging particles is somewhat arbitrary. Sunlight does not mitigate deep dielectric charging.

Total radiation dose is measured by the energy deposited in materials by charged particles passing through them. Dosage results from the totality of ionizing radiation that reaches the site of interest and is thus strongly affected by surrounding shielding. Sufficiently high levels can damage most materials, including dielectrics and optical materials. In most cases semiconductors are the most sensitive elements on a spacecraft. Some devices experience degradation at tens of kilorads, while radiation hard devices can tolerate 10 to 100 times more. Dosage is mostly cumulative, as semiconductors self heal only a little.

Single event upsets (SEUs) result when an ionizing particle leaves enough charge (equivalently energy) in the sensitive volume of a semiconductor device to flip the logical

state of the device. Generally, there is no permanent damage. The sensitive volumes are of micron size, and the required energy is 1 - 100 MeV depending upon the device. Neither electrons or protons have high enough LET (Linear Energy Transfer) to leave so much energy in a small volume. Only more highly charged particles such as alphas (in some cases) and $Z > 2$ particles can do this. However, protons that have nuclear collisions (called stars from their appearance in photographic film) in the sensitive volume can break up a nucleus and the resulting fragments leave enough energy to cause SEUs. Protons are so much more numerous than heavier particles that these nuclear collisions are the principal cause of SEUs.

The strategy that has evolved for a successful CEASE instrument consists of making a limited number of high-energy particle measurements using a pair of dosimeters and a solid-state telescope. We believe that if the right radiation parameters are sampled, then these data may be interpreted to identify and forecast environmental conditions that may affect the operation or longevity of a spacecraft. The issue is what parameters to measure with what accuracy and dynamic range and how to make those measurements.

A review of previous research including experimental measurements and theoretical modeling has identified five different environments that are occasionally characterized by extreme conditions that may damage or disrupt spacecraft operations. We have examined records of these environments and used theoretical models to augment existing data bases to develop spectral characteristics. These data provided the dynamic range and temporal behavior of the environments. We then knew what and how much was needed to be measured and had some idea of how accurate the measurements needed to be. We also used this information to create five test vectors (energy/flux models) that could be used to evaluate the performance of our instrument design in each critical environment.

The nature of solid-state detectors and telescopes is that there are possible ambiguities in their measurements. Discriminating electrons from protons or heavier masses can be impossible under some circumstances. Particles that stop entirely in the first detector or fly through both detectors or enter through the sides or back of the telescope confuse simple interpretation of the detector outputs. Appropriate selection of absorber thickness, detector thickness and area, and pulse processing electronics can minimize confusion. The electro/mechanical design of the telescope and dosimeter are critical to their usefulness.

A thorough knowledge of the spectral characteristics of the environment may also be used to guide the detector design toward placing regions of possible detector ambiguity at places where the natural environment would not contain components that trigger that uncertainty. For example, we may not be able to distinguish electrons from protons in a certain energy region, but we know that the natural environment consists of only one of the two species in that range.

It is also possible to design these ambiguity regions into areas where it is not relevant to discriminate the triggering event since it either doesn't portend a possible anomaly or in the case of SEUs (Single Event Upsets) the precise identification of the energetic ion doesn't mitigate or influence the SEU probability.

Lastly, a knowledge of the natural spectral shape of the environment may allow the identification of an ambiguous detector response by designing the electro/mechanical system such that naturally occurring events that may not be unambiguously resolved also trigger

unambiguous responses at other energies. An intelligent data processing algorithm may be designed that integrates this natural spectral knowledge and uses it to interpret detector responses. Knowledge of the probable spectral shape of an environment may be used to sum count rates into quantatized total-dosage estimates without extensive knowledge of the individual event characteristics.

It is the deductive and selective nature of CEASE that distinguishes it from a scientific experiment. It is designed to measure and discriminate only those environment parameters that are needed to forecast potential anomaly conditions.

2. Environments

Table 1 lists five environments. The first three represent extreme cases and use Inner (Trapped Radiation) Zone at the equator for maximum proton intensity, and Outer Zone, also at the equator, for maximum energetic electron intensity. Inner and Outer Zone environments include proton and electron intensity from AP8Min and AE6Max/AE8Max at low/high altitude. Present in the transient in GEO environment are anomalously large solar protons from CREME, and maximum storm electrons using a bi-maxwellian as listed in the Mil Std 1809, Space Environment for USAF Space Vehicles. Of all the environments these storm electrons produce the greatest counting rate in the front detector of the telescope if its absorber admits >30 keV electrons. The last two environments test the ability of CEASE to detect anomaly-causing conditions. Anomalously large solar protons scaled to the threshold of threatening flux in the presence of Outer Zone electrons allow us to examine the device's ability to warn of SEUs. Maximum storm electrons scaled to threshold intensity in the presence of Inner Zone protons verify the ability to warn of dielectric charging. Table 2 gives threshold conditions. If need be, other combinations may be used.

Table 1. - Environments

Environment	Source	Description
Inner Zone	AP8Min, AE6Max at equator	Represents max energetic protons
Outer Zone	AP8Min, AE8Max at equator	Represents max energetic electrons
Transient in GEO	CREME solar protons; Magnetic storm electrons from Mil Std 1809	Anomalously large solar protons; Maximum storm electrons from a bi-maxwellian
Solar Protons	Scaled protons and outer electrons	Anomalously large solar protons >20 MeV scaled to SEU threshold intensity; Outer zone electrons
Storm Electrons	Scaled electrons and inner protons	Maximum storm electrons >30 keV scaled to dielectric charging threshold; Inner zone protons

Table 2. - Anomaly Causes and Thresholds

Anomaly	Cause	Threshold
Surface Dielectric Charge (SDC)	Electrons 30 - 250 keV	Intensity > 5×10^5/cm²-sec and
Deep Dielectric Charge (DDC)	Electrons > 250 keV	Fluence > 2×10^{10}/cm² in last 10 hrs
SEUs	Protons > 25 MeV or High LET	5×10^{-5} SEU/bit-day: >120 protons or >2.4×10^{-3}/cm²-sec high LET
Surface Dose (SDose)	Protons > 2 MeV	10 krad
Total Dose (TDose)	Protons > 20 MeV Electrons > 1 MeV	10 krad

The sources listed in Table 1 were used to compile electron and proton energy intensity test vectors for each environment. Figures 1 and 2 show the test vectors that are used to validate candidate detector models. (Please see the next two pages)

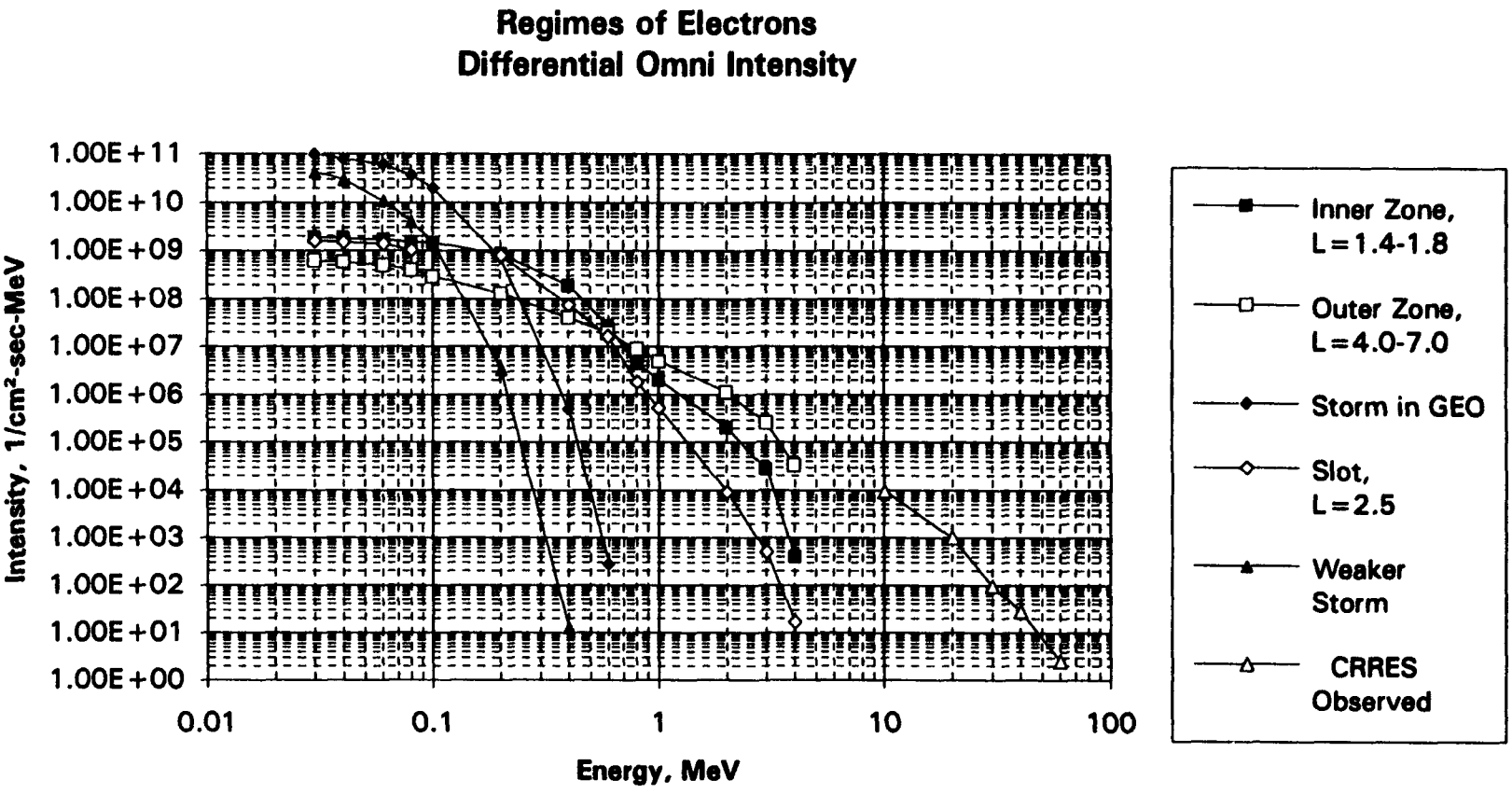

Figure 1. Electron Spectra of Selected Environments

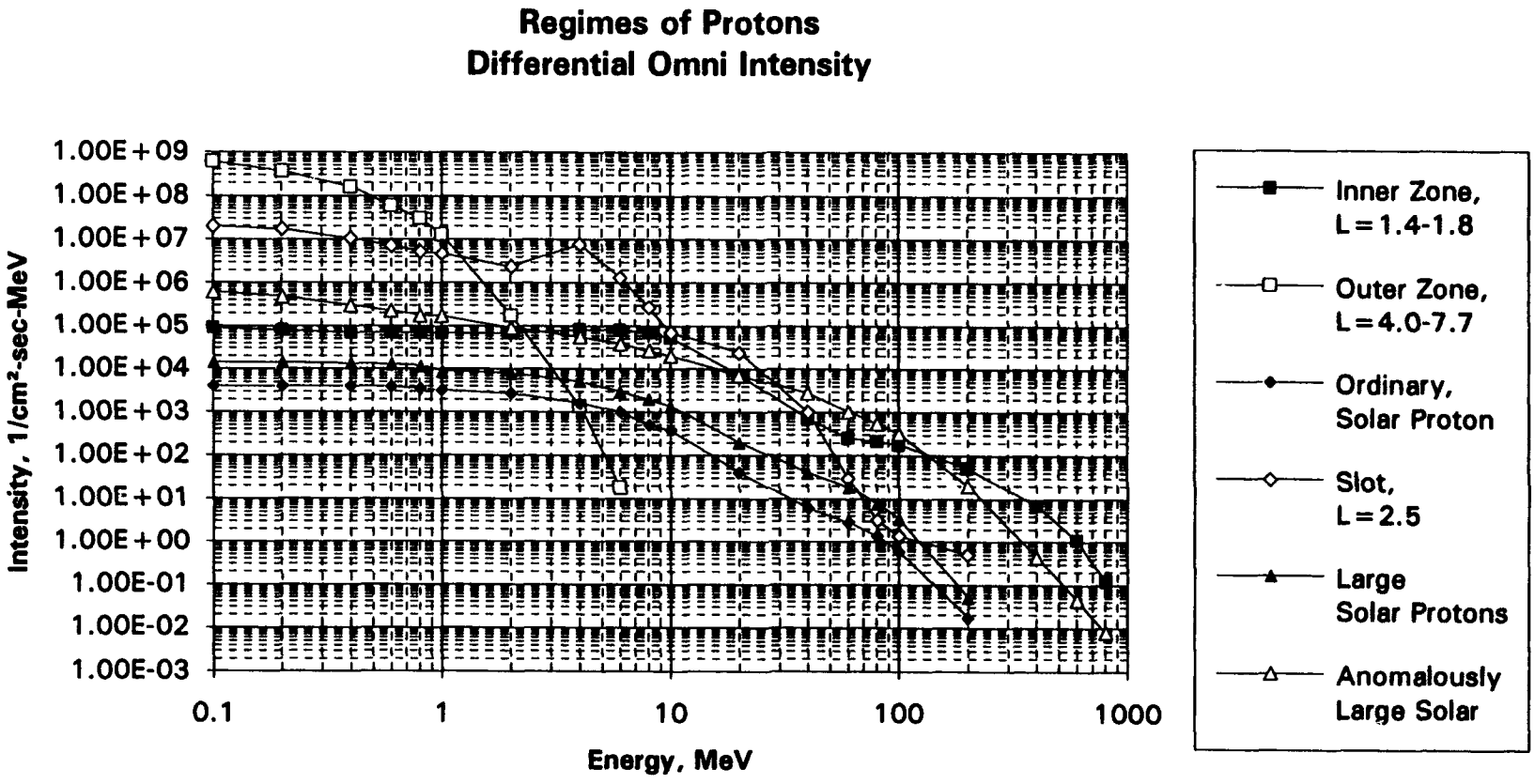

Figure 2. Ion spectra of selected environments

3. Modeled Sensors

3.1 Requirements

For all detectors, the maximum counting rate of the detector-preamplifier and logic chain should be as great as possible to achieve a large dynamic range. This affords maximum sensitivity and response to smaller fluxes. In the geometrical designs, we scaled the geometric factors to yield 2.5×10^5 counts per second in the most intense environments.

3.1.1 Telescope

In the telescope, the front detector D1 must be fully depleted to minimize the energy range in which electrons and protons are indistinguishable. For the same reason D1 should be as thin as possible consistent with measuring minimum ionizing particles. The rate of energy loss by a minimum ionizing (relativistic) singly charged particle is about 2 MeV per g/cm^2. This requires 150 μg/cm^2 or about 65 μm of silicon to exceed 30 keV energy loss. As a practical matter, fully depleted ion implant detectors are available down to only 150 μm thick; surface barrier detectors are made much thinner. The back detector D2 should be thicker than 500 μm, preferably substantially thicker, to separate protons from electrons over as wide an energy range as possible. The areas of D1 and D2 are not as critical because the collimator and aperture limit entrance of particles. However, their respons : to particles scattering and penetrating the shield on the back and sides depends on size. It is of advantage to mount D1 and D2 as close as possible to minimize their sizes.

There is no particular reason to push the minimum energy-loss threshold as low as possible. The detector-preamp noise-counting rate above this threshold must remain insignificant throughout the life of a CEASE instrument. As the instrument may be stored for extended periods, and will not be cooled or closely temperature controlled, we choose a 30 keV energy loss (pulse-height) threshold.

3.1.2 Dosimeter

The size of the detector in the dosimeter is critical as there is no aperture. The sensitivity to incident intensity depends therefore upon area and volume. It is necessary to know the total sensitive volume accurately in order to convert energy loss to rad-Si.

3.2 Geometrical Design

We have modeled geometrical designs of the telescope and dosimeter including recommended detector types. We choose the telescope aperture and dosimeter detector sizes so that in the most extreme environment counting rates do not exceed 250 kHz. These sizes may change if tests of the prototype show that a different maximum rate is appropriate or to adapt CEASE to various missions that encounter differing environments.

3.2.1 Coincidence Telescope

Figure 3 shows the design for the coincidence telescope. It has a 1.5 cm thick (4.1 g/cm^2) aluminum shield and collimator that accepts particles from 90° field of view. Following is a small aperture and thin absorber before the detectors D1 and D2. We intend that the front be removable so that the aperture size and absorber may be changed. We have carried out calculations for two absorber thicknesses, thick and thin. CEASE will use only one telescope with an absorber between these two limits. With thicker absorber, the maximum rate due to storm electrons is less, which allows a larger aperture. Both detectors are 150 mm^2 area and 150 and 700 μm thick, respectively. If subsequent analysis shows that a thicker D2 is required, we can stack these detectors.

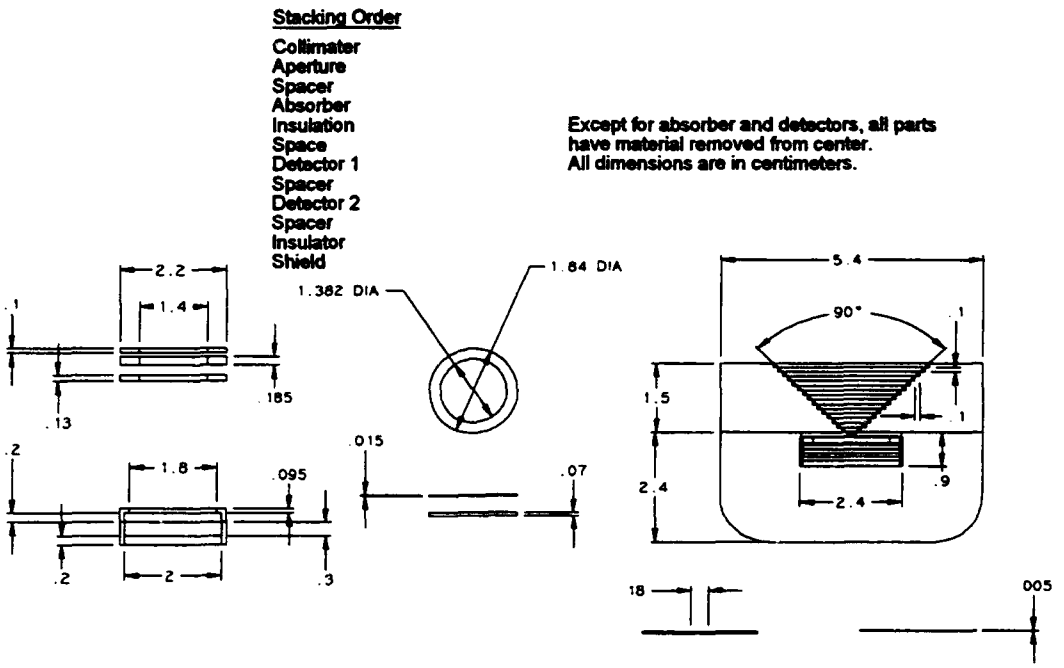

Figure 3. Solid State Telescope Assembly

3.2.2 Dosimeter

The dosimeters use a single solid state detector close behind a planar absorber with 1.5 cm of aluminum surrounding the rest of the dosimeter. The detector has ~170° FOV through the absorber. Dosimeters #1 and 2 have absorbers 0.43 and 1.7 g/cm^2 thick respectively, which corresponds to electron/proton minimum energies of 1.1/18 MeV and 3.2/37 MeV. Figure 4 shows the design for dosimeter 1, with the thin absorber and smaller detector. Figure 5 is Dosimeter 2 with the thicker absorber and large detector. CEASE uses both dosimeters.

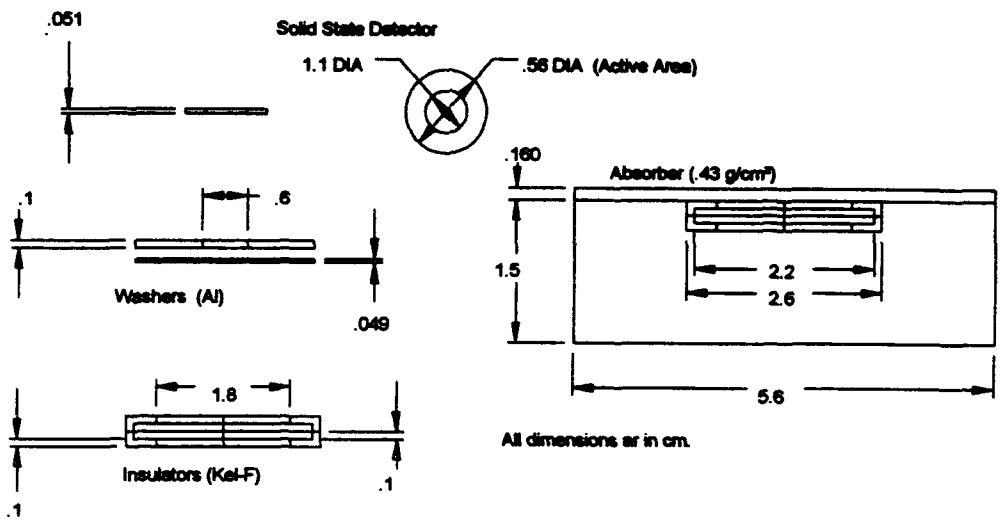

Figure 4. Dosimeter 1 Assembly – Thin Absorber

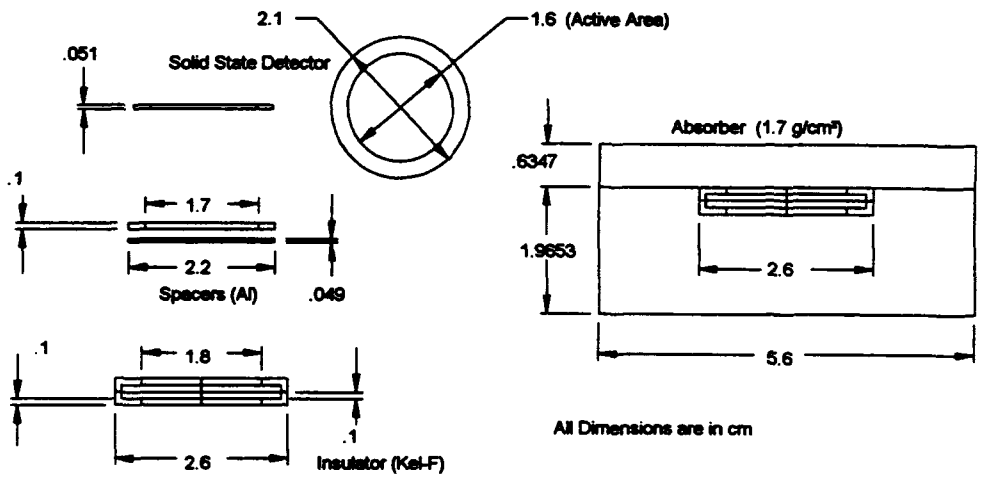

Figure 5. Dosimeter 2 Assembly – Thick Absorber

If counting rates with these detectors prove too high, smaller areas can be made on special order. Table 3 shows the absorber cross section thicknesses. Table 4 tabulates the geometric factors of all of the sensors.

Table 3. CEASE Detector Absorber Depths

Device	Part	Description
Dosimeter 1	Abs:	430 mg/cm² Al
	Det 1	115 mg/cm² Si
Dosimeter 2	Abs:	1.7 g/cm² Al
	Det 1	115 mg/cm² Si
Thick SST	Abs:	13.5 mg/cm² Al
	Det 1	34.5 mg/cm² Si
	Det 2	161 mg/cm² Si
Thin SST	Abs:	1.6 mg/cm² Al
	Det 1	34.5 mg/cm² Si
	Det 2	161 mg/cm² Si

Table 4. CEASE Detector Forward and Reverse Geometric Factors

Device	Dir	Area (cm²)	Opening Angle (deg)	Geometric Factor (cm²-sr)
Dosimeter 1	F	0.25	170	0.7794
	R	0.25	170	0.7794
Dosimeter 2	F	2	170	6.2355
	R	2	170	6.2355
Thick SST	F	0.016	90	0.0251
	R	2×1.5	90	2×2.3562
Thin SST	F	0.0016	90	0.0025
	R	2×1.5	90	2×2.3562

Note that the aperture for the thick SST has ten time the area of the thin SST. The geometric factors of the two reflect that ratio, and this results in the counting rates that are tabulated on Table 6. Under some circumstances the thicker absorber results in higher count rates, which at first seems counter-intuitive until the larger aperture area is considered.

3.3 Model Response

From the five standard environments and the geometries listed earlier in this report, the program *detresp* computes the energy loss in the detectors from range-energy tables for protons and Integrated *detresp* TIGER Series (ITS) Monte Carlo (See Appendix A) routines for electrons. The *detresp* program takes account of incoming intensity, geometric factor, and the effect of oblique transmission through the instruments. Briefly, *detresp* calculates the energy loss per unit energy interval in each detector for the given environment.

Figure 6 is the result for the telescope from Inner Zone electrons and protons entering the front aperture. The two axes are the energy losses (pulse heights) in the two detectors. The shading represents the amount of response according to the scale on the right. Starting with low incident energy, the protons register in the lower left and with increasing incident energy extend to the right along the bottom of the box until they penetrate D1 and start producing response in D2. The response then rises in D2 while slightly dropping in D1 until the protons penetrate D2. Then, the response drops in both detectors as it merges into the electron ``blob." To some extent, electrons follow the same pattern except the response is lower and considerably blurred by energy straggling and angular scattering.

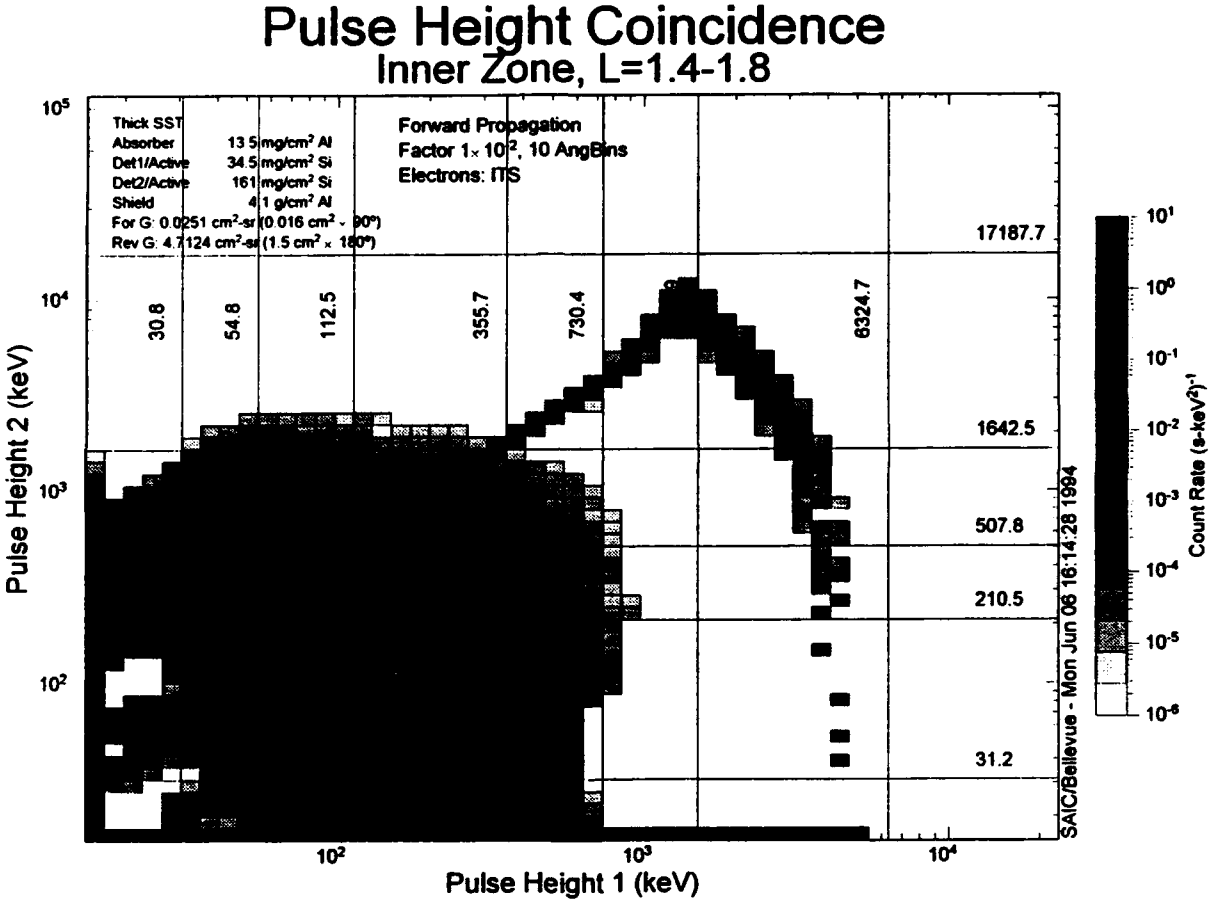

Figure 6. Telescope Response to Inner Zone Particles entering the aperture

The text in the upper left describes the device. The grid superimposed on D1-D2 space are the boxes that correspond to where we set electronic thresholds in the detector system and the count rates that accumulate in each box. The grid also shows the values of the thresholds. Appendix A contains is the complete set of these plots along with plots that show the count rate from electrons and protons in each box.

We assume that particles with pulse height below 30 keV are not detected. Hence, the box in the lower left corner has no corresponding counting channel. The boxes along the bottom of

the plot correspond to count with anti-coincidence in D2. The boxes along the left are anti-coincidence with D1.

Figure 7 shows the boxes along with the range of incident energies in each box. The value of the energy range for electrons is not precise because the electrons of a given input energy go into several boxes. Hence, there are boxes that clearly have electron response that do not have an energy range in Figure 7. Appendix A shows these thresholds for both telescope combinations. The *detresp* program also calculates the response independently in the detectors.

For each device and particle input spectra, we calculate both forward through the primary absorber and backwards through the shield. Forward particles are those that enter through the telescope aperture and collimator. Table 6 shows the total rates for each detector.

The dosimeters have planar absorbers and accept particles from a cone of ~170° full opening angle. Their effective geometric factor are therefore $\sim\pi \times$ (area of detector). (It is π, not 2π, because integration is carried out with the projected area of the flat detector.)

An aluminum shield surrounds the back and sides of the dosimeters and telescope; the same shield covers the front of the telescope except in the collimator. Using ITS, we ran electrons through various thicknesses of aluminum. At 1.5 cm (4.1 g/cm^2), essentially no electrons penetrate the detector. Thus, we chose that thickness for the shield of the telescope. The penetrating protons within an acceptance angle of somewhat more than 90° can produce coincidences whether moving forward or backward. The geometric factor for such particles is the area of the detector times the solid angle. The factor ×2 accounts for both forward and backward motion through the shield. This mechanism enhances the telescope's sensitivity to protons that cause SEUs. In addition, protons can enter the shield on the sides but not produce coincidences.

We ran each environment from the back of the devices through the shield. Over a 90° FOV, *detresp* calculates the total counting rate in each detector as well as the pulse height distribution, which gives the count rate in each box.

Table 6 shows the total counting rates in the detectors that result from each environment entering the front aperture of the instrument and also penetrating the shield. In the case of the dosimeter, this calculation includes the entire shield. For the telescope it is protons from directions that can cause coincidence. Table 5 shows the counting rates in the individual telescope detectors caused by protons from the side. These numbers are estimated from the area of the detectors and the integral proton fluxes and are not calculated by *detresp*; no energy loss distribution is available. To suppress accidental coincidences, the CEASE coincidence time gates should be as small as possible.

In the geometrical designs the apertures and dosimeter sizes are adjusted to yield a maximum counting rate of 2.5×10^5/sec. The counting rates from particles penetrating the shield do not change as the telescope aperture changes, but do scale with detector size. We can make more detailed calculations of the shield's effect after the prototype is built and calibrated in a particle beam.

Table 5. Counting Rates in telescope due to protons penetrating the sides

Detector	Inner	Outer	Trans GEO	Solar Protons	Storm Electrons
SST D1	8×10^3	40	119	8×10^3	8×10^3
SST D2	9×10^3	45	135	9×10^3	9×10^3

Table 6. Counting Rates through aperture or front (F) and shield (R) 4.1 g/cm^2

Device	Det	Dir	Inner	Outer	Trans GEO	Solar Protons	Storm Electrons
Dosimeter 1	1	F	13,551	52,753	8,455	52,778	4,002
		R	986	0	1,285	3	986
Dosimeter 2	1	F	12,190	3,438	24,877	3,508	12,072
		R	7,890	0	10,278	27	7,890
Thick SST	1	F	234,821	59,330	231,646	59,302	1,831
		R	7,516	94	11,657	125	7,503
	2	F	60,717	25,655	2,115	25,658	1,282
		R	7,660	201	12,171	234	7,632
Thin SST	1	F	48,667	14,092	360,557	11,504	372
		R	7,516	94	11,657	125	7,503
	2	F	8,597	3,139	709	3,140	141
		R	7,660	201	12,171	234	7,632

3.4 Preliminary Warning Logic

We combine the boxes into anomaly boxes that warn of various threats. For the telescope and referring to Figure 7, we number the boxes from the lower left, with the lower left box being (0,0), the box above it being (0,1), and so forth. Table 7 shows the makeup of the telescope anomaly boxes. For the dosimeters, the figures in Appendix A show the boxes, which number from the bottom with 0 being the box below 30 keV. Table 8 shows the makeup of the dosimeter anomaly boxes.

Table 7. Combination of Telescope Boxes into Anomaly Boxes

(Electron energies are approximate.)

Anomaly	Boxes	Detected Particles
SDC*	(1,0)+(2,0)+(3,0)	30-250 keV electrons
DDC	(1,1)+(1,2)+(1,3)+(2,1)+(3,0)+(3,1)+(3,2)+(4,0)	>250 keV electrons
SEUs	(4,4)+(0,4)	>25 MeV protons
SDose, protons	(5,0)+(5,4)+(6,0)+(6,1)+(6,2)+(6,3)+(6,4)	2-25 MeV protons

** With thicker absorber, electrons below 100 keV are not admitted. Very shallow surface charging would not be sensed.*

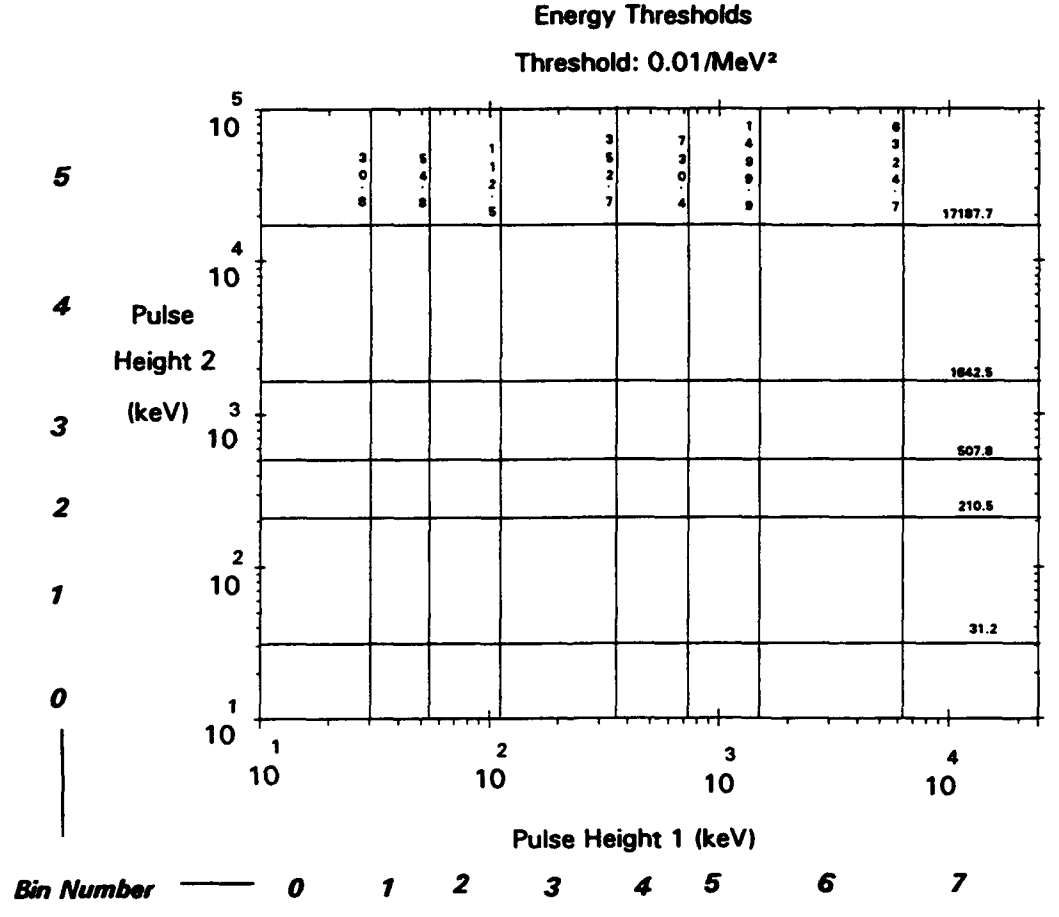

Figure 7. CEASE Telescope Anomaly Box Boundaries

The particle energies and types match the discussion of anomalies at the beginning of this report. Note that with the thicker absorber, essentially no electrons below 100 keV are detected, so that some surface dielectric charging is not sensed. Similarly, the absorbers on the two dosimeters preclude measuring electrons that cause surface dielectric charging. Table 9 shows count rates in the anomaly boxes from the five environments.

The SEU channel responds only to penetrating protons. In the outer zone, there is no SEU response. In the presence of threshold SEU fluxes (Solar Protons), there is sufficient response in the SEU channel to detect. Note that several environments cause SEUs and dielectric charging. Table 8 tabulates the anomaly derivation from the Dosimeter data.

For the charging channels, we cannot distinguish between protons and electrons that stop in D1. The electrons that stop there are significant for charging and cannot be ignored. The Storm Electron spectrum is threshold electrons combined with high proton flux and, hence, corresponds to the worst case for detecting charging. For the thick SST, of the 60 DDC counts, 31 are from protons; of the 122 SDC counts, 13 are from protons. For the thin SST 6 of 22 counts in DDC and 2 of 173 counts are from protons. Thus, even under the worst conditions, we can determine threshold charging.

Table 8. Dosimeter Boxes

Anomaly	Boxes	Detected Particles
DDC	1	Electrons >1.1 or 3.7 MeV
SEUs	3	Protons and Heavier
TDose	1+2+3	All particles

Table 9. Counting Rates in Anomaly Boxes

Anomaly	Device	Inner	Outer	Trans GEO	Solar Protons	Storm Electrons
DDC	Dosimeter 1	694	3,551	8	3,551	5
	Dosimeter 2	75	600	0	600	0
	Thick SST	135,697	32,977	60,203	32,965	60
	Thin SST	24,716	7,073	34,052	5,261	22
TDose	Dosimeter 1	14,537	52,753	9,739	52,781	4,989
	Dosimeter 2	20,080	3,438	35,155	3,536	19,962
SDC	Thick SST	171,715	33,412	229,298	33,406	122
	Thin SST	39,884	9,929	359,790	8,448	173
SDose	Thick SST	2,027	24	2,504	13	2,024
	Thin SST	643	297	1,773	6	643
SEUs	Dosimeter 1	1,383	0	2,730	8	1,383
	Dosimeter 2	2,775	0	7,817	23	2,775
	Thick SST	1,638	1	4,649	15	1,638
	Thin SST	1,566	0	4,470	13	1,566

For each anomaly, we can now construct a threshold value that corresponds to a threshold threat and a means of determining how much the threat from that anomaly exceeds that threshold.

3.4.1 SEUs

Recalling that we constructed the Solar Protons spectrum to correspond to threshold conditions for SEUs, we set the threshold levels in each device to the values for SEUs under Solar Protons in Table 6.

3.4.2 Dielectric Charging (DDC and SDC)

We constructed the Storm Electron spectrum to correspond to threshold dielectric charging for both Deep (DDC) and Surface (SDC) Dielectric charging. Therefore, the threshold levels in each device are the values for DDC and SDC under Storm Electrons in Table 6.

As Table 2 indicates, dielectric charging requires *both* that the electron intensity exceed a threshold *and* that the fluence accumulated at these intensities in the preceding ~10 hours (4×10^4 s) exceed the threshold intensity times 4×10^4 s. Thus, we have a threshold for both fluence and flux.

3.4.3 Dose (Sdose and Tdose)

The relationship between count rate and dose is

$$\text{Dose Rate} = 2 \times 10^{-3} \text{ rads/hr} \left(\frac{R}{1/s}\right)\left(\frac{E}{1 \text{ MeV}}\right)\left(\frac{0.03 \text{ g}}{m}\right) \qquad (1)$$

where R is the count rate, E is the mean *energy-loss* of particles (or energy loss of each particle that could be measured), m is the mass of the detector, which is 0.03 g for Dosimeter 1, 0.23 g for Dosimeter 2, 0.05 g for telescope D1, and 0.24 g for telescope D2.

Hence, we get different doses for each detector. For each box, we multiply counts by the geometric mean pulse height in the box, sum these, and multiply by the detector mass to get the dose.

3.4.4 Converting Output to Warning Flags

We define a base level for each anomaly at $10^{1/2}$ times the threshold level. If we use a 4 bit flag for each value, we compute the 4 bit flag by $2 \log_{10}$(level/base level). Thus, one flag occupies one-half byte and a value of two corresponds to the threshold level.

This leads to a total of 15 flags, two for dose for each of the dosimeters, two for surface dose in the two detectors in the telescope, three for all devices times two (flux and fluence) for deep dielectric charging, two for surface dielectric charging from the telescope, and three for SEUs from each device. These 15 flags should be available to all clients on request.

However, most clients won't want that much information on threats. We want to reduce the flags to five summary flags to correspond to the five threats. The final determination on how to do this must await some experience during testing, calibration, and ultimately operation.

For the summary SEU and dose (TDose and SDose) flags, our initial cut is simply to average the individual parts. For charging, we must deal with flux vs. fluence. We suggest using primarily the flux flag. If the fluence flag is less than threshold (2), subtract 2 and add the fluence flag:

$$\text{Charging Flag (SDC, DDC)} = \begin{cases} J, K \geq 2 \\ J - 2 + K, K \leq 2 \end{cases} \qquad (2)$$

where J is the flux flag and K is the fluence flag. It would seem like a good idea to disseminate time averages of these flags over the last hour or so.

An operational plan for CEASE should include a plan on how to disseminate these flags as well as plans for interrupts and other data. Also,it can further address how to combine flags as well as their definition.

4. Hardware

The baseline hardware that was projected for CEASE in the second annual report (Report PL-TR-92-2307;ADA261729) is still valid. Figure 8 depicts the current configuration including the two dosimeter sites. Note that the telescope has a collimator (90°) built into the housing.

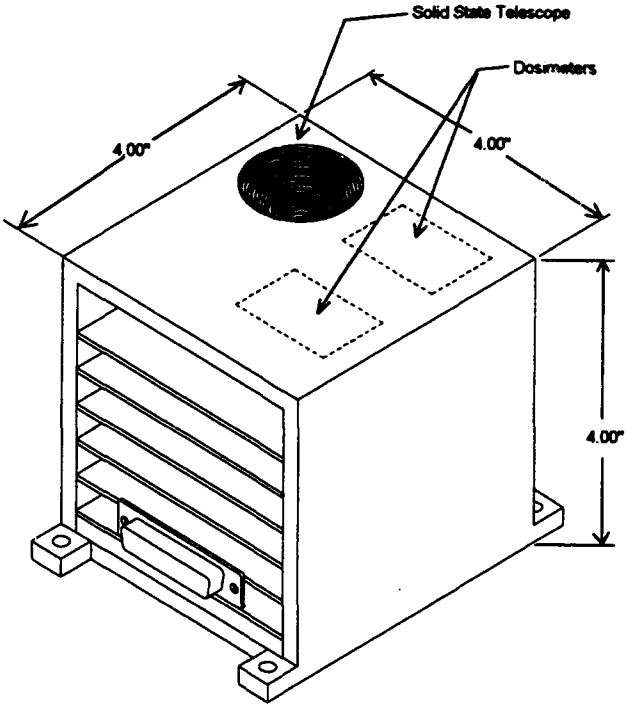

Figure 8. CEASE Concept Package with Telescope and Two Dosimeters

The current designed dimensions of the dosimeters and solid state telescope allow both mounting and are within the weight budget. We are working toward hybridizing the electronics to accommodate this enclosure size.

4.1 HUTSAT

The Helsinki University of Technology is assembling a small satellite, HUTSAT. Its small size demands tight experiment constraints of power and volume. The CEASE Dosimeter has similar constraints, and its development and fabrication schedule parallel the HUTSAT schedule. It may be possible to use the HUTSAT as a test bed for the CEASE dosimeter. This possibility is being explored. At present, little activity is occurring as we await activation of the Finish portion of the program.

4.2 STEP 4

STEP 4 is one of a series of Air Force Satellites design as test beds for small satellite technology. Amptek, Inc. is presently developing designs for an instrument on STEP 4 which will use a CEASE type dosimeter and a microproceessing system patterned after the CEASE hybrid architecture. We have provided preliminary mechanical housing drawings, weight and power estimates. TRW is the integrating contractor. Figures 9 and 10 depict the current STEP 4 design envelopes.

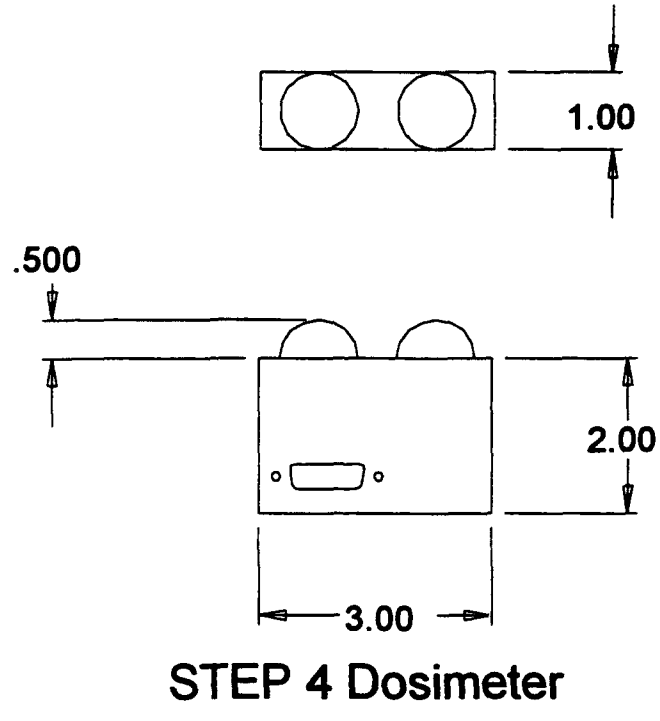

Figure 9. STEP 4 Dosimeter (Remote operation)

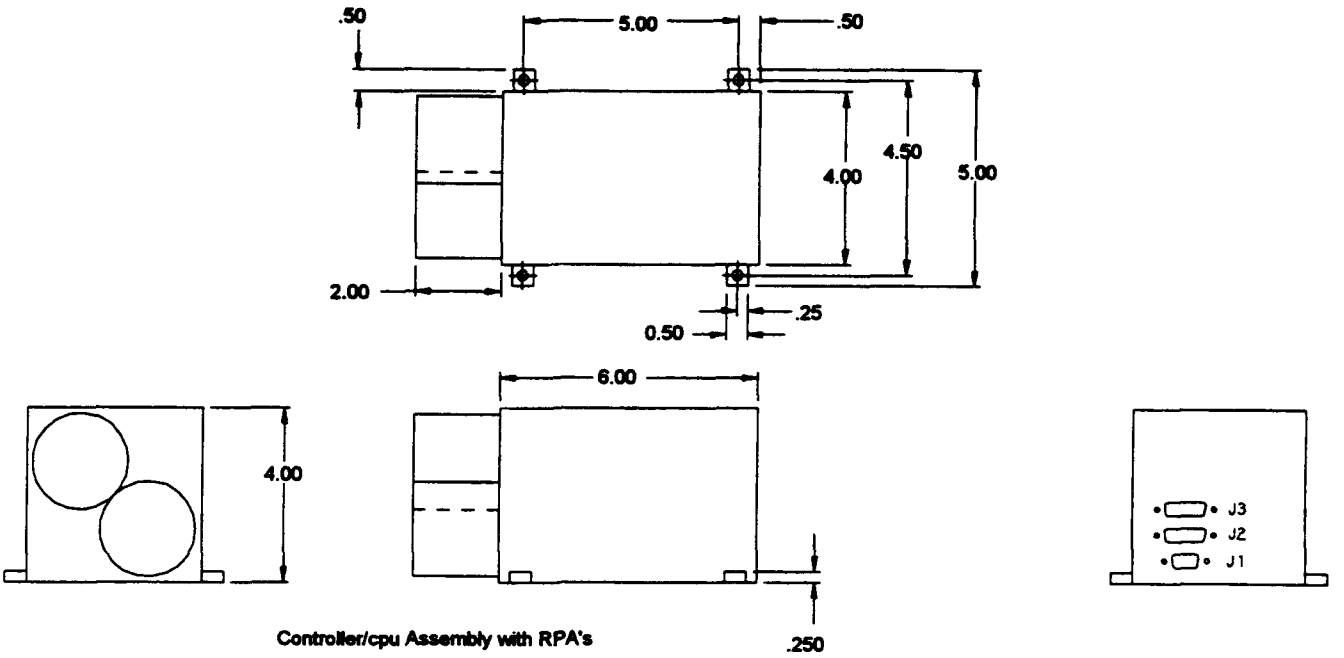

Figure 10. STEP 4 Main Electronics Box

The above drawings are preliminary, but are providing base lining for TRW engineers.

Specifics of projected design are:

Dosimeter Box	0.75 pounds
Drift meters and electronics	3.62
Cable	0.58
Engineering margin	0.55

5. Software

Most of the software work this year has been targeted toward developing and testing algorithms to convert CEASE diagnostics data into warning flags and hazard notices. Some thought has been given to optional data packets that contain scientific data as well as the hazard alerts. This feature would make in-flight testing of the CEASE much easier and more accurate.

Appendix A. Modeled Response of Instrument Suite in Five Environments

Pulse height coincidence and bin accumulation for the thick and thin absorber telescope for three environments, both forward and reverse propagation.

CEASE Solid State Telescope Energy Thresholds, Forward and Reverse; two absorber thicknesses.

CEASE Dosimeter Response Figures, five environments, both forward and reverse propagation

Pulse Height Coincidence

Inner Zone, L=1.4-1.8

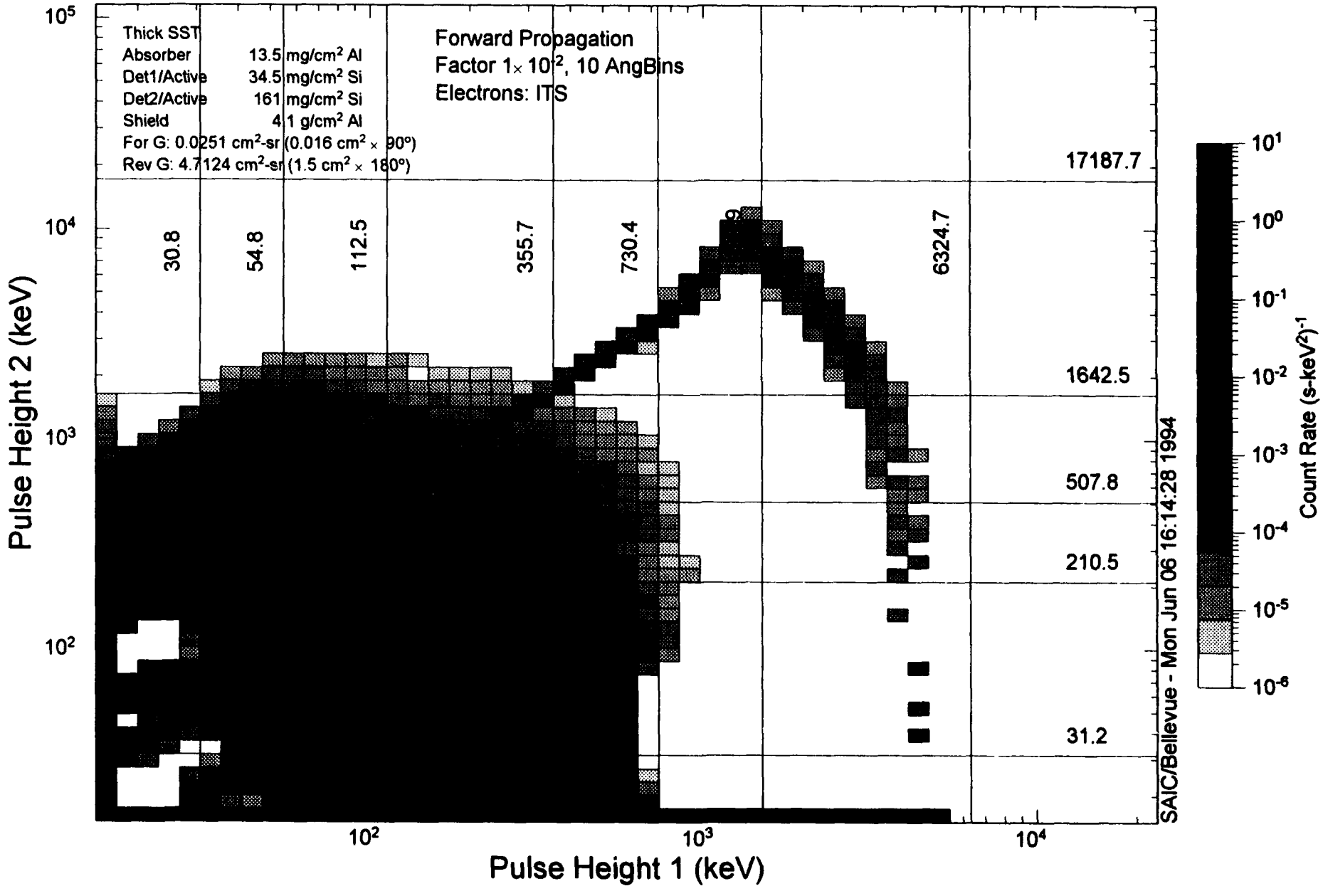

22

Pulse Height Coincidence

Inner Zone, L=1.4-1.8

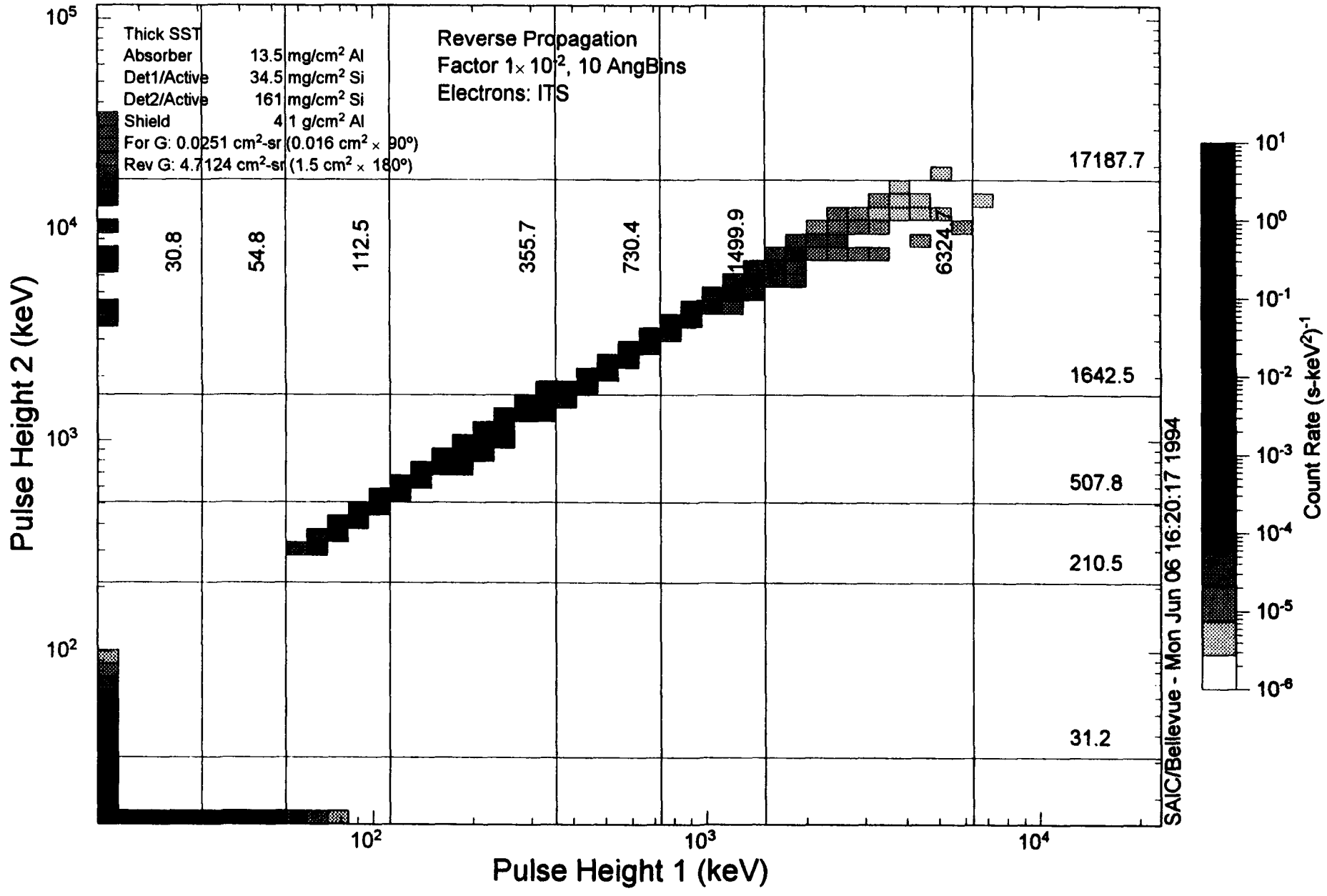

Pulse Height Coincidence

Outer zone, L=4-6. Quiet

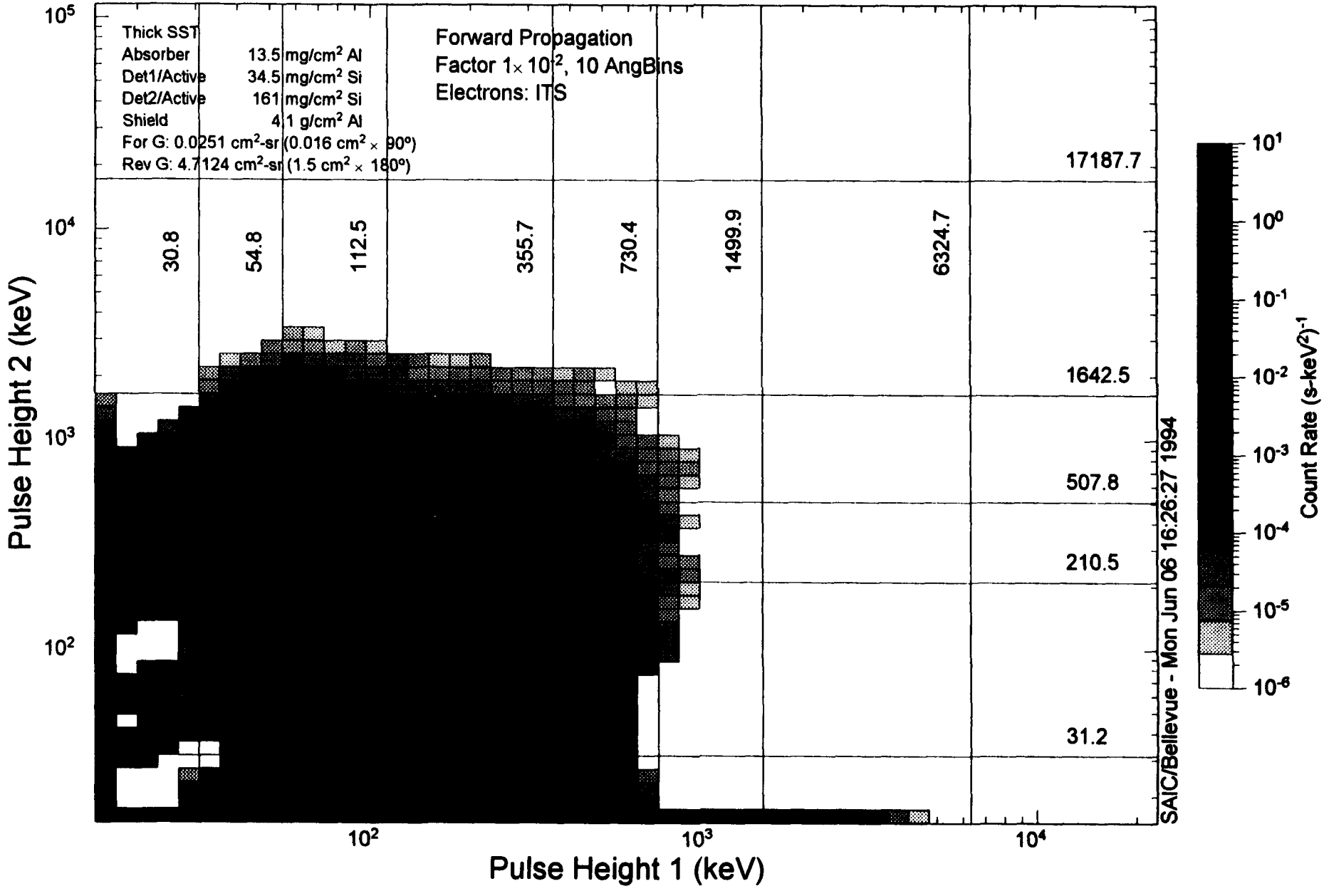

Pulse Height Coincidence

Outer zone, L=4-6. Quiet

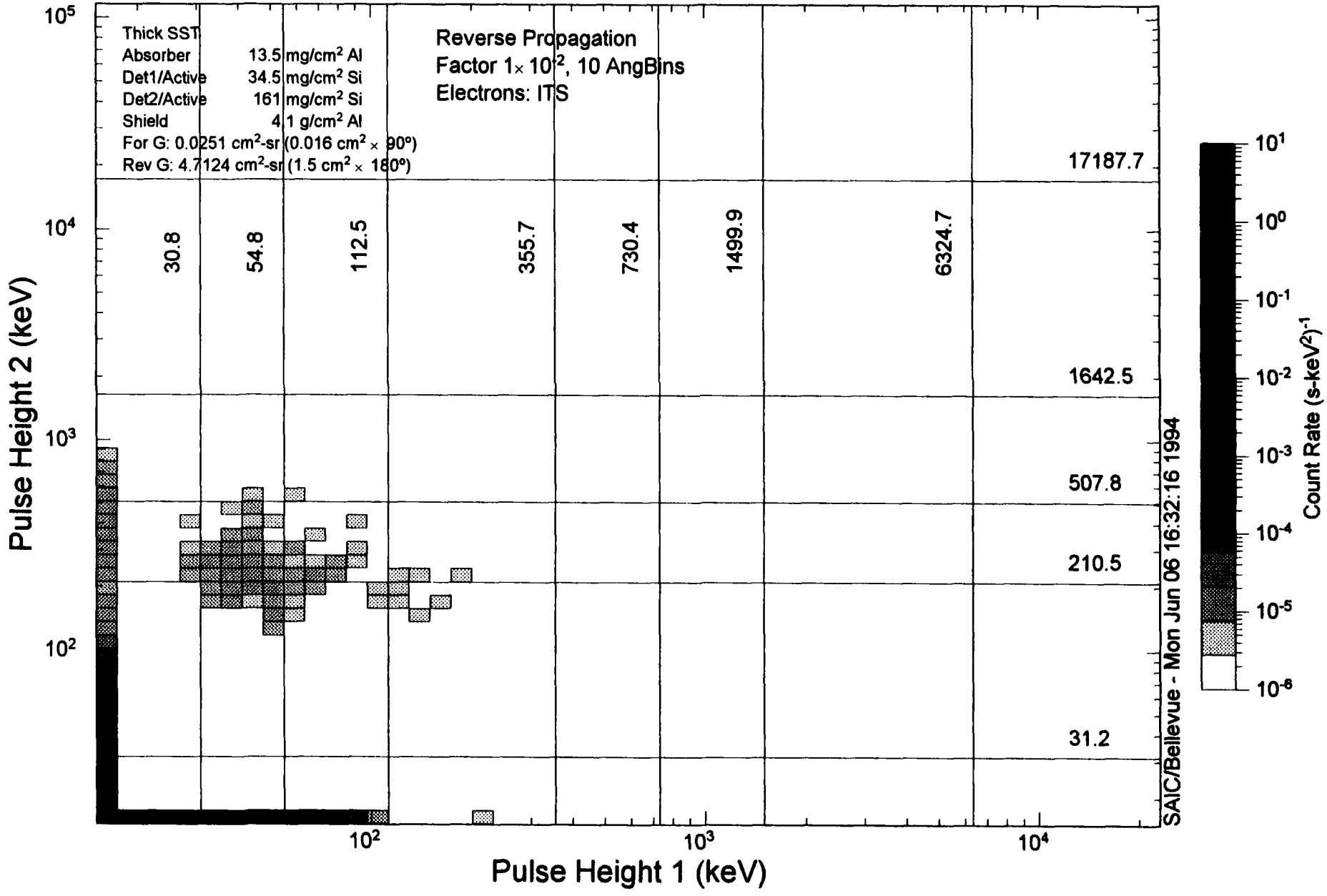

25

Pulse Height Coincidence
Outer zone and GEO, transient.

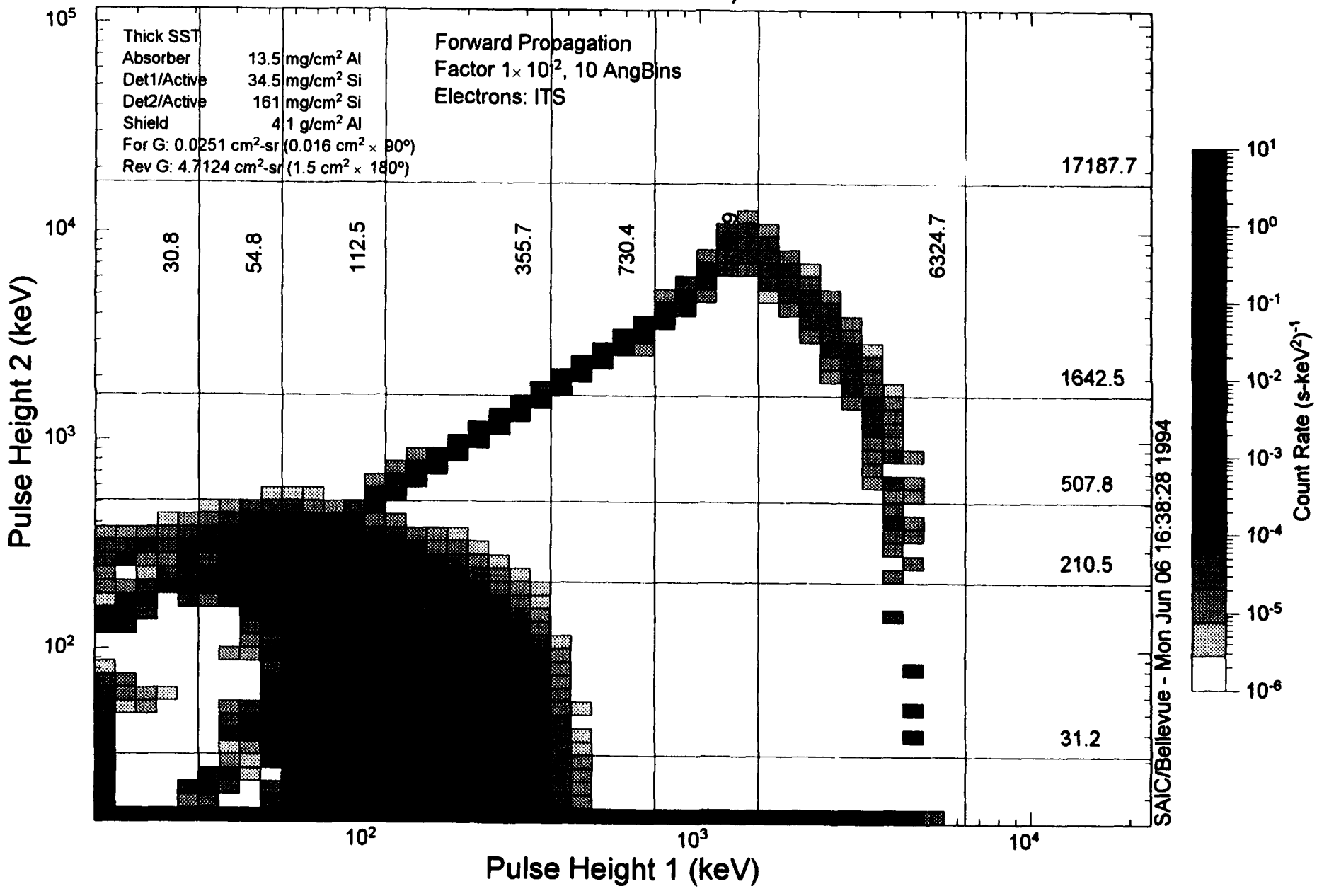

Pulse Height Coincidence

Outer zone and GEO, transient.

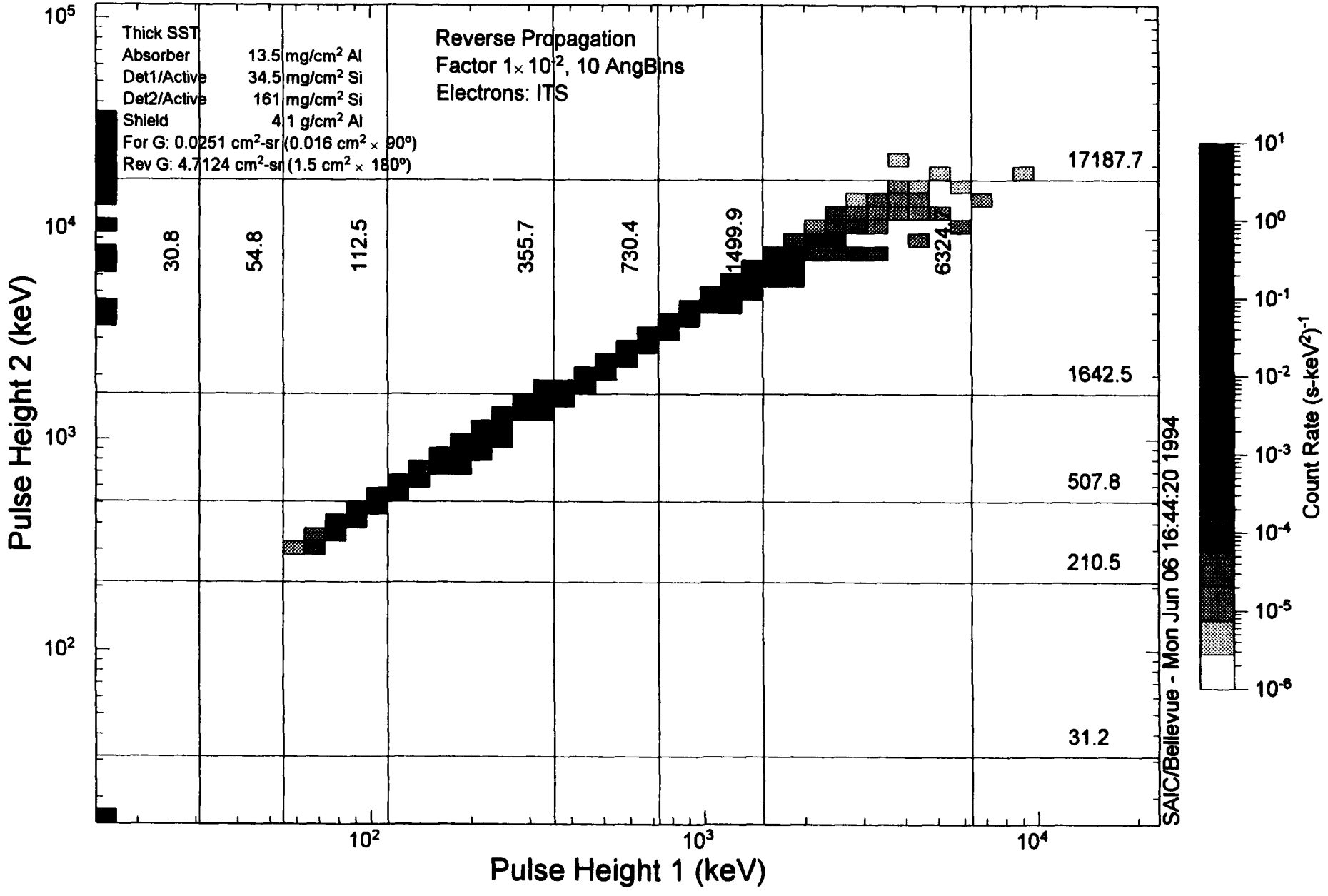

27

Pulse Height Coincidence
Inner Zone, L=1.4-1.8

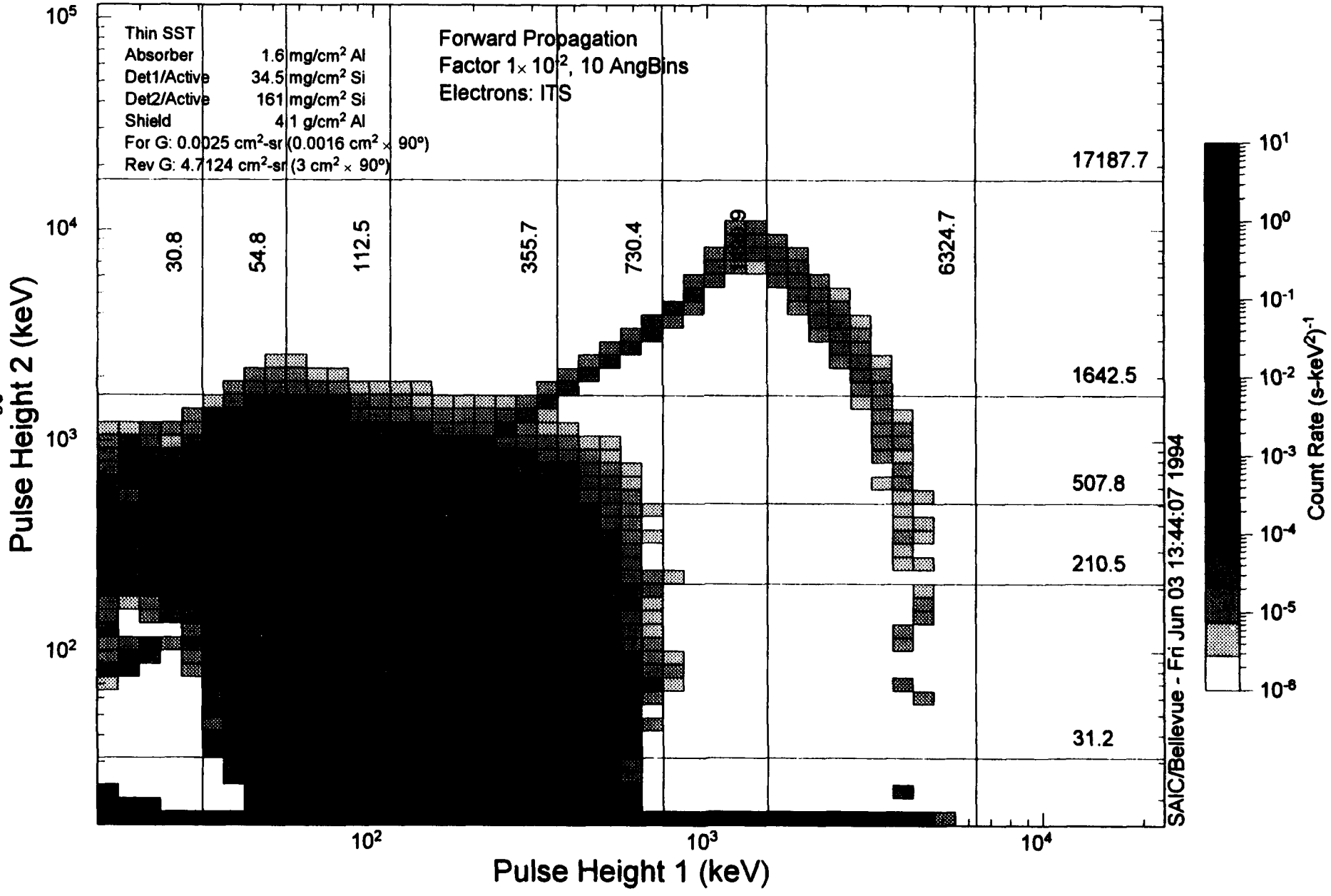

Bin Accumulation
Inner Zone, L=1.4-1.8

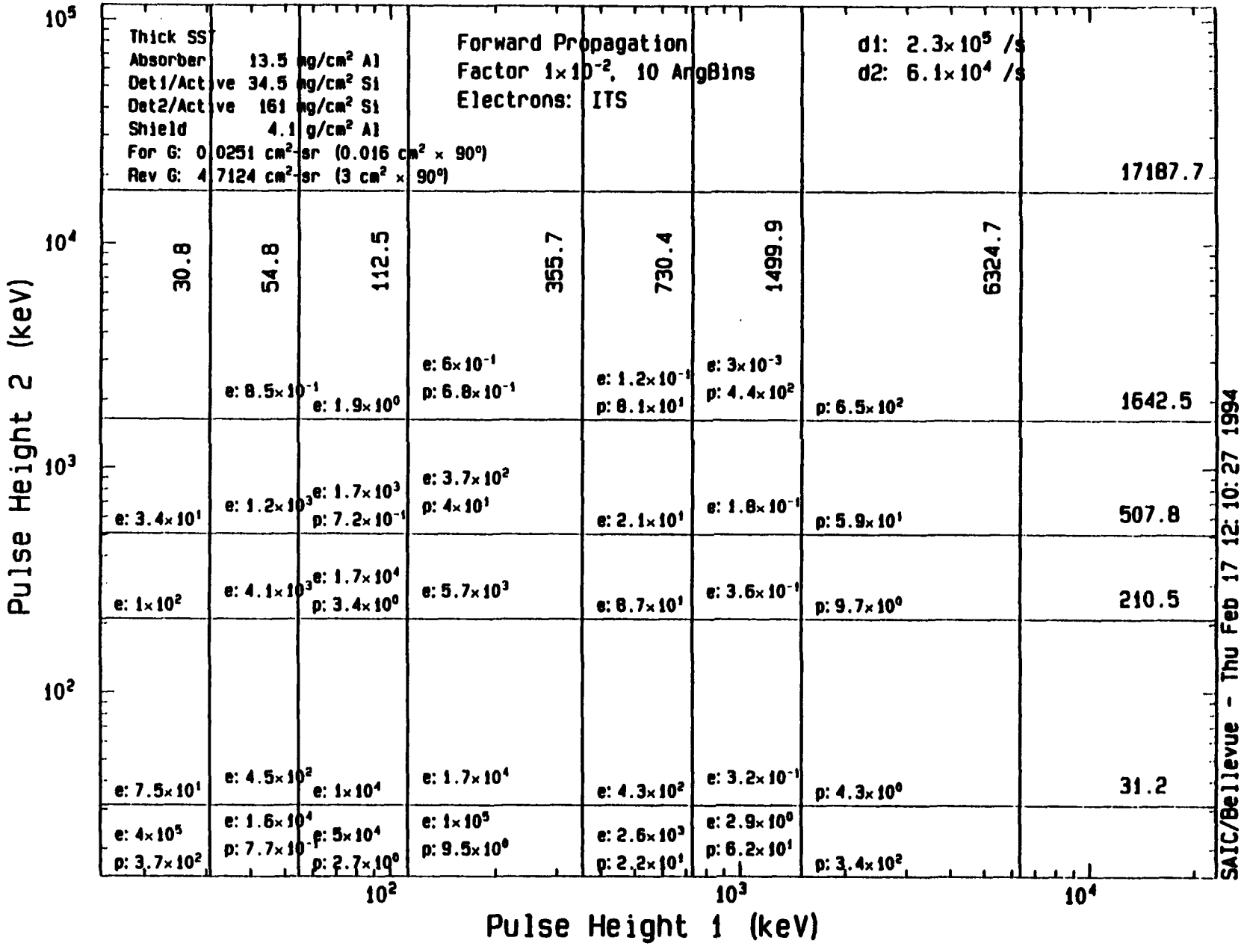

Bin Accumulation
Inner Zone, L=1.4-1.8

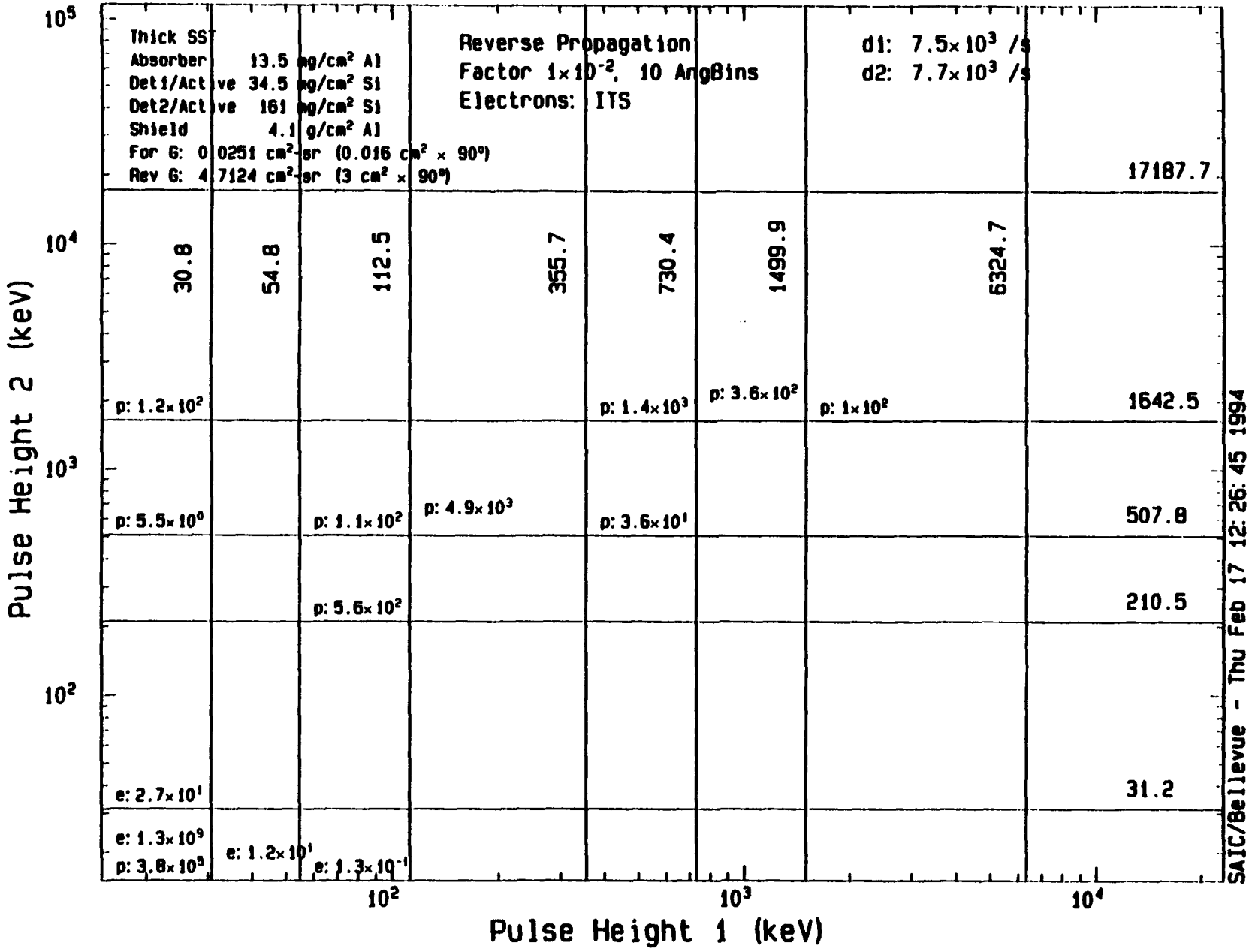

Bin Accumulation

Outer zone, L=4-6. Quiet

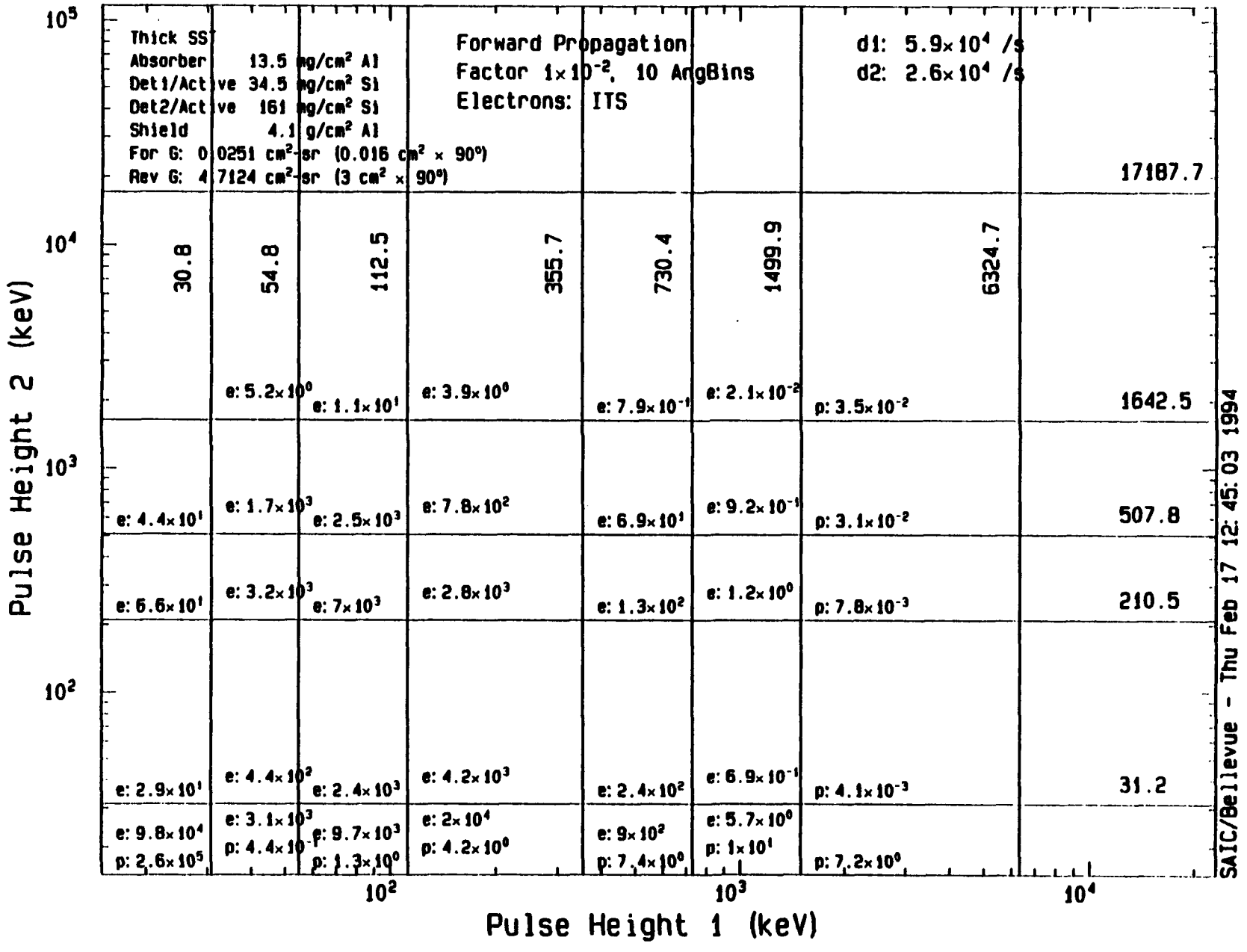

Bin Accumulation

Outer zone, L=4-6. Quiet

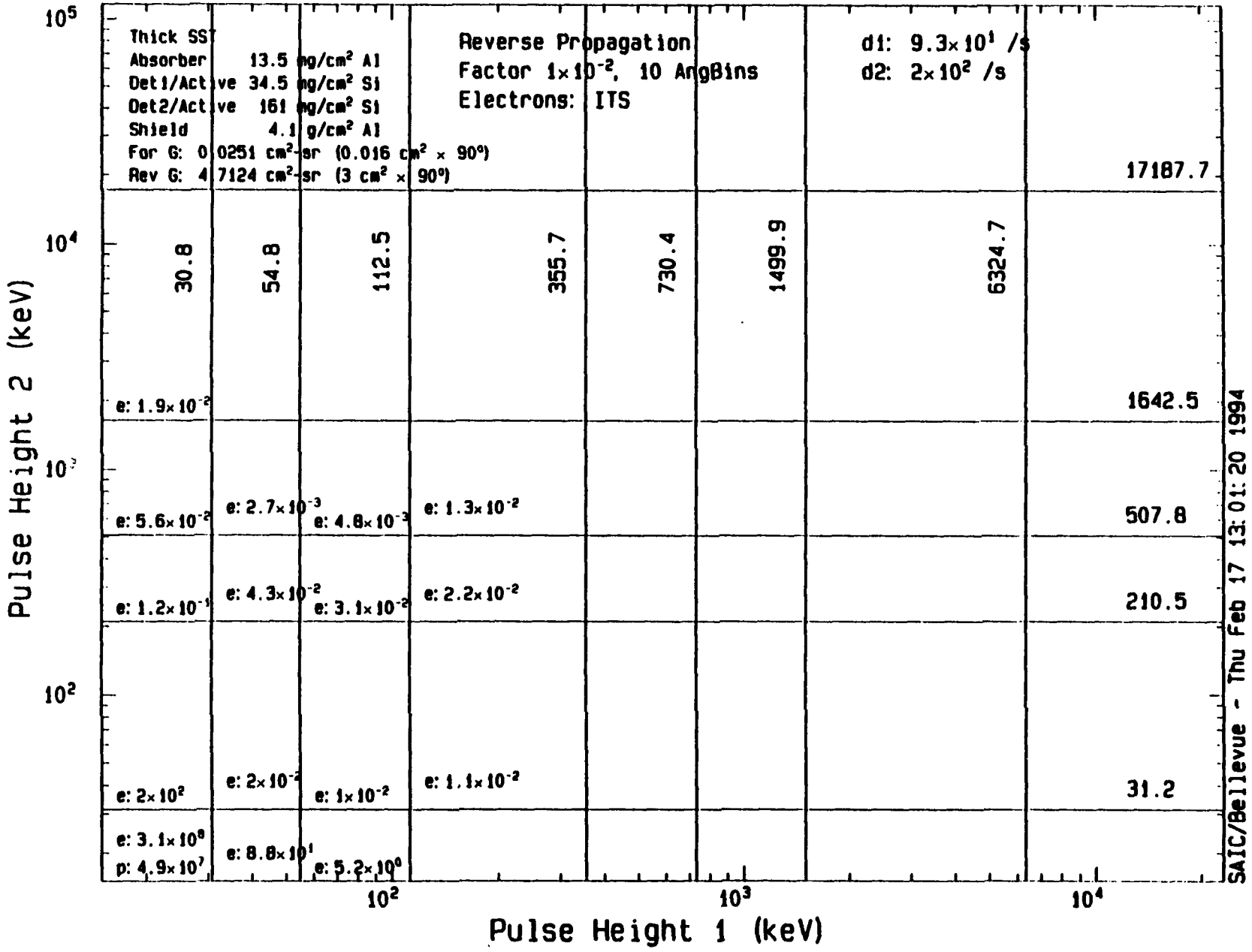

Bin Accumulation

Outer zone and GEO, transient.

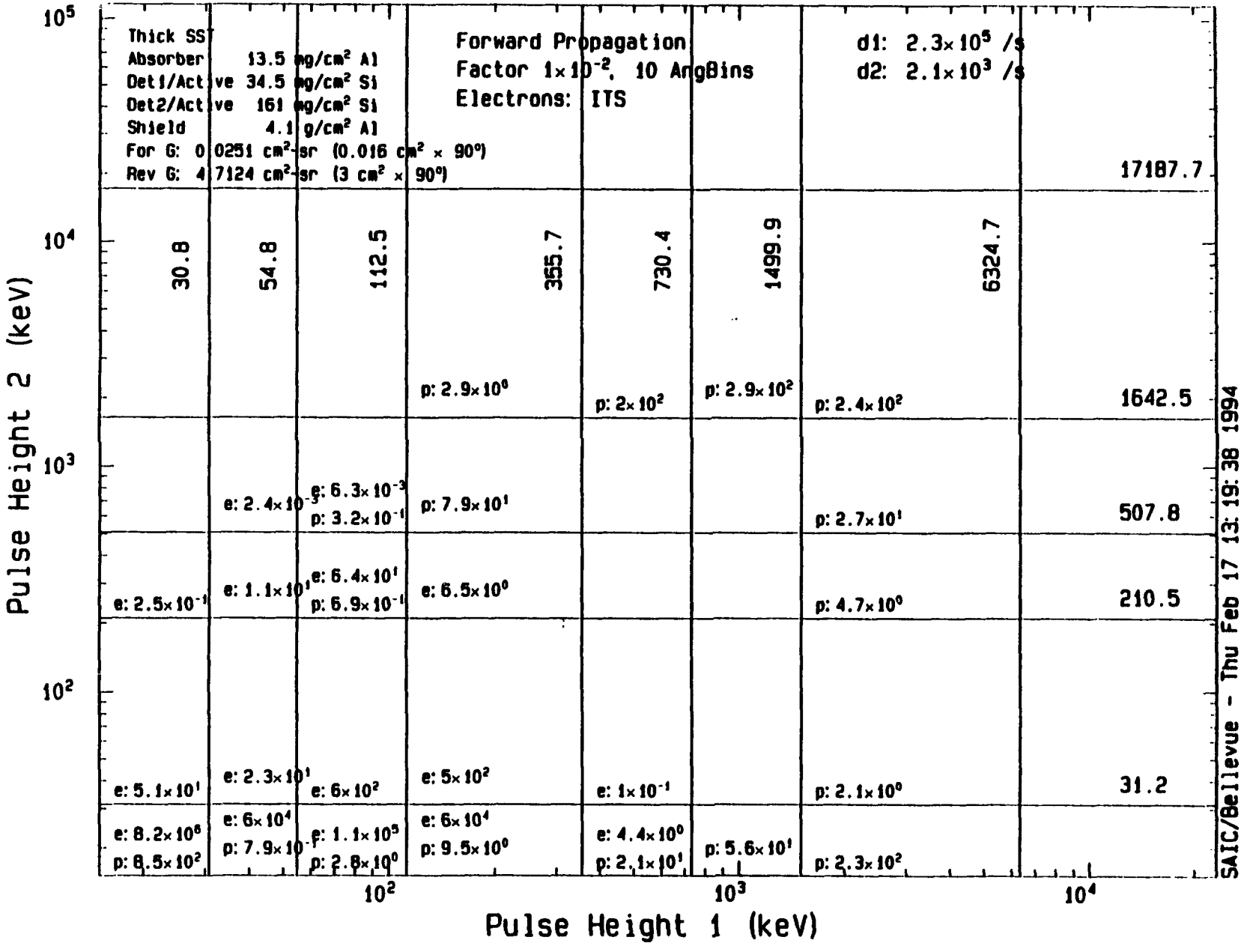

Bin Accumulation

Outer zone and GEO, transient.

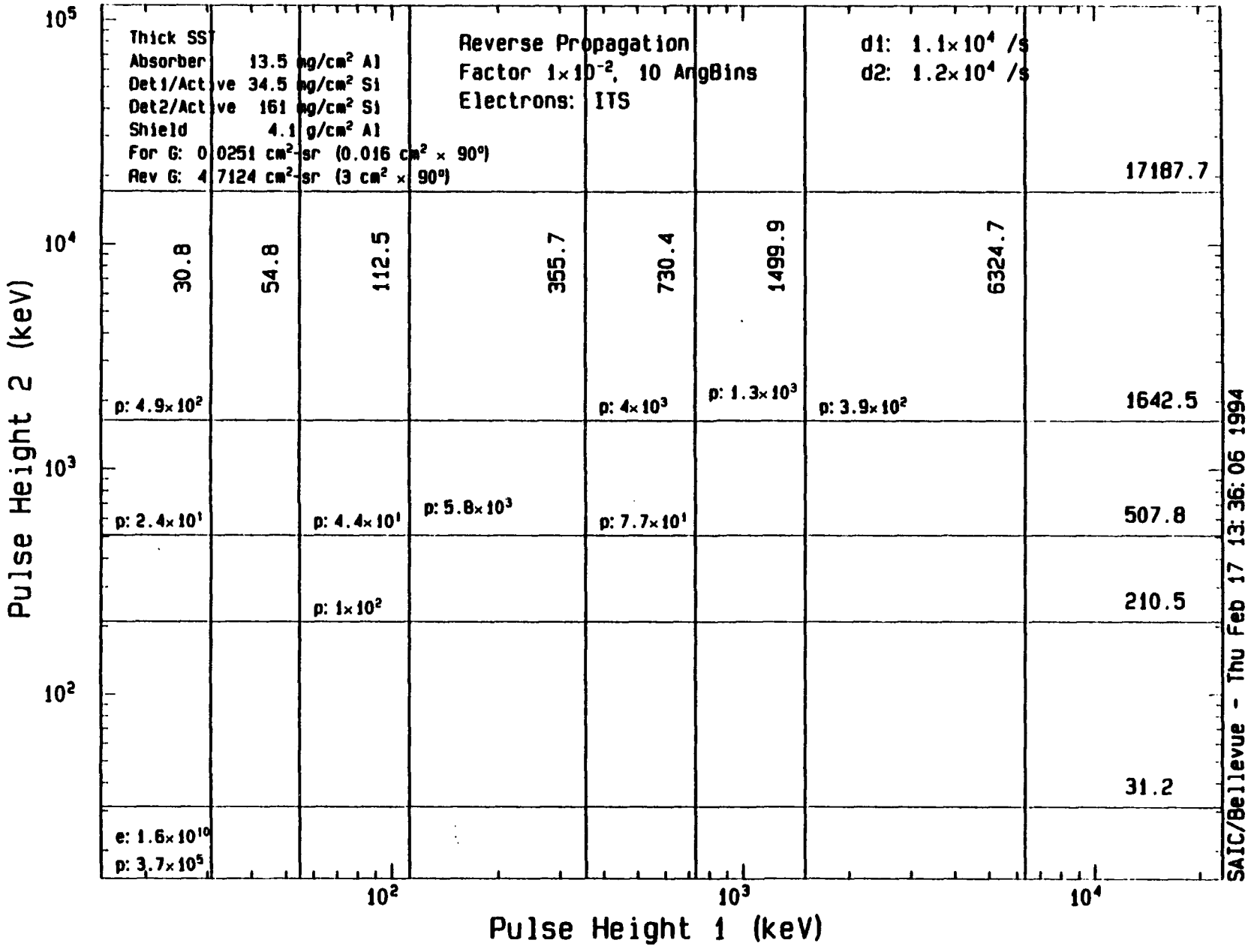

Pulse Height Coincidence

Inner Zone, L=1.4-1.8

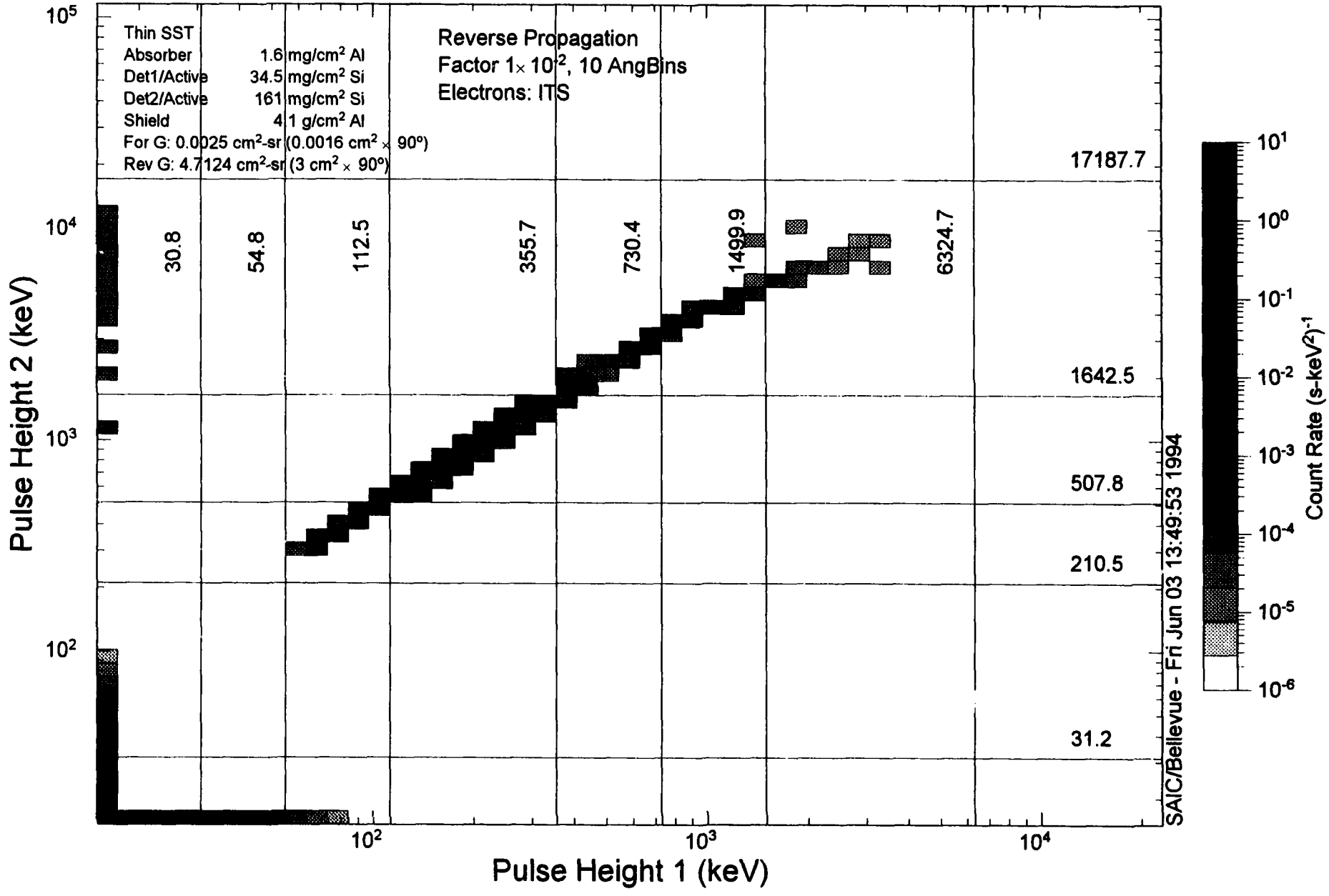

35

Pulse Height Coincidence

Outer zone, L=4-6. Quiet

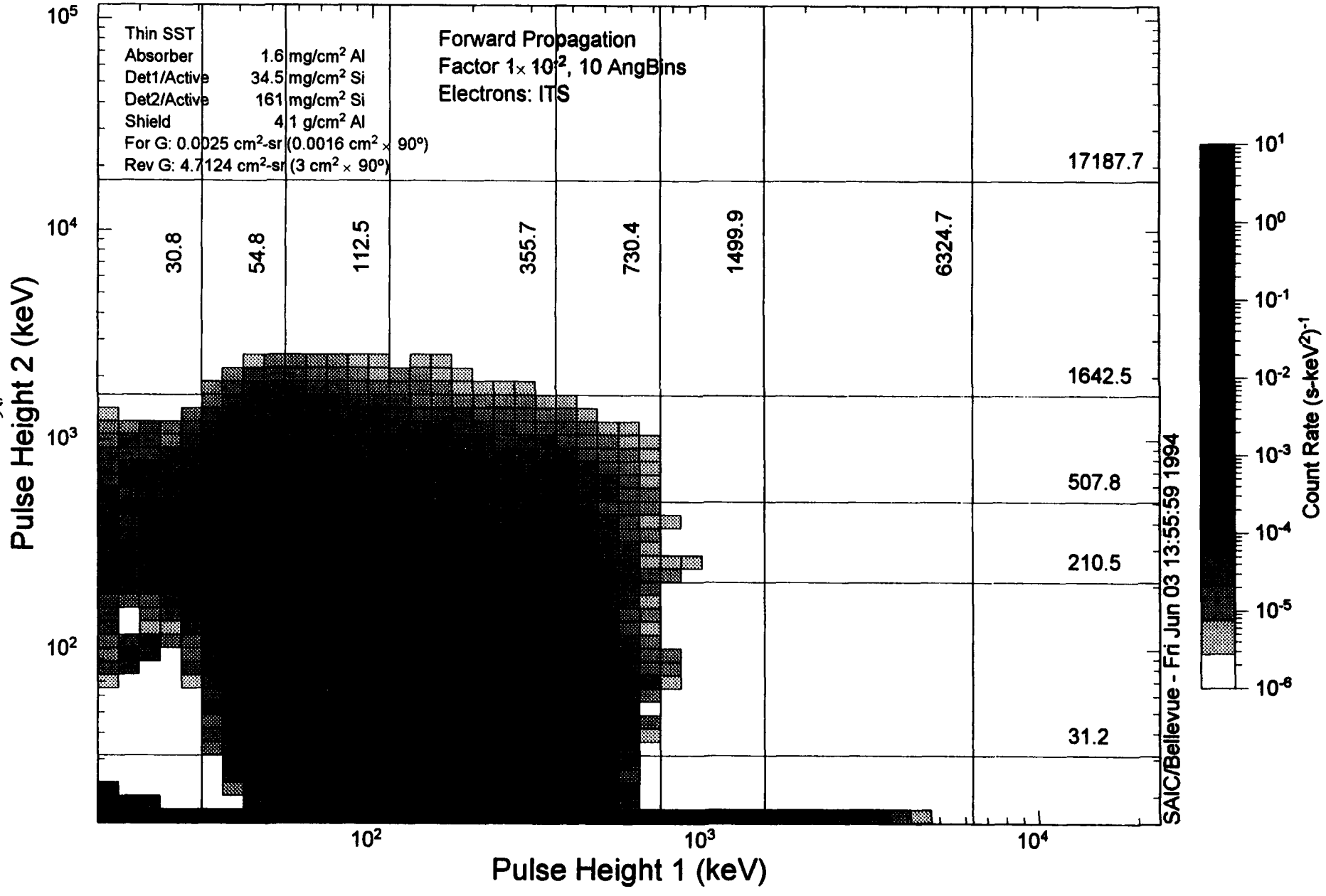

Pulse Height Coincidence

Outer zone, L=4-6. Quiet

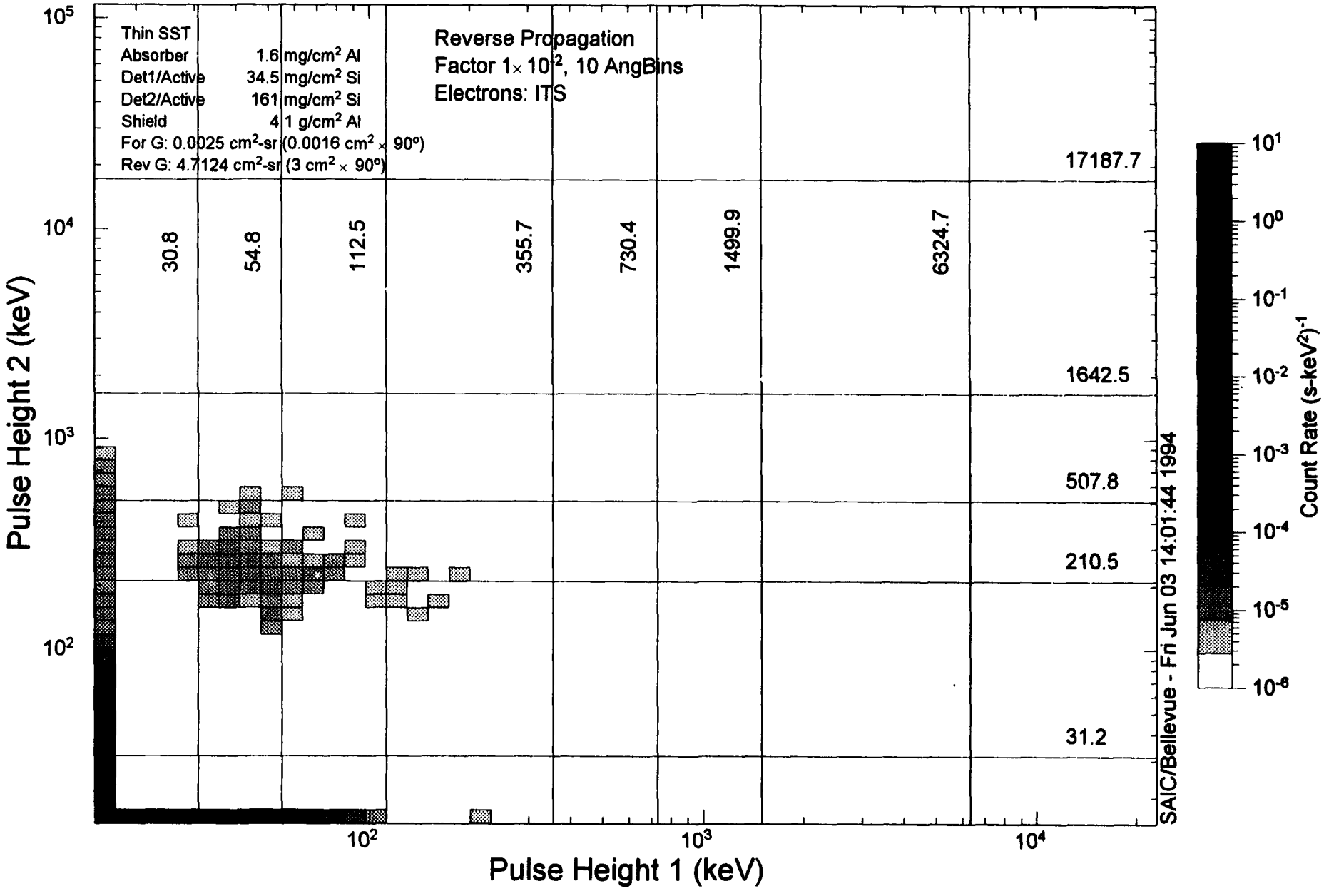

Pulse Height Coincidence
Outer zone and GEO, transient.

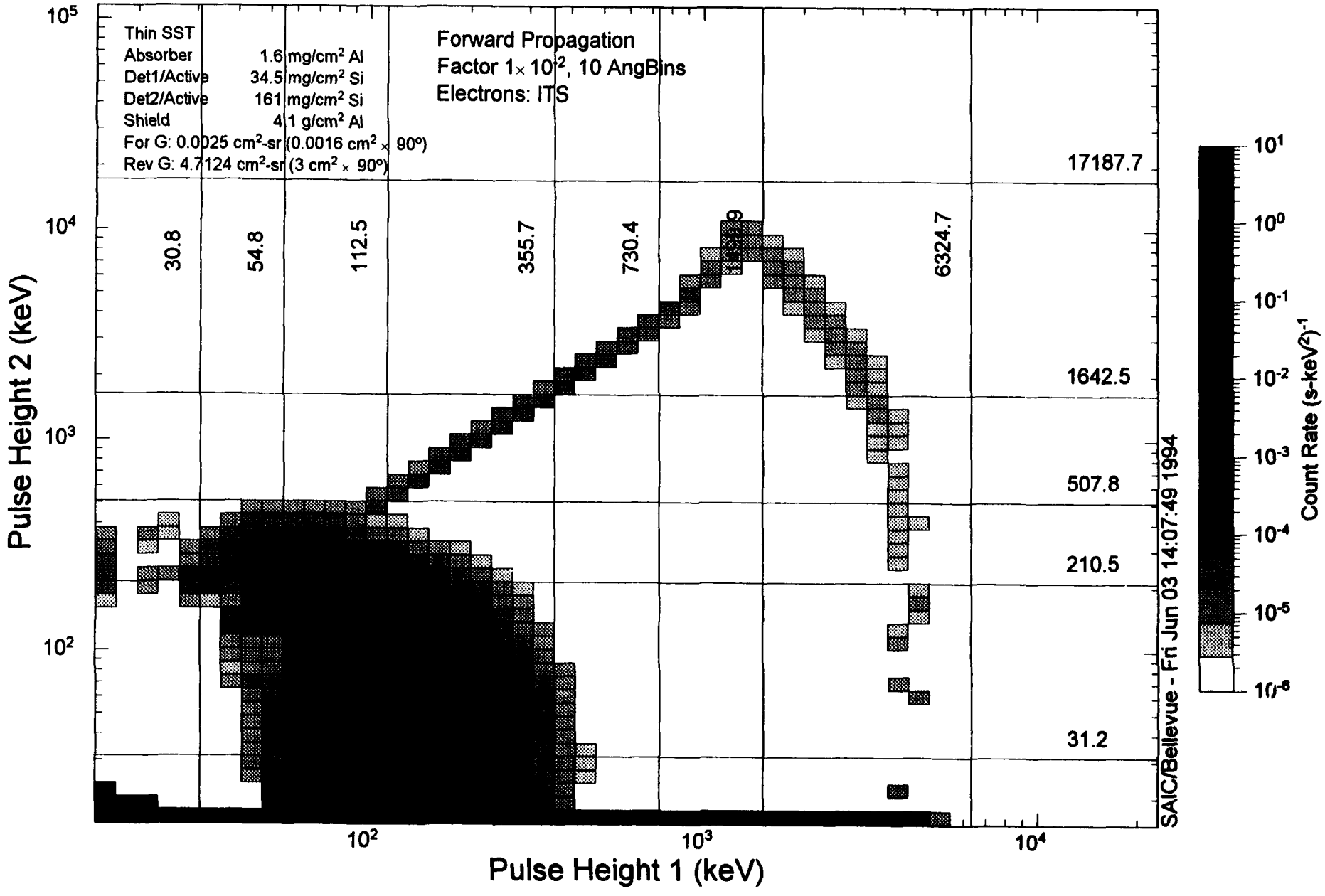

Pulse Height Coincidence

Outer zone and GEO, transient.

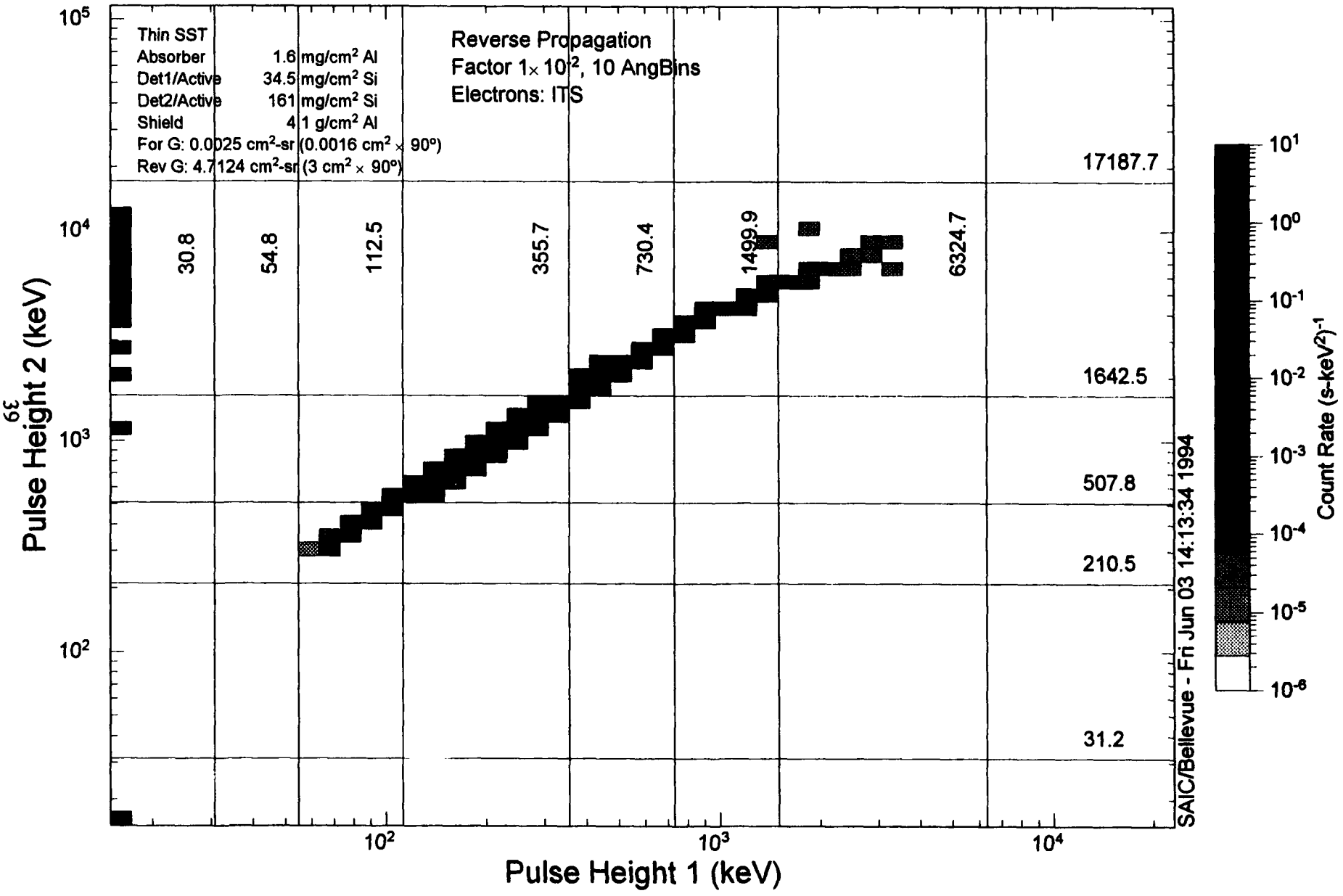

Bin Accumulation
Inner Zone, L=1.4-1.8

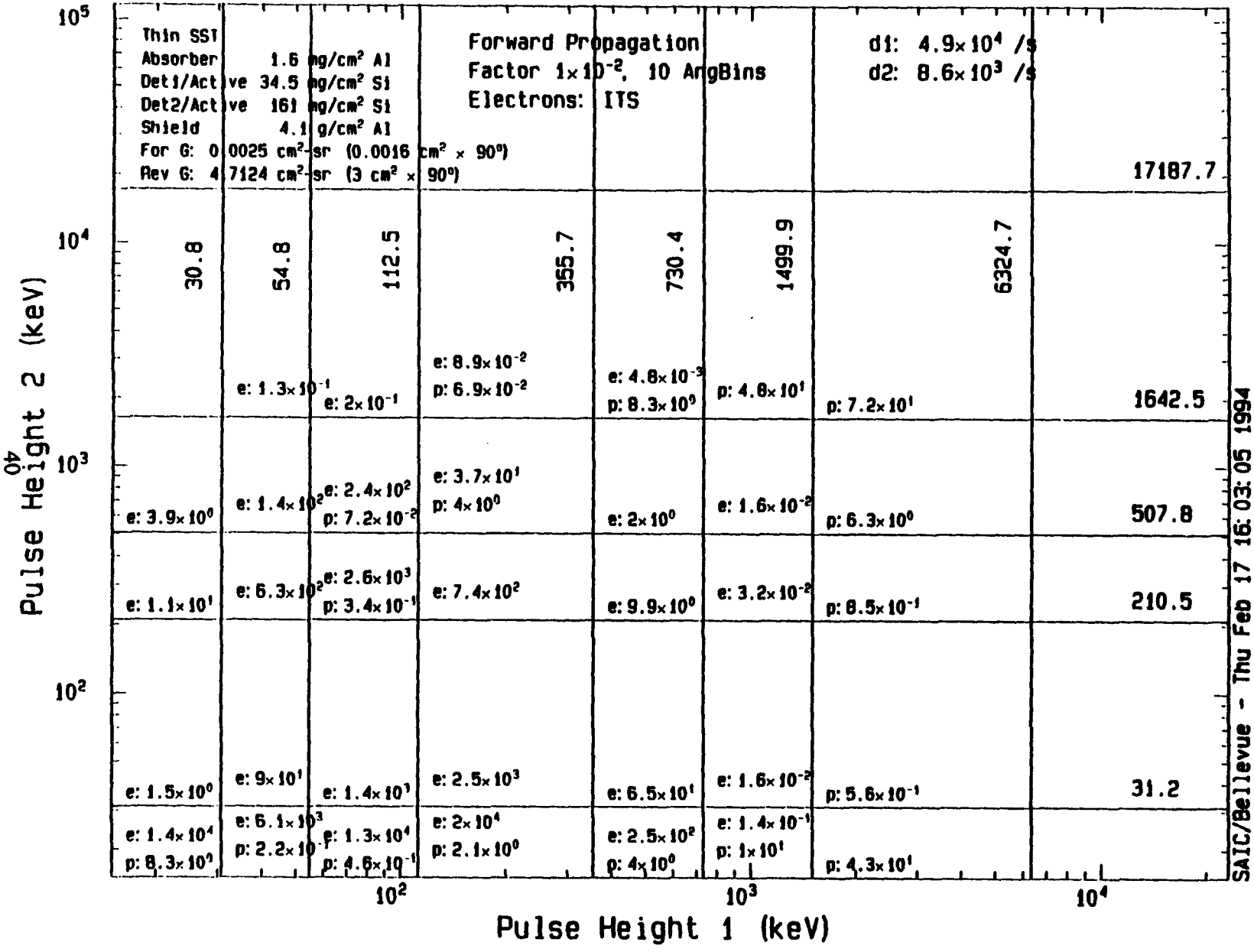

Bin Accumulation

Inner Zone, L=1.4-1.8

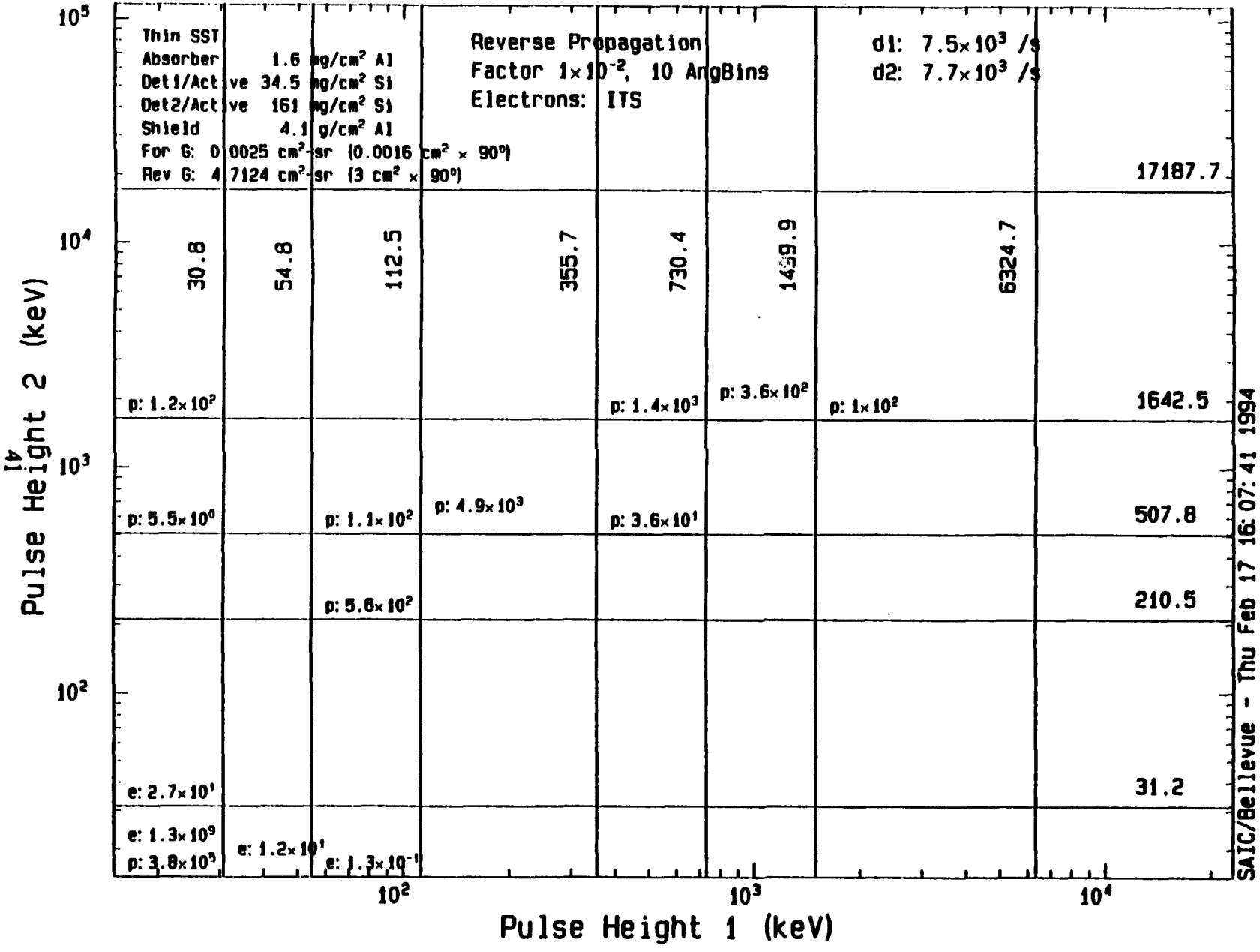

Bin Accumulation

Outer zone, L=4-6. Quiet

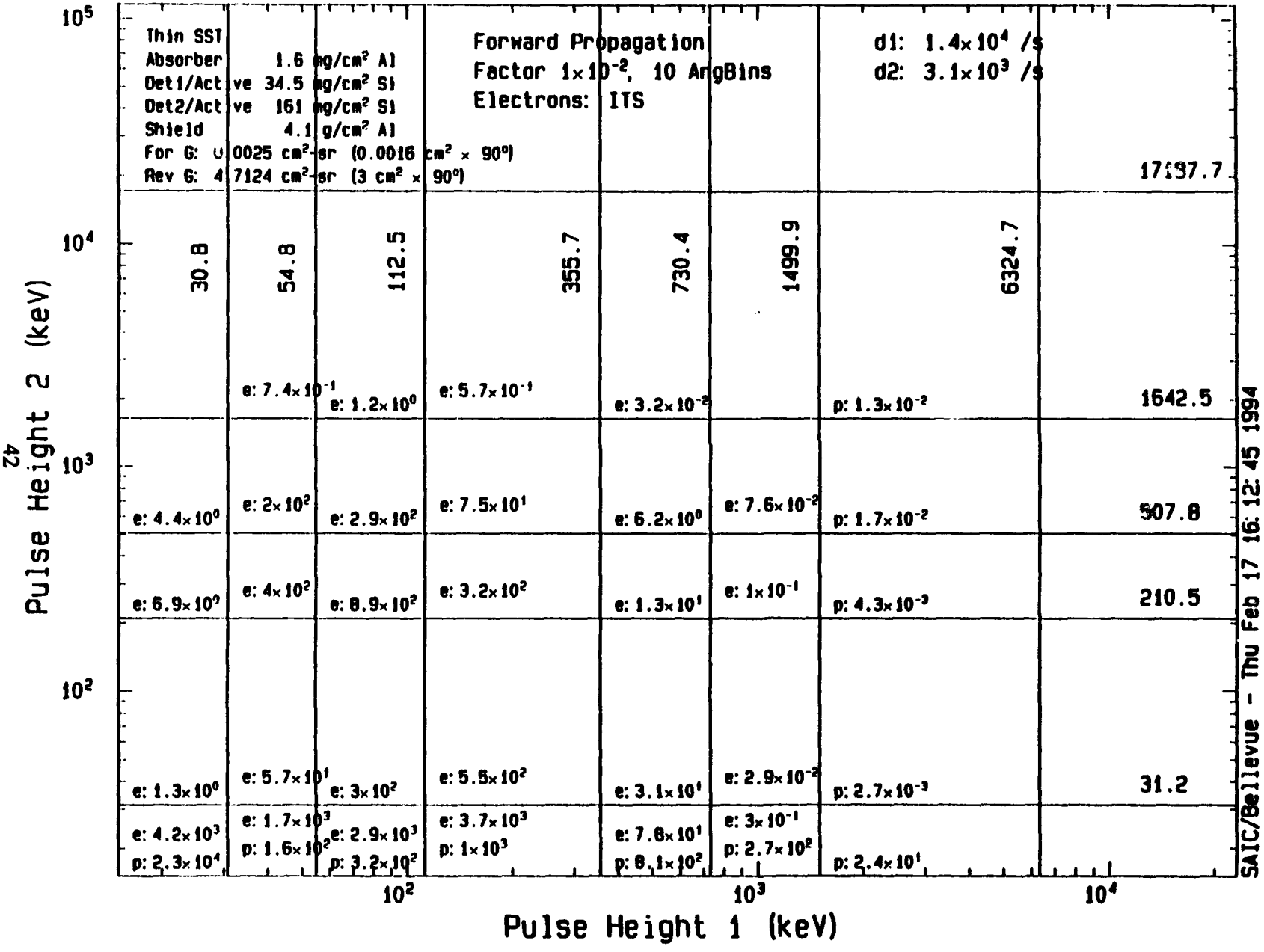

SAIC/Bellevue - Thu Feb 17 16:12:45 1994

Bin Accumulation

Outer zone, L=4-6. Quiet

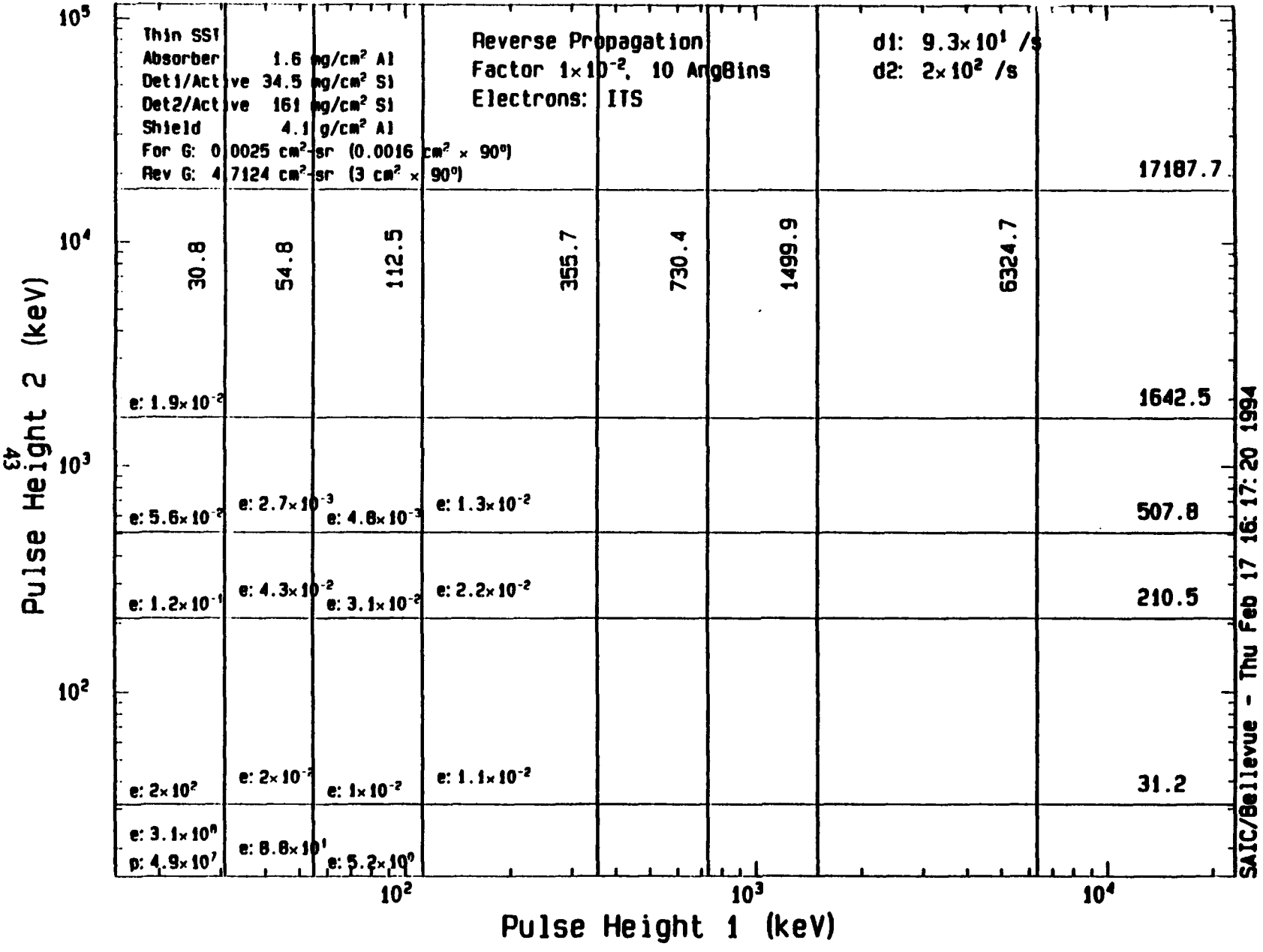

Bin Accumulation

Outer zone and GEO, transient.

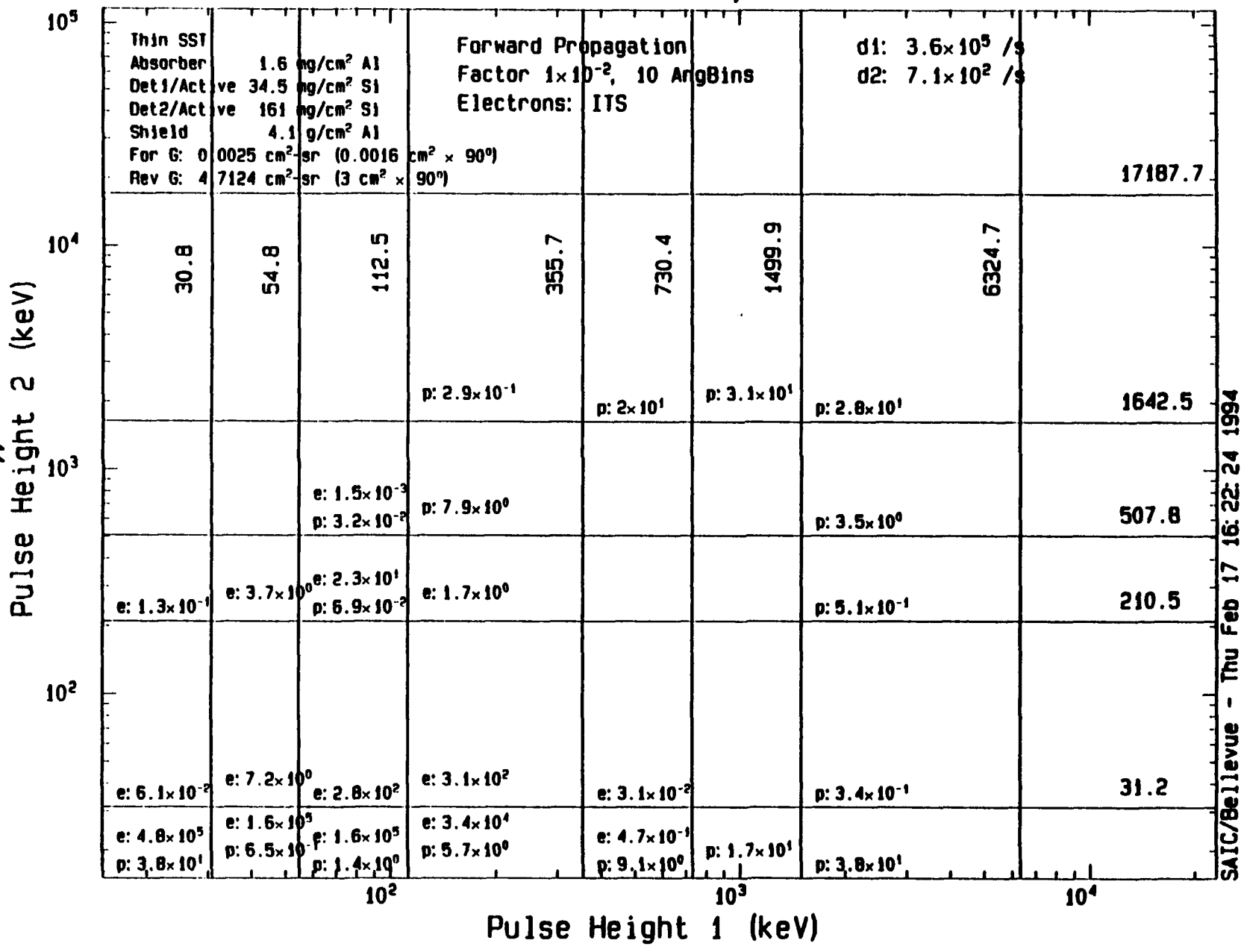

Bin Accumulation

Outer zone and GEO, transient.

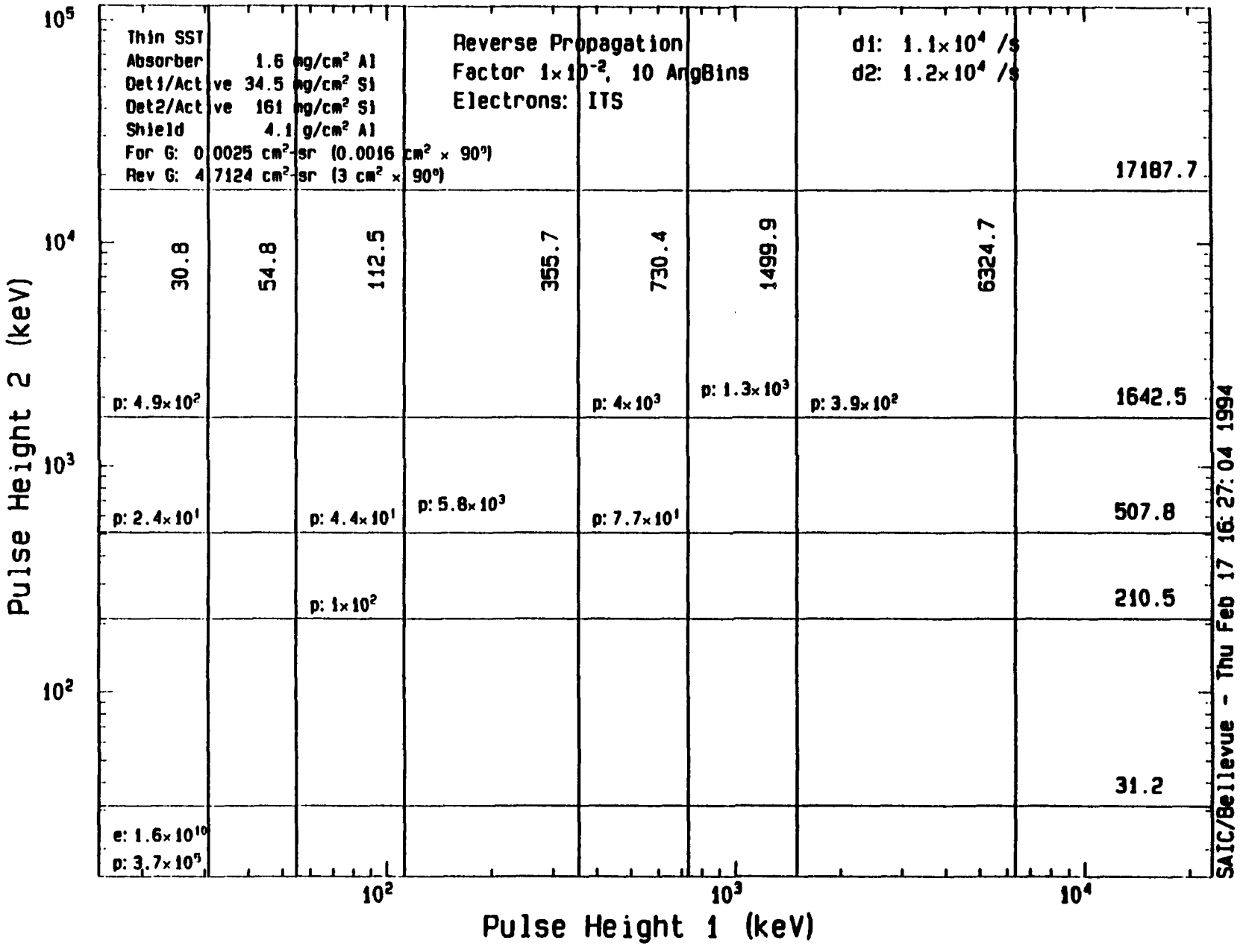

Energy Thresholds

Threshold: 0.01/MeV^2

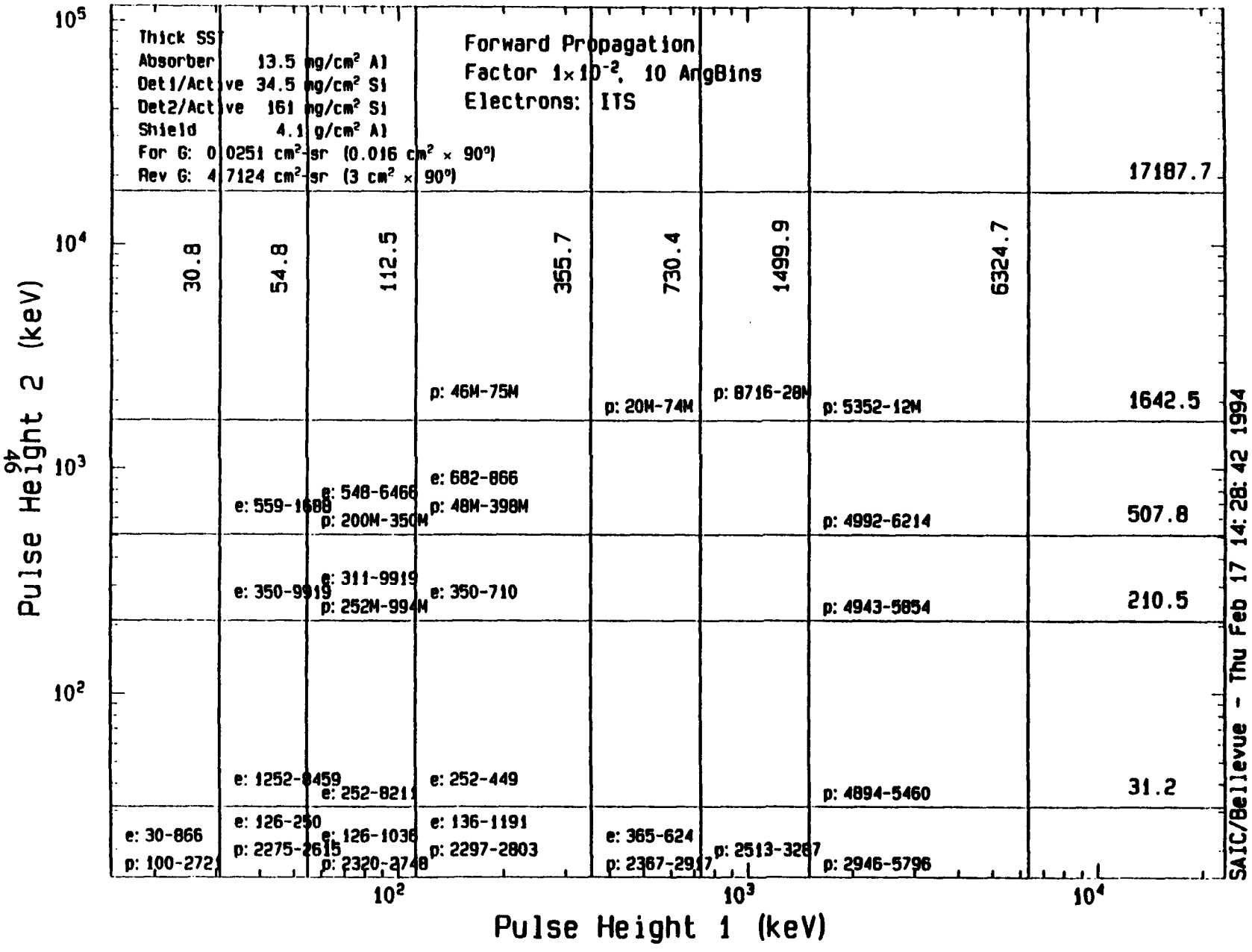

Energy Thresholds

Threshold: 0.01/MeV^2

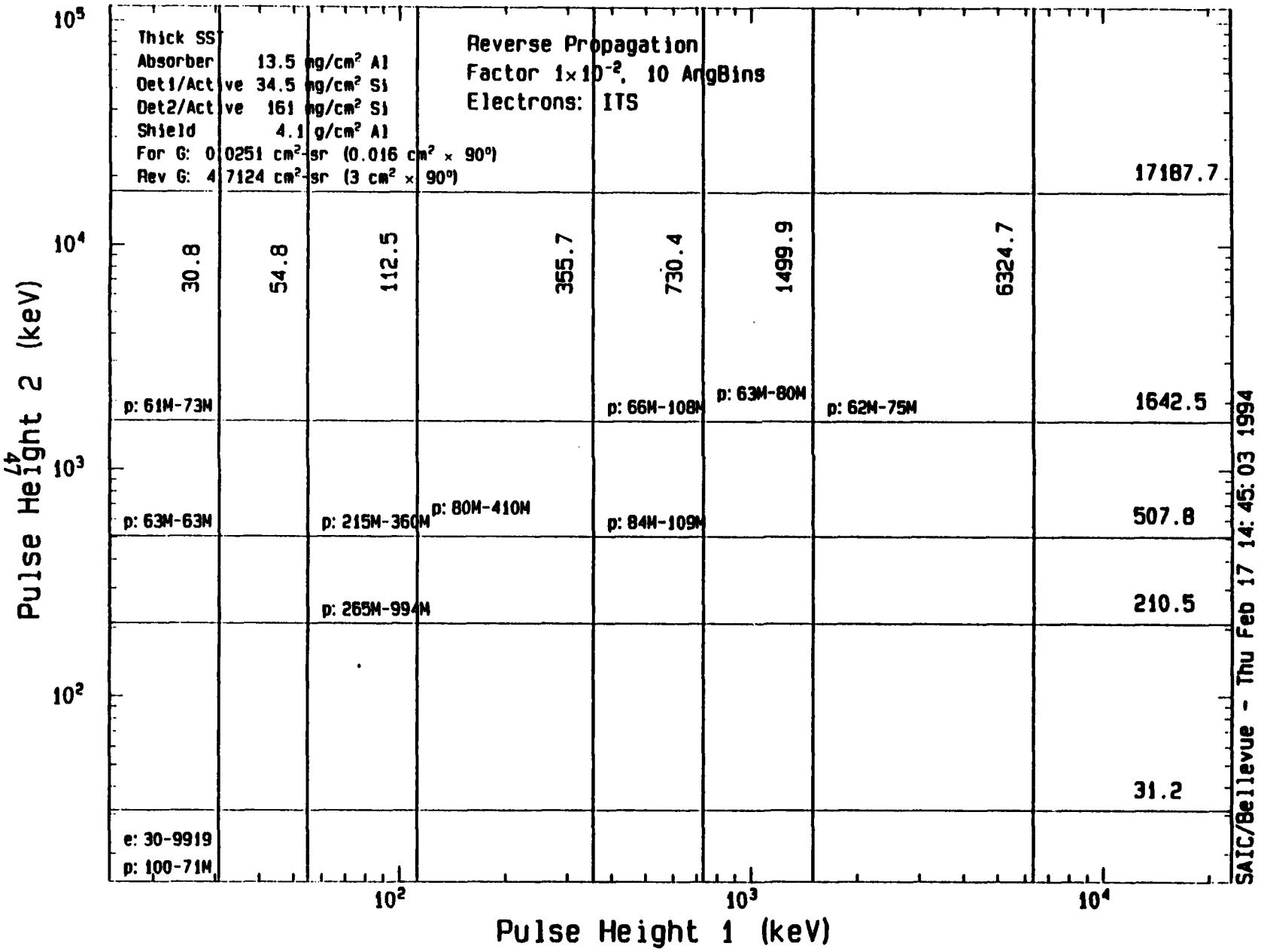

Energy Thresholds

Threshold: 0.01/MeV^2

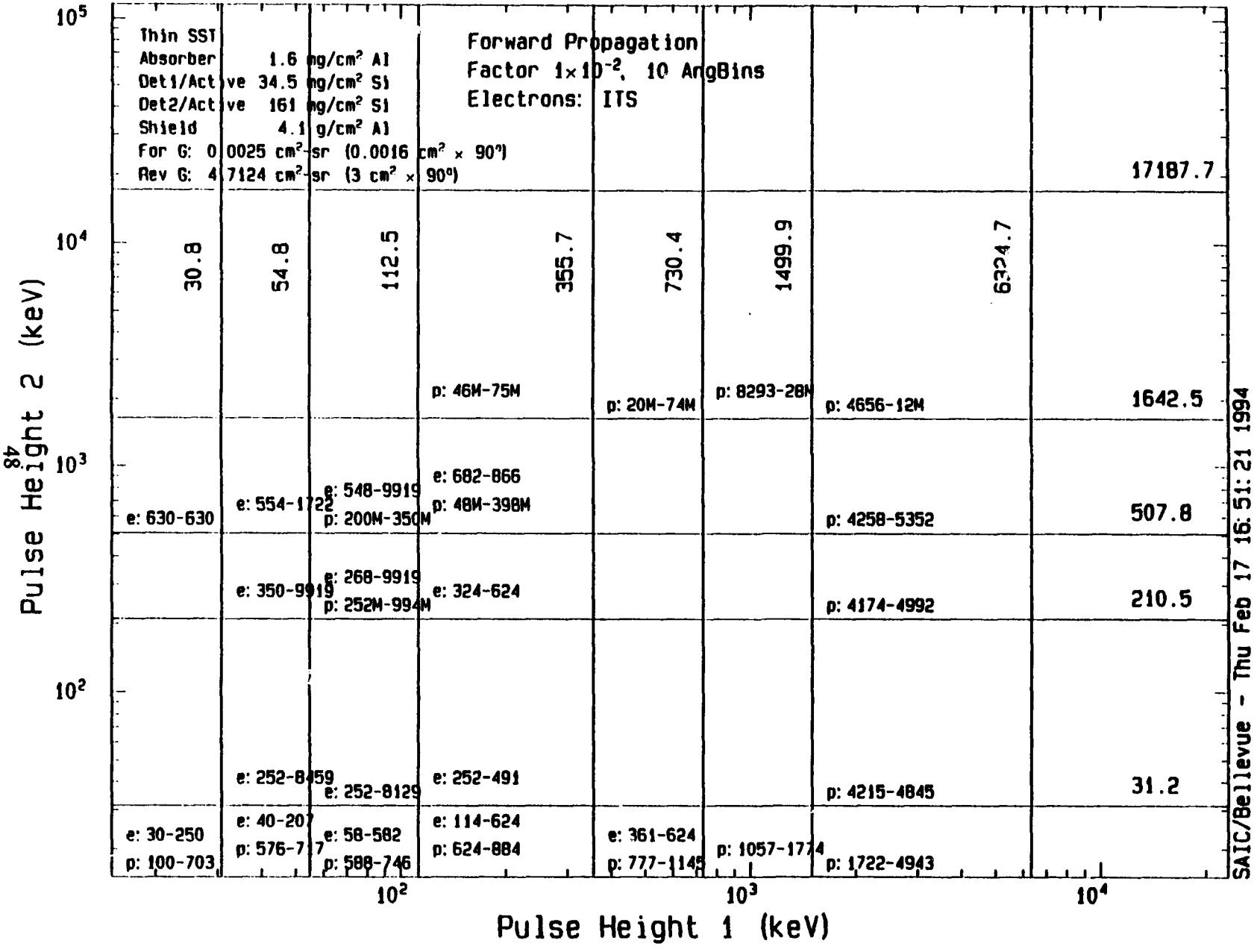

Energy Thresholds

Threshold: 0.01/MeV^2

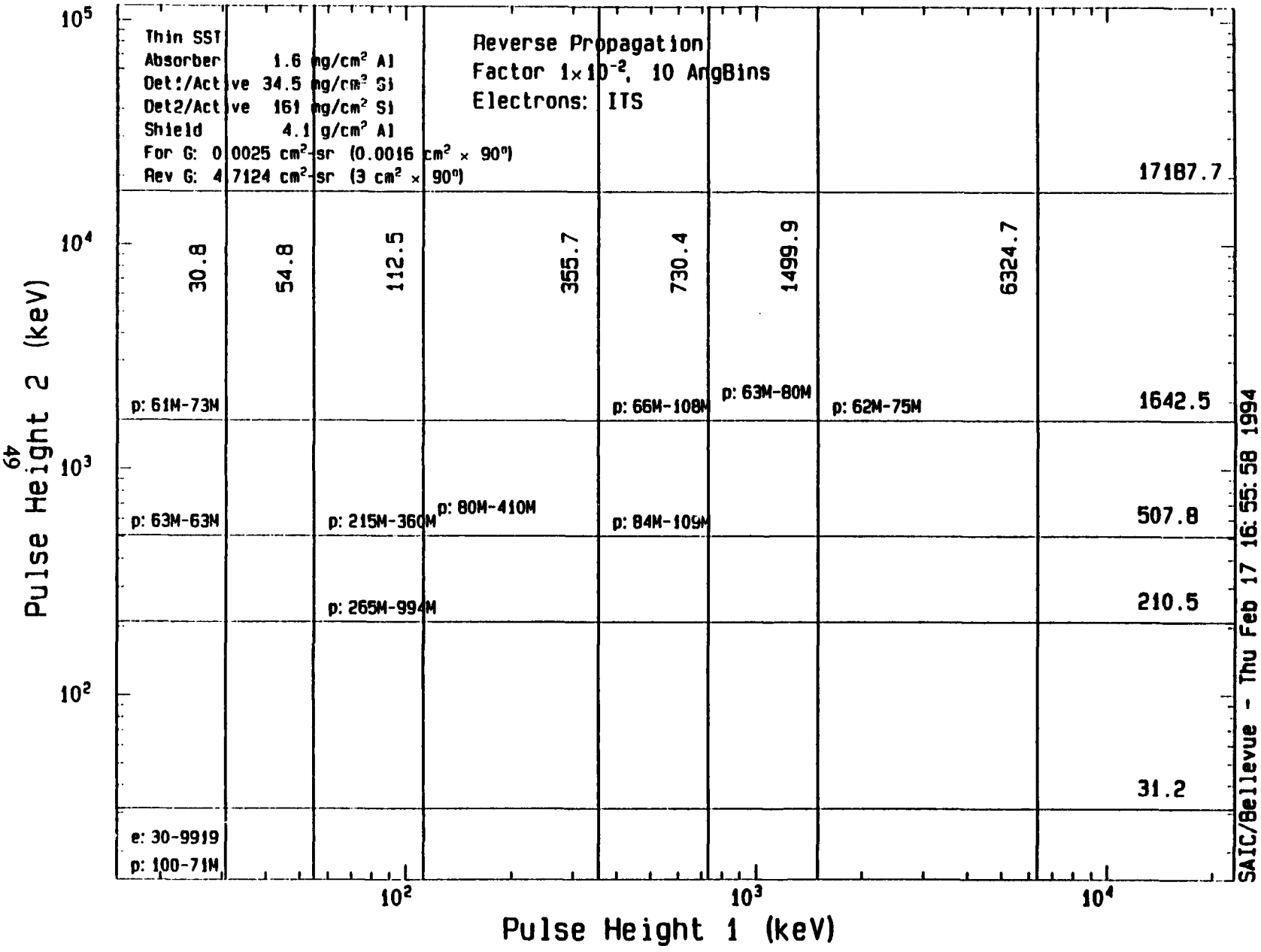

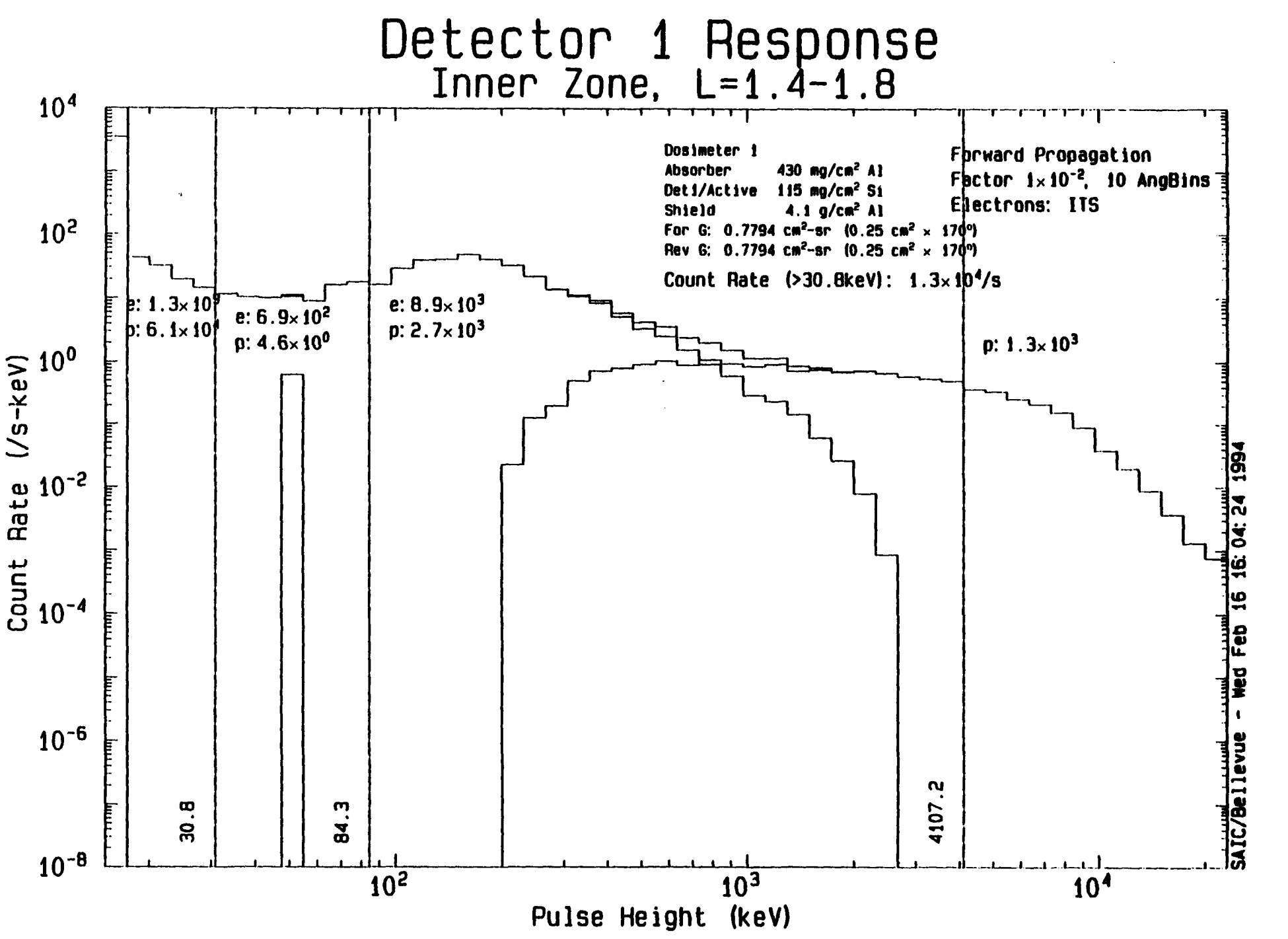
Detector 1 Response
Inner Zone, L=1.4-1.8
Dosimeter 1
Absorber 430 mg/cm² Al
Det1/Active 115 mg/cm² Si
Shield 4.1 g/cm² Al
For G: 0.7794 cm²-sr (0.25 cm² × 170°)
Rev G: 0.7794 cm²-sr (0.25 cm² × 170°)
Count Rate (>30.8keV): 1.3×10⁴/s
Forward Propagation
Factor 1×10⁻², 10 AngBins
Electrons: ITS
e: 1.3×10⁹
p: 6.1×10⁴
e: 6.9×10²
p: 4.6×10⁰
e: 8.9×10³
p: 2.7×10³
p: 1.3×10³
30.8
84.3
4107.2
Count Rate (/s-keV)
Pulse Height (keV)
SAIC/Bellevue - Wed Feb 16 16:04:24 1994

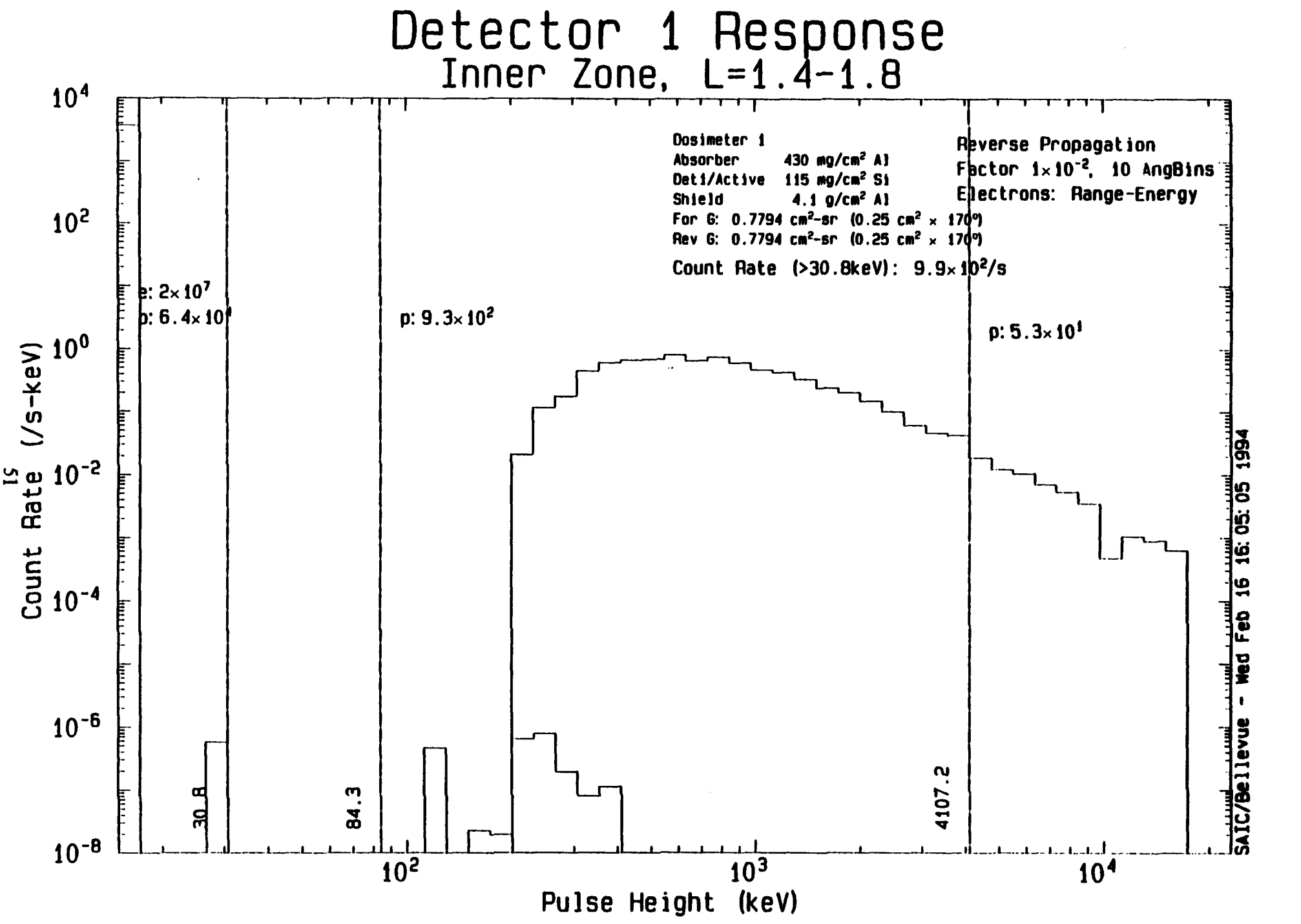
Detector 1 Response
Inner Zone, L=1.4-1.8
Dosimeter 1
Absorber 430 mg/cm² Al
Det1/Active 115 mg/cm² Si
Shield 4.1 g/cm² Al
For G: 0.7794 cm²-sr (0.25 cm² x 170°)
Rev G: 0.7794 cm²-sr (0.25 cm² x 170°)
Count Rate (>30.8keV): 9.9x10²/s
Reverse Propagation
Factor 1x10⁻², 10 AngBins
Electrons: Range-Energy
e: 2x10⁷
p: 6.4x10⁴
p: 9.3x10²
p: 5.3x10¹
30.8
84.3
4107.2
Count Rate (/s-keV)
Pulse Height (keV)
SAIC/Bellevue - Wed Feb 16 16:05:05 1994

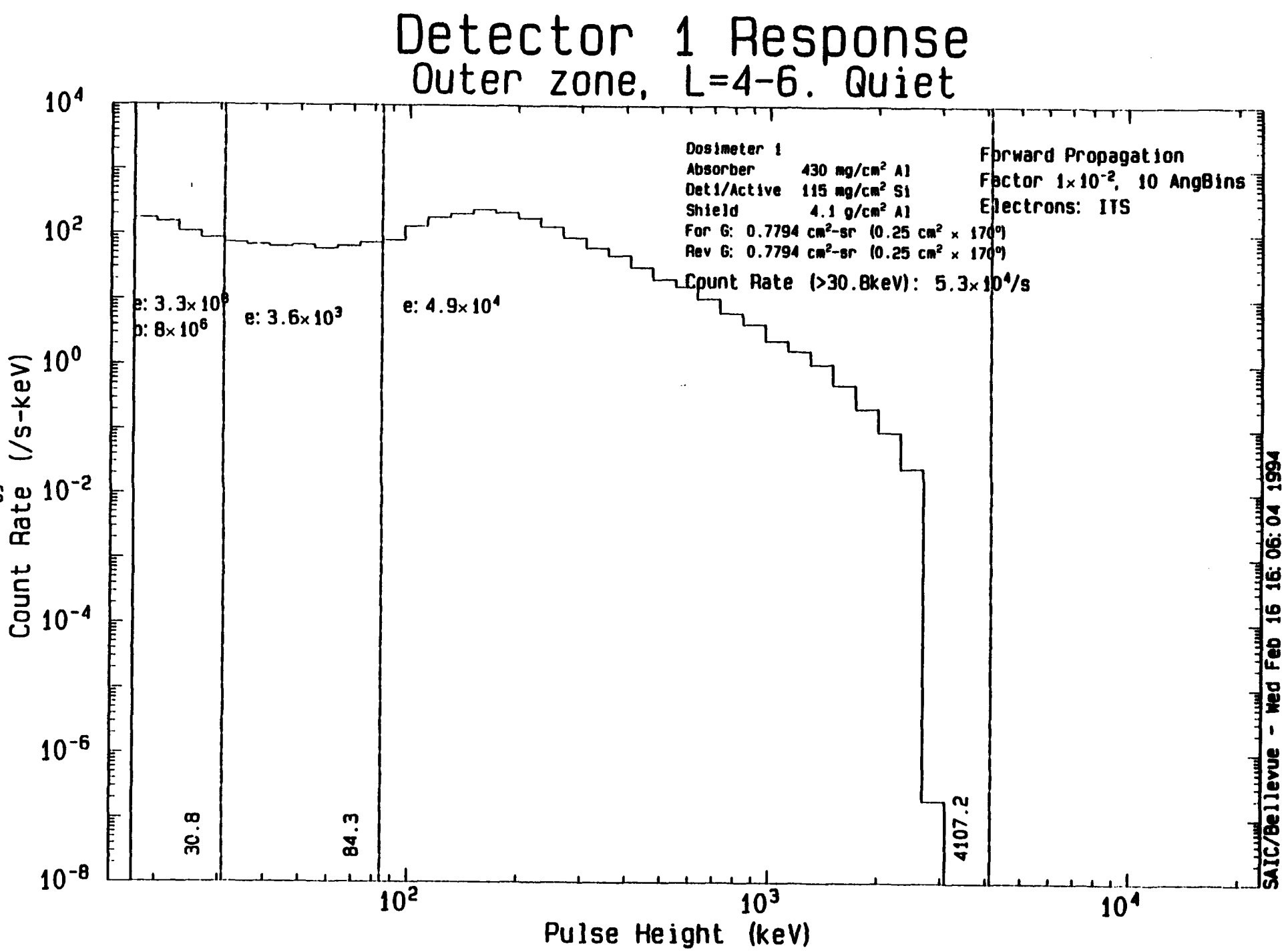
Detector 1 Response
Outer zone, L=4-6. Quiet
Dosimeter 1
Absorber 430 mg/cm² Al
Det1/Active 115 mg/cm² Si
Shield 4.1 g/cm² Al
For G: 0.7794 cm²-sr (0.25 cm² x 170°)
Rev G: 0.7794 cm²-sr (0.25 cm² x 170°)
Count Rate (>30.8keV): 5.3x10⁴/s
Forward Propagation
Factor 1x10⁻², 10 AngBins
Electrons: ITS
e: 3.3x10⁹
p: 8x10⁶
e: 3.6x10³
e: 4.9x10⁴
30.8
84.3
4107.2
Count Rate (/s-keV)
Pulse Height (keV)
SAIC/Bellevue - Wed Feb 16 16:06:04 1994

Detector 1 Response

Outer zone, L=4-6. Quiet

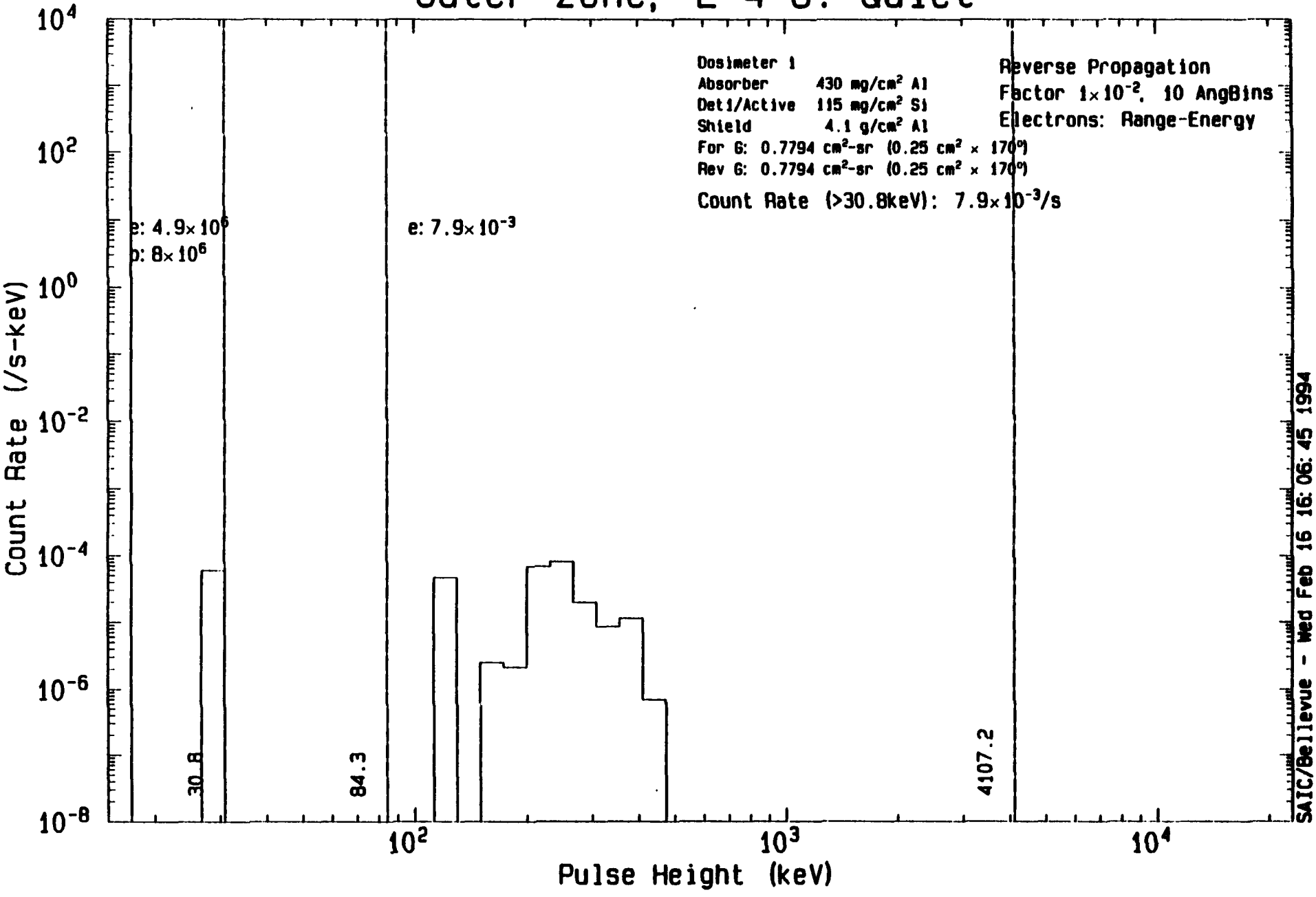

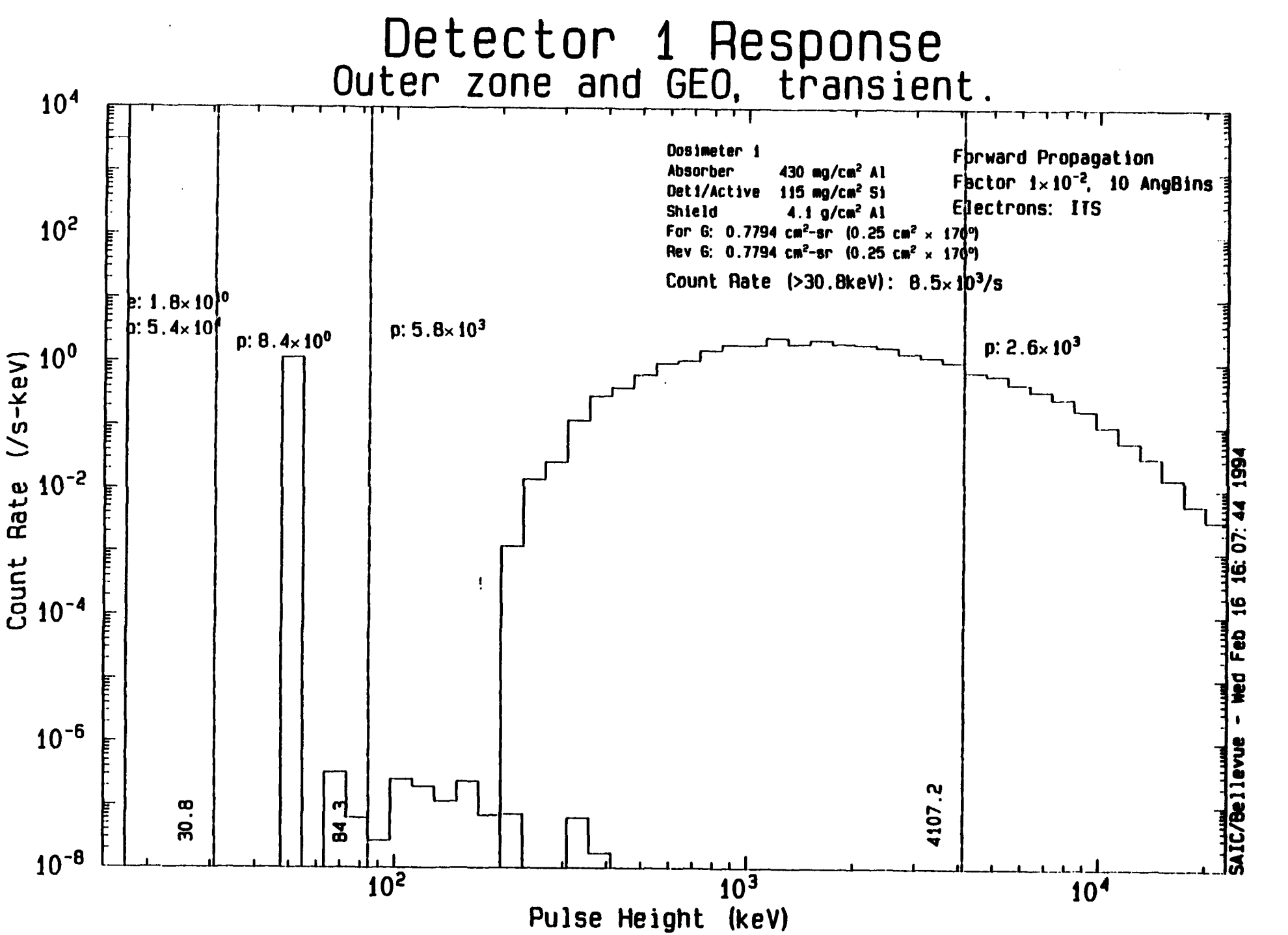
Detector 1 Response
Outer zone and GEO, transient.
Dosimeter 1
Absorber 430 mg/cm² Al
Det1/Active 115 mg/cm² Si
Shield 4.1 g/cm² Al
For G: 0.7794 cm²-sr (0.25 cm² × 170°)
Rev G: 0.7794 cm²-sr (0.25 cm² × 170°)
Count Rate (>30.8keV): 8.5×10³/s
Forward Propagation
Factor 1×10⁻², 10 AngBins
Electrons: ITS
e: 1.8×10⁰
p: 5.4×10⁰
p: 8.4×10⁰
p: 5.8×10³
p: 2.6×10³
30.8
84.3
4107.2
Count Rate (/s-keV)
Pulse Height (keV)
SAIC/Bellevue - Wed Feb 16 16:07:44 1994

Detector 1 Response

Outer zone and GEO, transient.

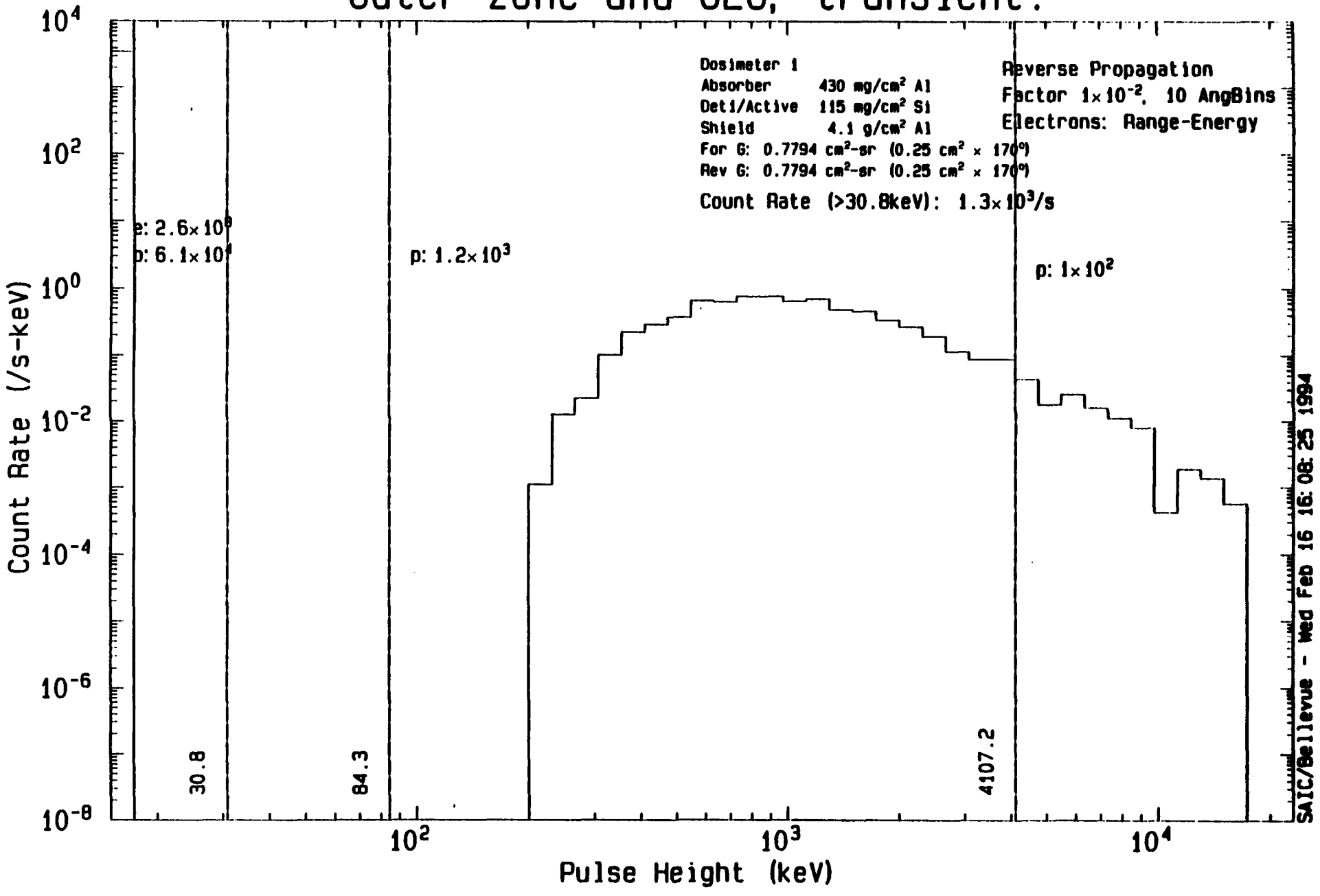

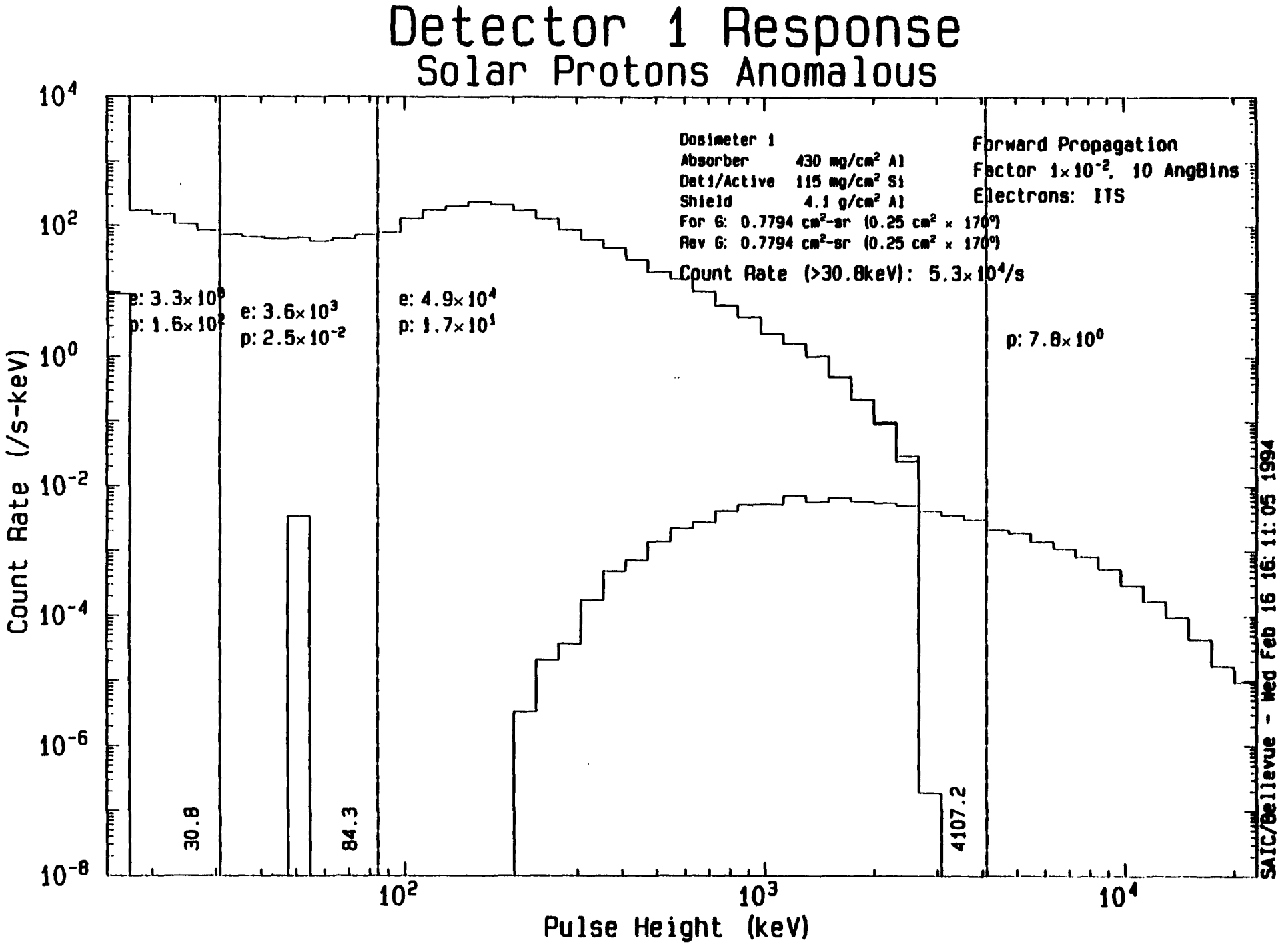
Detector 1 Response
Solar Protons Anomalous
Dosimeter 1
Absorber 430 mg/cm² Al
Det1/Active 115 mg/cm² Si
Shield 4.1 g/cm² Al
For G: 0.7794 cm²-sr (0.25 cm² x 170°)
Rev G: 0.7794 cm²-sr (0.25 cm² x 170°)
Count Rate (>30.8keV): 5.3x10⁴/s
Forward Propagation
Factor 1x10⁻², 10 AngBins
Electrons: ITS
e: 3.3x10⁰
p: 1.6x10²
e: 3.6x10³
p: 2.5x10⁻²
e: 4.9x10⁴
p: 1.7x10¹
p: 7.8x10⁰
30.8
84.3
4107.2
Count Rate (/s-keV)
Pulse Height (keV)
SAIC/Bellevue - Wed Feb 16 16:11:05 1994

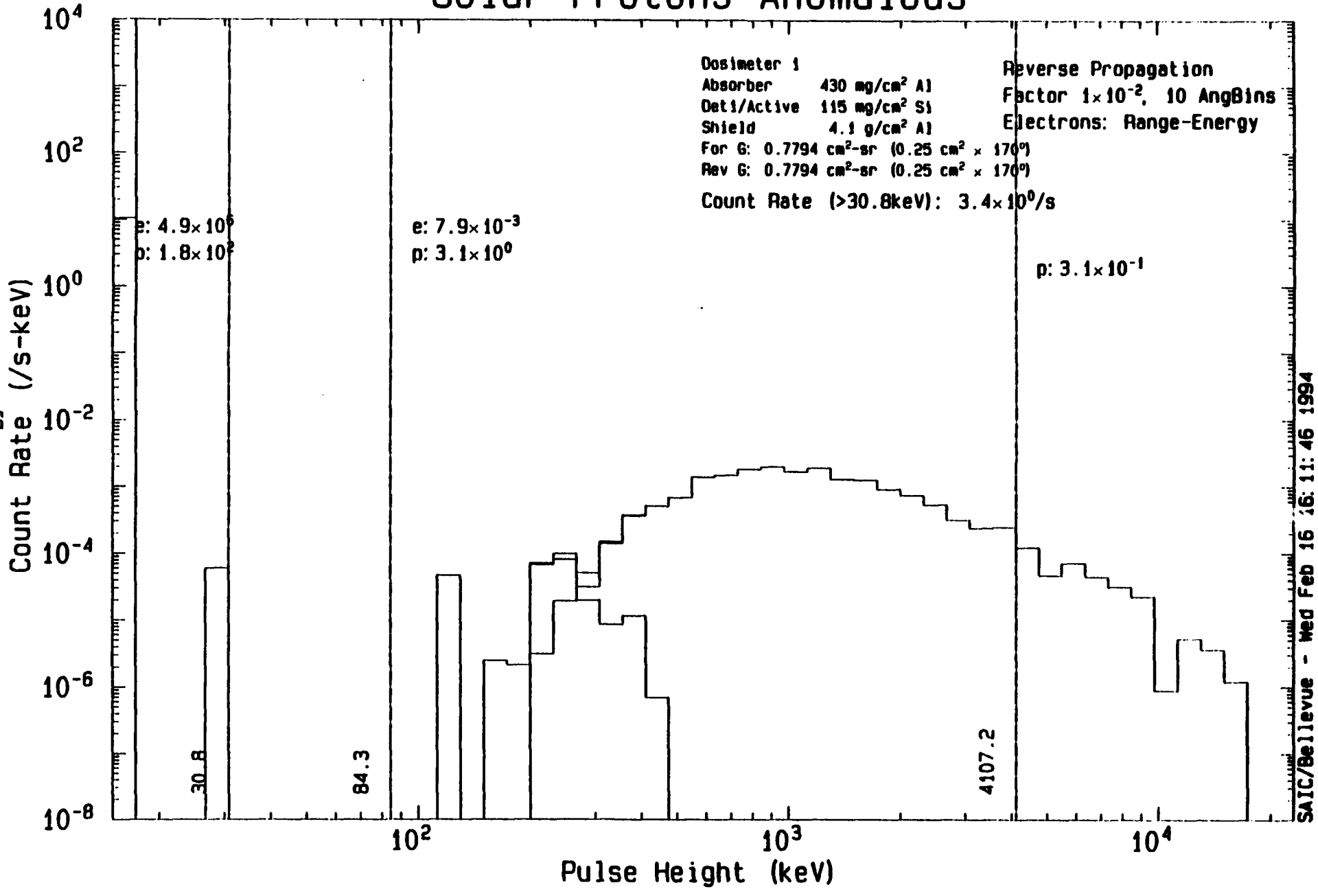
Detector 1 Response
Solar Protons Anomalous
Dosimeter 1
Absorber 430 mg/cm² Al
Det1/Active 115 mg/cm² Si
Shield 4.1 g/cm² Al
For G: 0.7794 cm²-sr (0.25 cm² x 170°)
Rev G: 0.7794 cm²-sr (0.25 cm² x 170°)
Count Rate (>30.8keV): 3.4x10⁰/s
Reverse Propagation
Factor 1x10⁻², 10 AngBins
Electrons: Range-Energy
e: 4.9x10⁶
p: 1.8x10²
e: 7.9x10⁻³
p: 3.1x10⁰
p: 3.1x10⁻¹
30.8
84.3
4107.2
Count Rate (/s-keV)
Pulse Height (keV)
SAIC/Bellevue - Wed Feb 16 16:11:46 1994

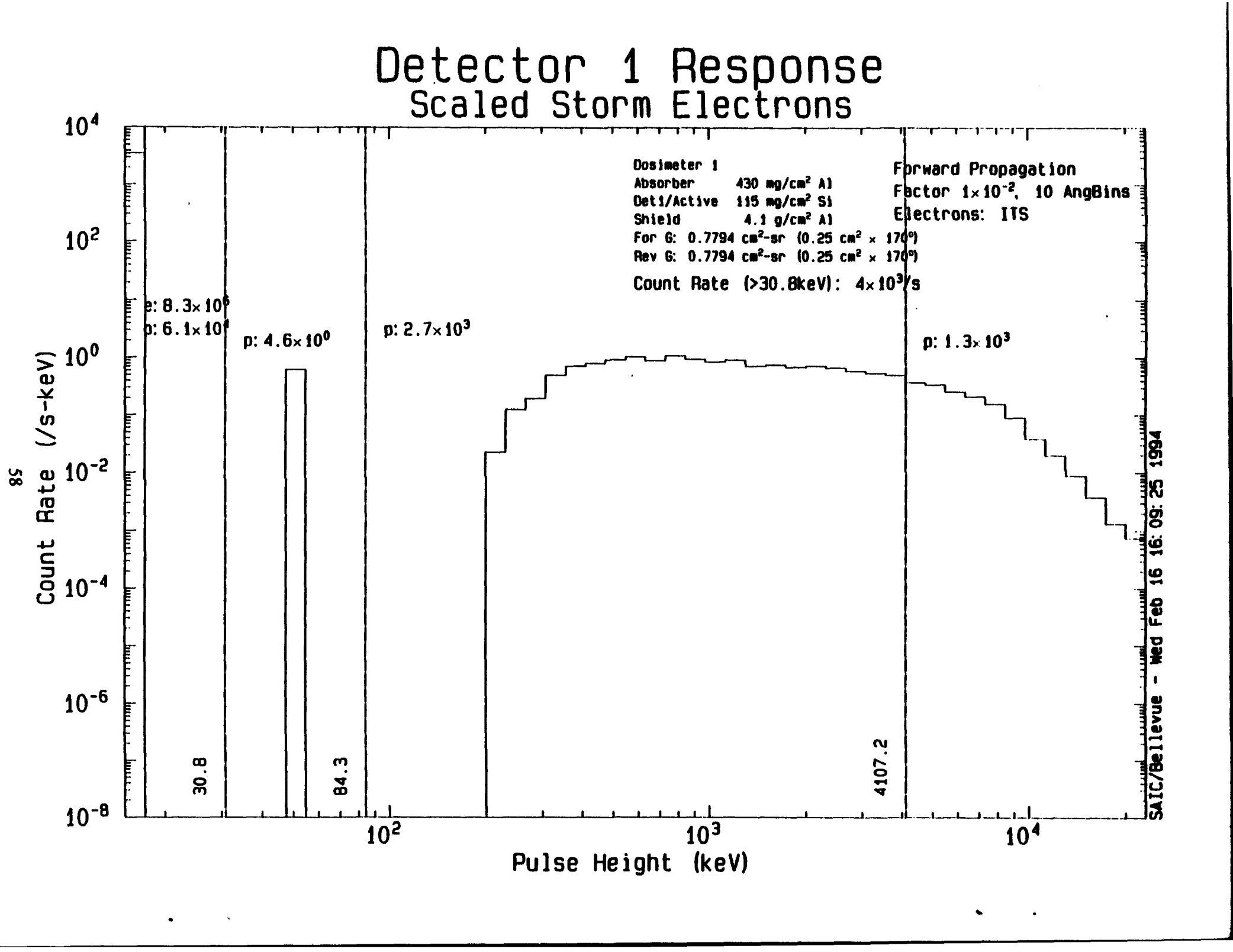
Detector 1 Response
Scaled Storm Electrons
Dosimeter 1
Absorber 430 mg/cm² Al
Det1/Active 115 mg/cm² Si
Shield 4.1 g/cm² Al
For G: 0.7794 cm²-sr (0.25 cm² × 170°)
Rev G: 0.7794 cm²-sr (0.25 cm² × 170°)
Count Rate (>30.8keV): 4×10³/s
Forward Propagation
Factor 1×10⁻², 10 AngBins
Electrons: ITS
e: 8.3×10⁶
p: 6.1×10⁴
p: 4.6×10⁰
p: 2.7×10³
p: 1.3×10³
30.8
84.3
4107.2
Count Rate (/s-keV)
Pulse Height (keV)
SAIC/Bellevue - Wed Feb 16 16:09:25 1994

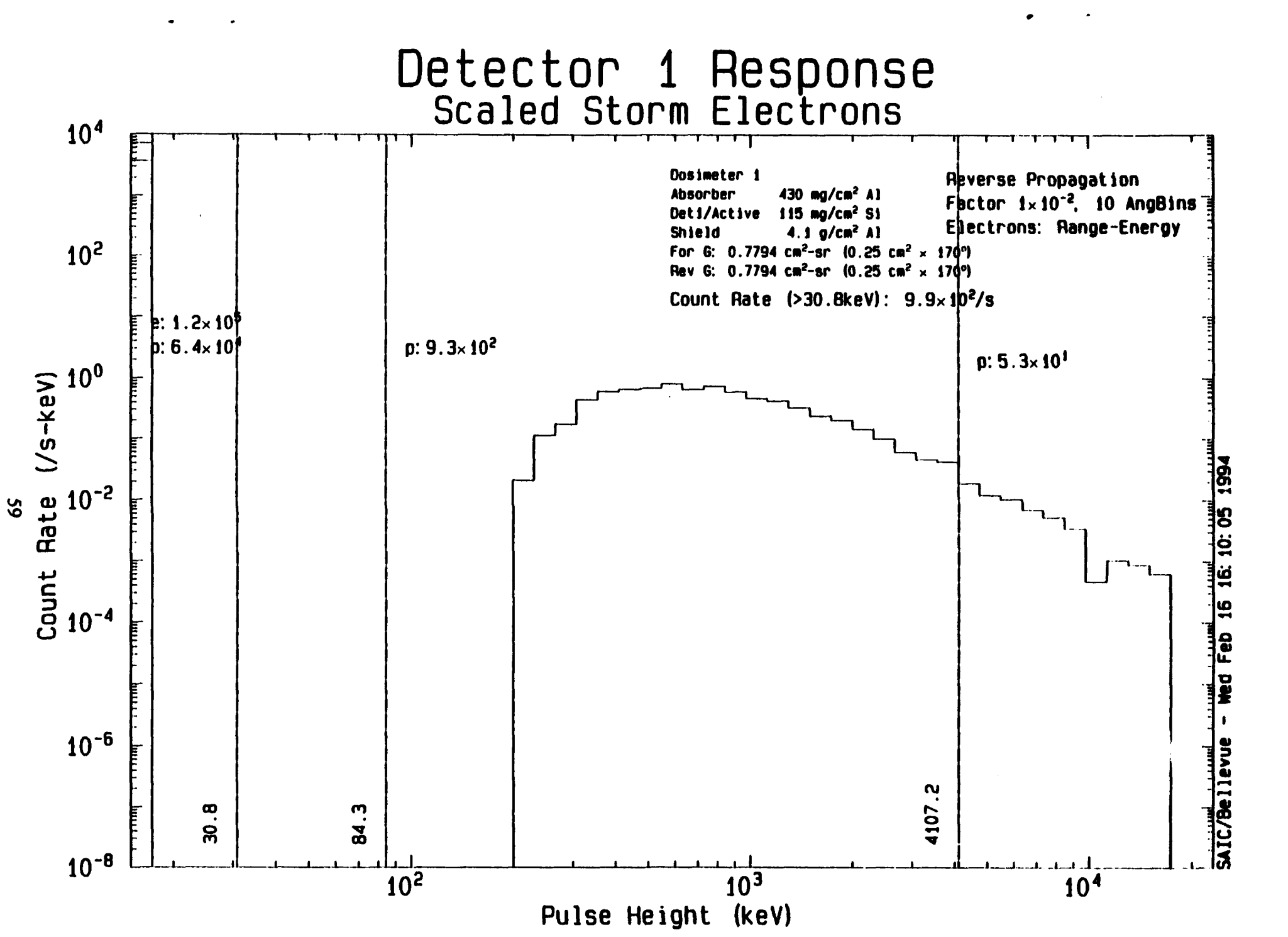
Detector 1 Response
Scaled Storm Electrons
Dosimeter 1
Absorber 430 mg/cm² Al
Det1/Active 115 mg/cm² Si
Shield 4.1 g/cm² Al
For G: 0.7794 cm²-sr (0.25 cm² x 170°)
Rev G: 0.7794 cm²-sr (0.25 cm² x 170°)
Count Rate (>30.8keV): 9.9x10²/s
Reverse Propagation
Factor 1x10⁻², 10 AngBins
Electrons: Range-Energy
e: 1.2x10⁵
p: 6.4x10⁴
p: 9.3x10²
p: 5.3x10¹
30.8
84.3
4107.2
Count Rate (/s-keV)
Pulse Height (keV)
SAIC/Bellevue - Wed Feb 16 16:10:05 1994

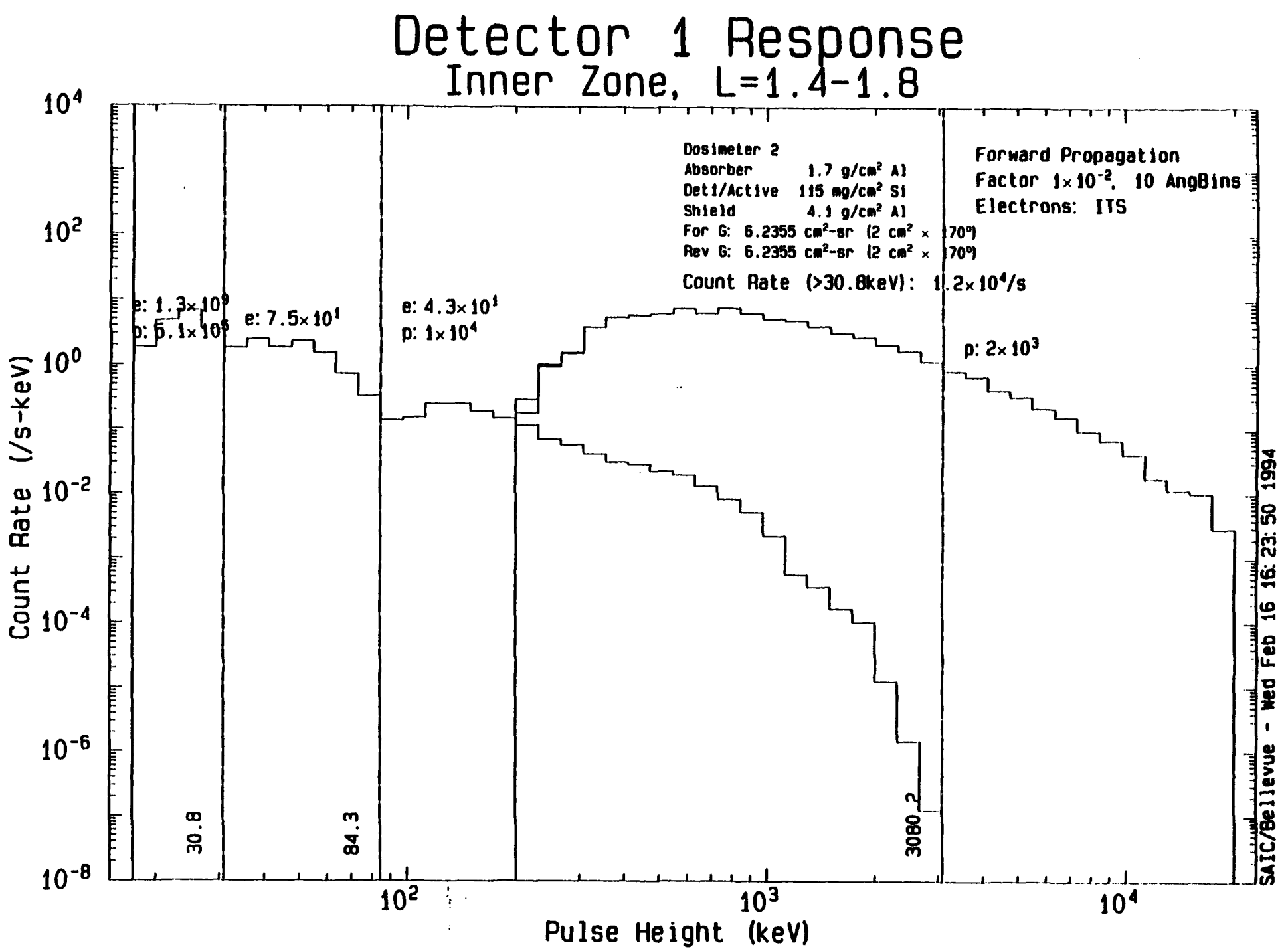
Detector 1 Response
Inner Zone, L=1.4-1.8
Dosimeter 2
Absorber 1.7 g/cm² Al
Det1/Active 115 mg/cm² Si
Shield 4.1 g/cm² Al
For G: 6.2355 cm²-sr (2 cm² × 170°)
Rev G: 6.2355 cm²-sr (2 cm² × 170°)
Count Rate (>30.8keV): 1.2×10⁴/s
Forward Propagation
Factor 1×10⁻², 10 AngBins
Electrons: ITS
e: 1.3×10⁹
p: 5.1×10⁶
e: 7.5×10¹
e: 4.3×10¹
p: 1×10⁴
p: 2×10³
30.8
84.3
3080.2
Count Rate (/s-keV)
Pulse Height (keV)
SAIC/Bellevue - Wed Feb 16 16:23:50 1994

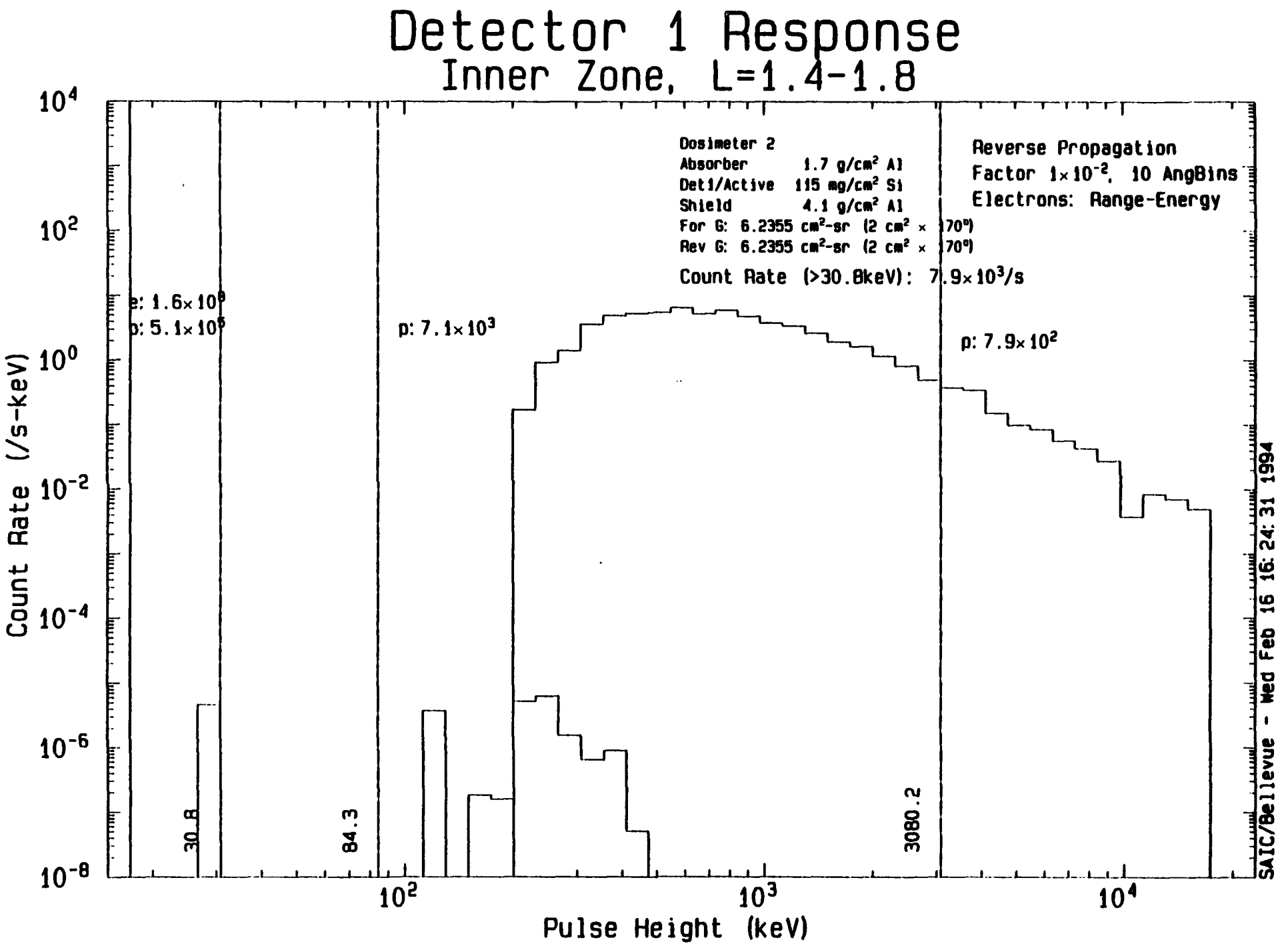
Detector 1 Response
Inner Zone, L=1.4-1.8
Dosimeter 2
Absorber 1.7 g/cm² Al
Det1/Active 115 mg/cm² Si
Shield 4.1 g/cm² Al
For G: 6.2355 cm²-sr (2 cm² × 70°)
Rev G: 6.2355 cm²-sr (2 cm² × 70°)
Count Rate (>30.8keV): 7.9×10³/s
Reverse Propagation
Factor 1×10⁻², 10 AngBins
Electrons: Range-Energy
e: 1.6×10⁶
p: 5.1×10⁵
p: 7.1×10³
p: 7.9×10²
30.8
84.3
3080.2
Count Rate (/s-keV)
Pulse Height (keV)
SAIC/Bellevue - Wed Feb 16 16:24:31 1994

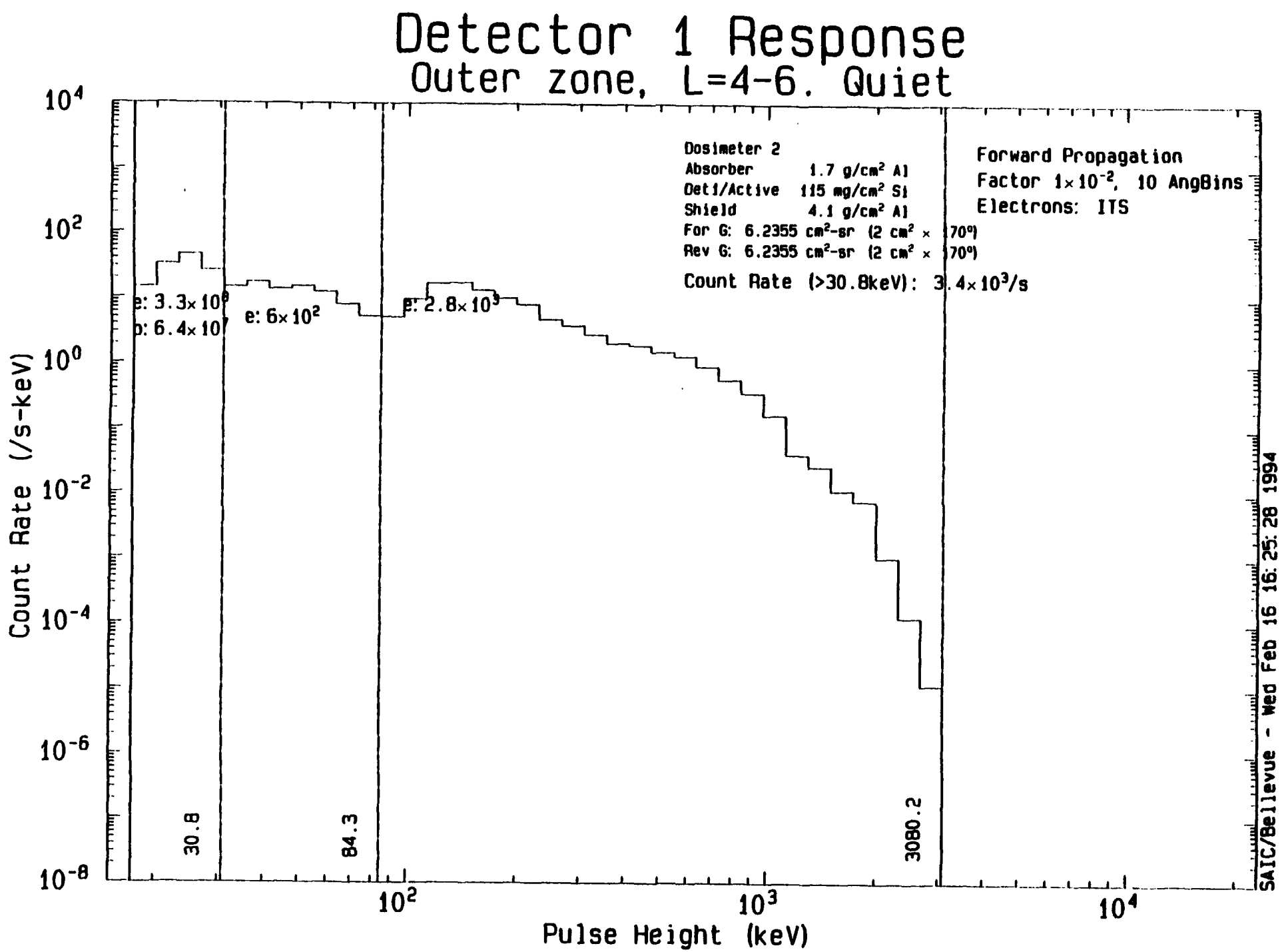
Detector 1 Response
Outer zone, L=4-6. Quiet
Dosimeter 2
Absorber 1.7 g/cm² Al
Det1/Active 115 mg/cm² Si
Shield 4.1 g/cm² Al
For G: 6.2355 cm²-sr (2 cm² × 70°)
Rev G: 6.2355 cm²-sr (2 cm² × 70°)
Count Rate (>30.8keV): 3.4×10³/s
Forward Propagation
Factor 1×10⁻², 10 AngBins
Electrons: ITS
e: 3.3×10
p: 6.4×10
e: 6×10²
e: 2.8×10³
30.8
84.3
3080.2
Count Rate (/s-keV)
Pulse Height (keV)
SAIC/Bellevue - Wed Feb 16 16:25:28 1994

Detector 1 Response

Outer zone, L=4-6. Quiet

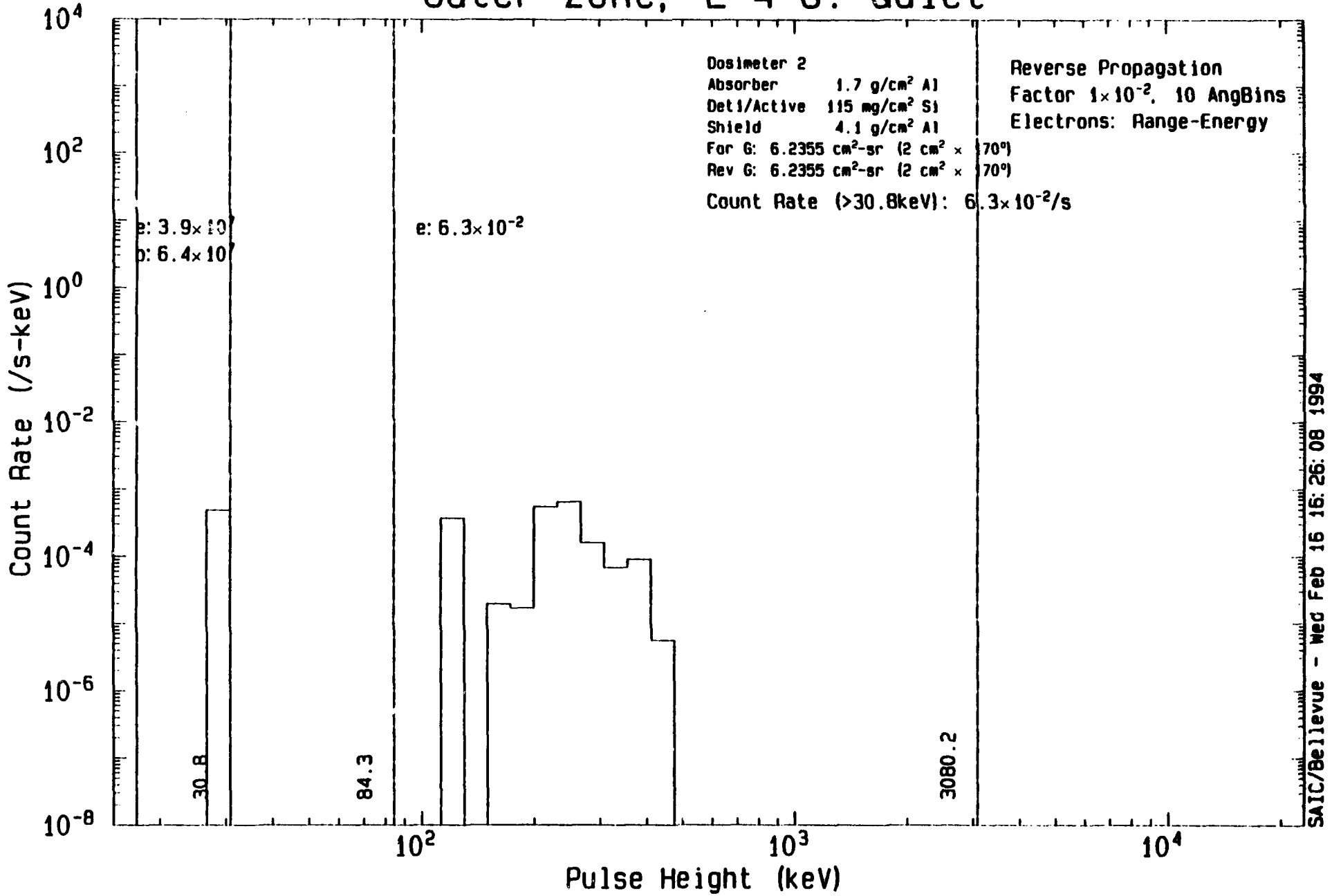

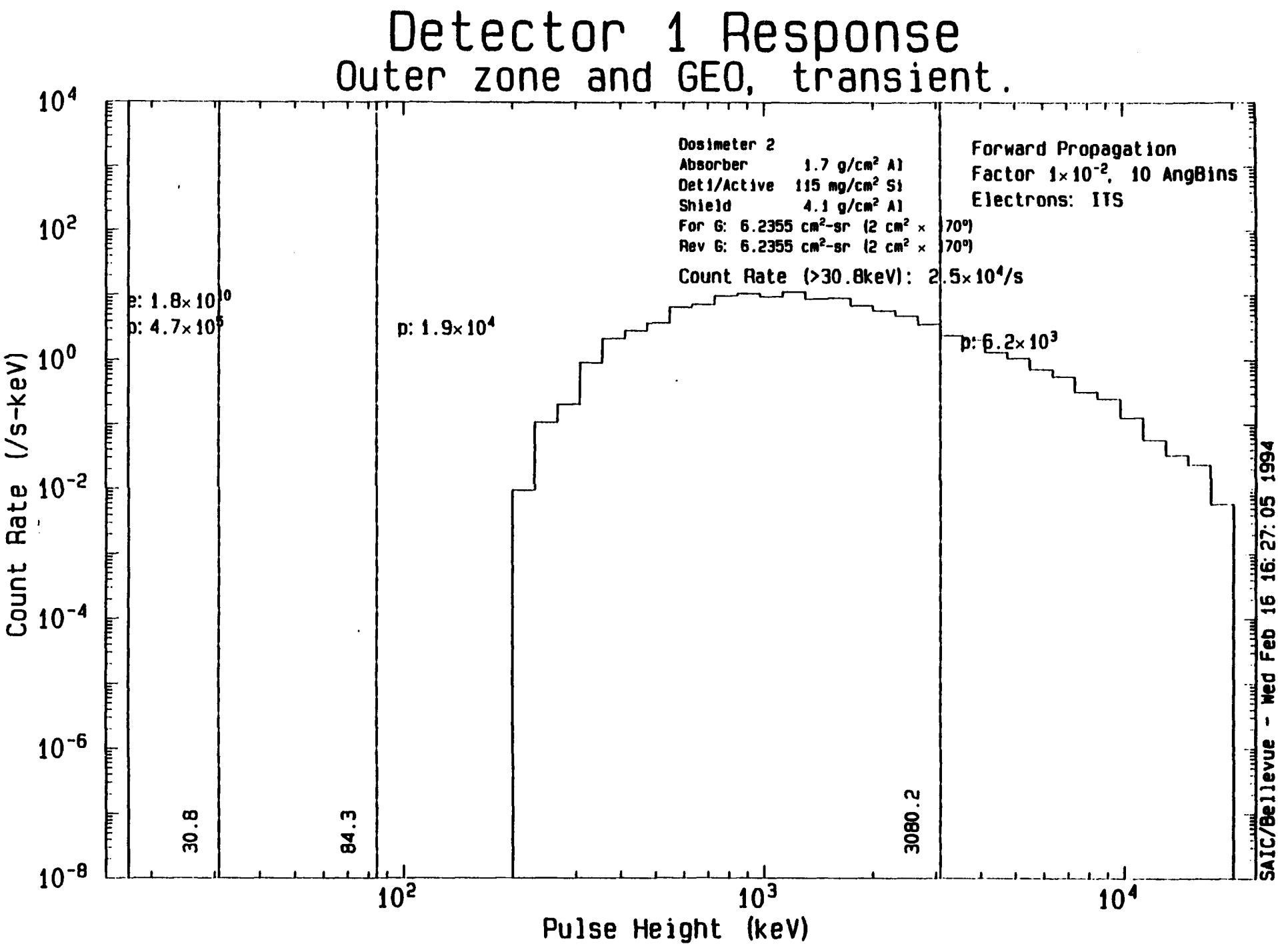
Detector 1 Response
Outer zone and GEO, transient.
Dosimeter 2
Absorber 1.7 g/cm² Al
Det1/Active 115 mg/cm² Si
Shield 4.1 g/cm² Al
For G: 6.2355 cm²-sr (2 cm² × 170°)
Rev G: 6.2355 cm²-sr (2 cm² × 170°)
Count Rate (>30.8keV): 2.5×10⁴/s
Forward Propagation
Factor 1×10⁻², 10 AngBins
Electrons: ITS
e: 1.8×10¹⁰
p: 4.7×10⁵
p: 1.9×10⁴
p: 6.2×10³
30.8
84.3
3080.2
Count Rate (/s-keV)
Pulse Height (keV)
SAIC/Bellevue - Wed Feb 16 16:27:05 1994

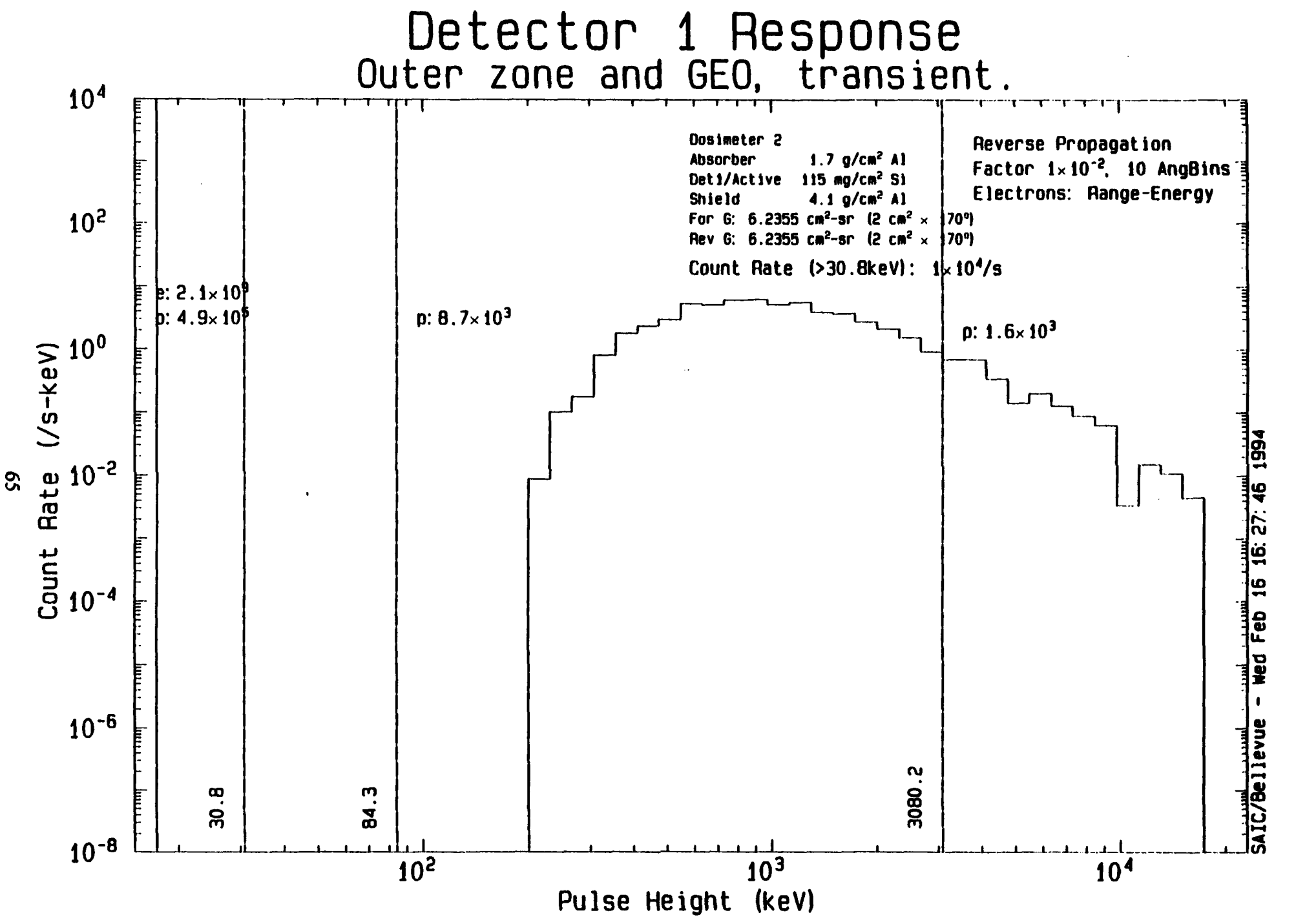
Detector 1 Response
Outer zone and GEO, transient.
Dosimeter 2
Absorber 1.7 g/cm² Al
Det1/Active 115 mg/cm² Si
Shield 4.1 g/cm² Al
For G: 6.2355 cm²-sr (2 cm² × 70°)
Rev G: 6.2355 cm²-sr (2 cm² × 70°)
Count Rate (>30.8keV): 1×10⁴/s
Reverse Propagation
Factor 1×10⁻², 10 AngBins
Electrons: Range-Energy
e: 2.1×10⁹
p: 4.9×10⁶
p: 8.7×10³
p: 1.6×10³
30.8
84.3
3080.2
Count Rate (/s-keV)
Pulse Height (keV)
SAIC/Bellevue - Wed Feb 16 16:27:46 1994

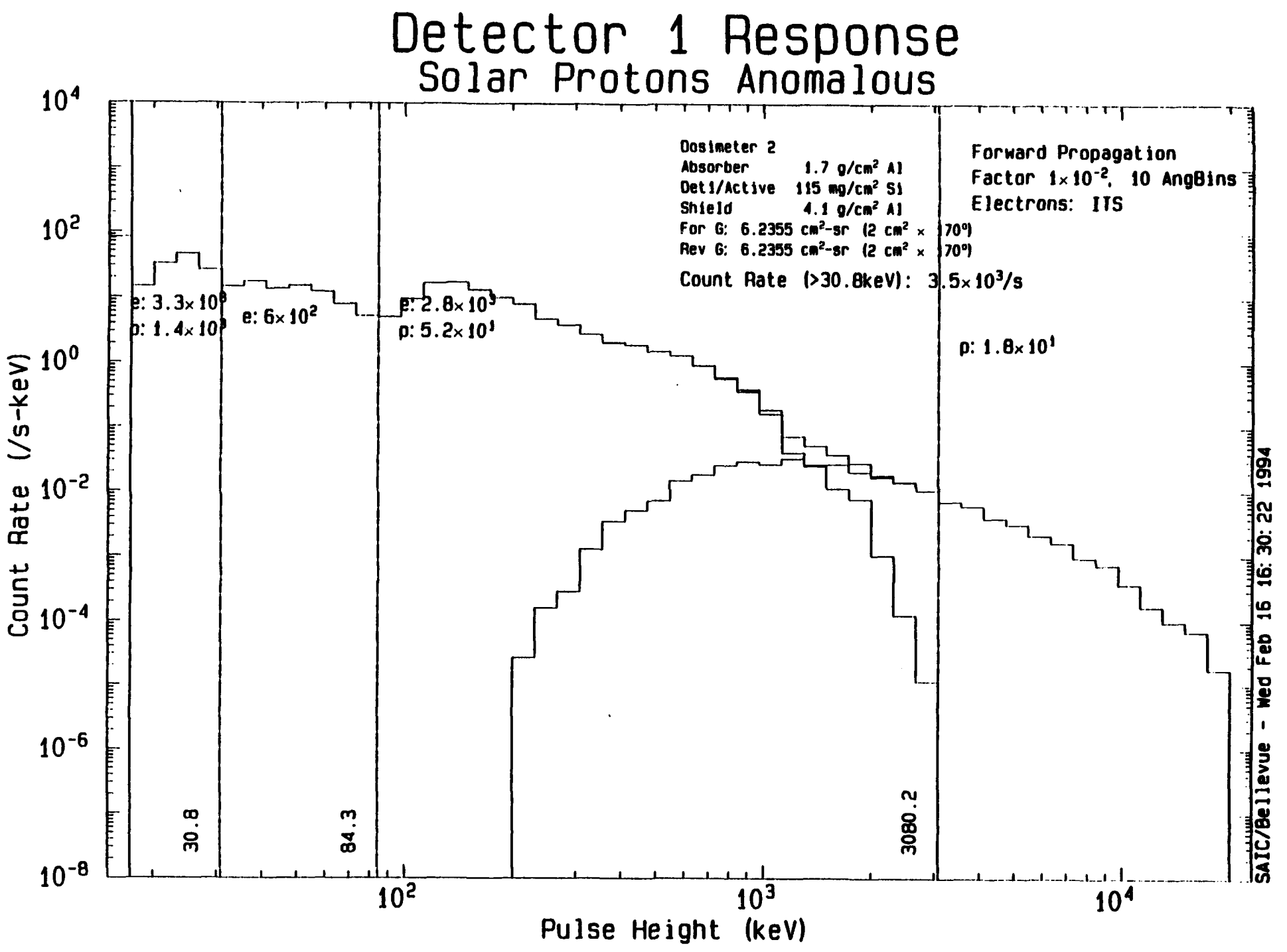
Detector 1 Response
Solar Protons Anomalous
Dosimeter 2
Absorber 1.7 g/cm² Al
Det1/Active 115 mg/cm² Si
Shield 4.1 g/cm² Al
For G: 6.2355 cm²-sr (2 cm² × 170°)
Rev G: 6.2355 cm²-sr (2 cm² × 170°)
Count Rate (>30.8keV): 3.5×10³/s
Forward Propagation
Factor 1×10⁻², 10 AngBins
Electrons: ITS
e: 3.3×10³
p: 1.4×10³
e: 6×10²
p: 2.8×10³
p: 5.2×10¹
p: 1.8×10¹
30.8
84.3
3080.2
Count Rate (/s-keV)
Pulse Height (keV)
SAIC/Bellevue - Wed Feb 16 16:30:22 1994

99

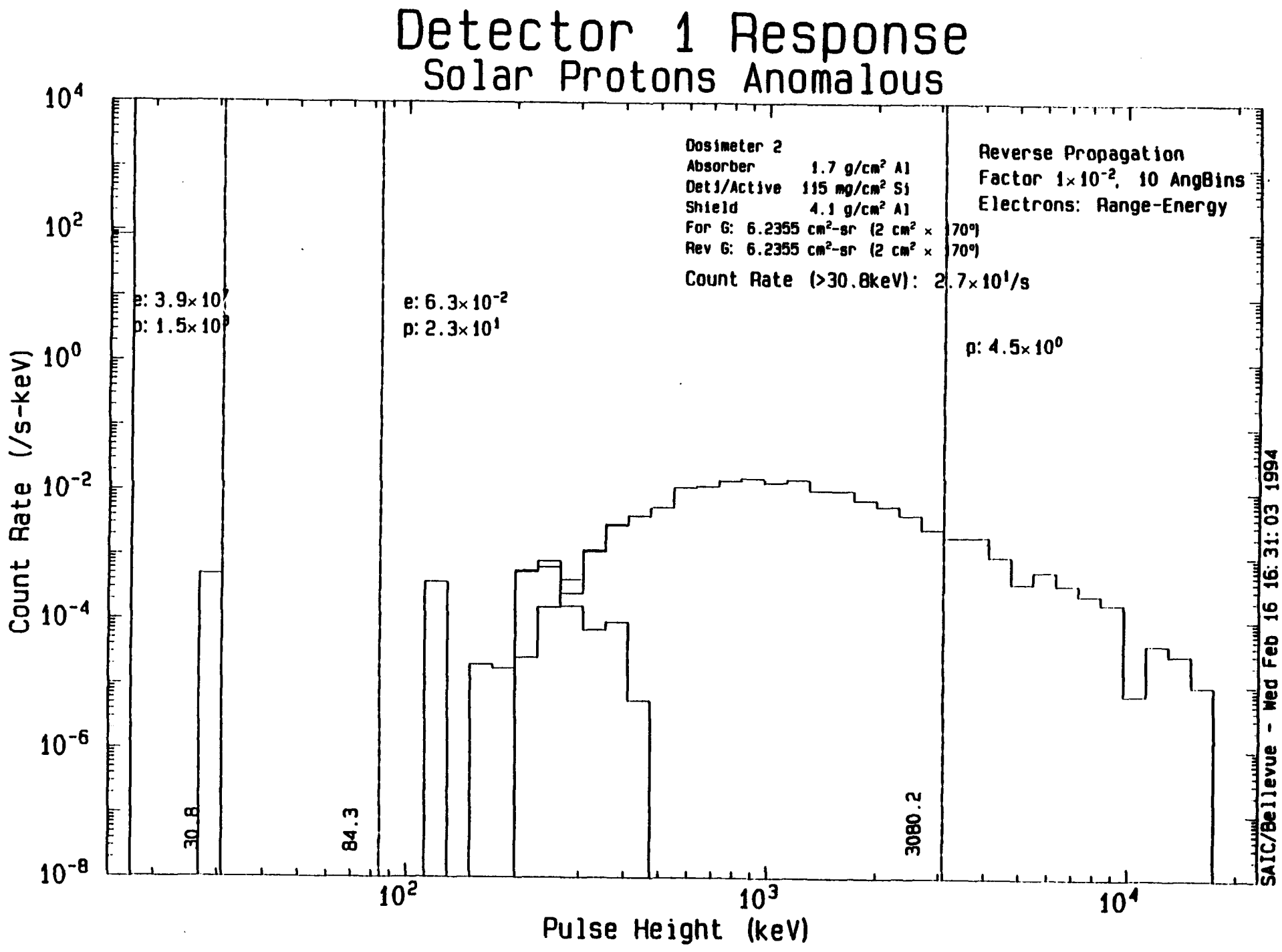
Detector 1 Response
Solar Protons Anomalous
Dosimeter 2
Absorber 1.7 g/cm² Al
Det1/Active 115 mg/cm² Si
Shield 4.1 g/cm² Al
For G: 6.2355 cm²-sr (2 cm² × 70°)
Rev G: 6.2355 cm²-sr (2 cm² × 70°)
Count Rate (>30.8keV): 2.7×10¹/s
Reverse Propagation
Factor 1×10⁻², 10 AngBins
Electrons: Range-Energy
e: 3.9×10
p: 1.5×10
e: 6.3×10⁻²
p: 2.3×10¹
p: 4.5×10⁰
30.8
84.3
3080.2
Count Rate (/s-keV)
Pulse Height (keV)
SAIC/Bellevue - Wed Feb 16 16:31:03 1994

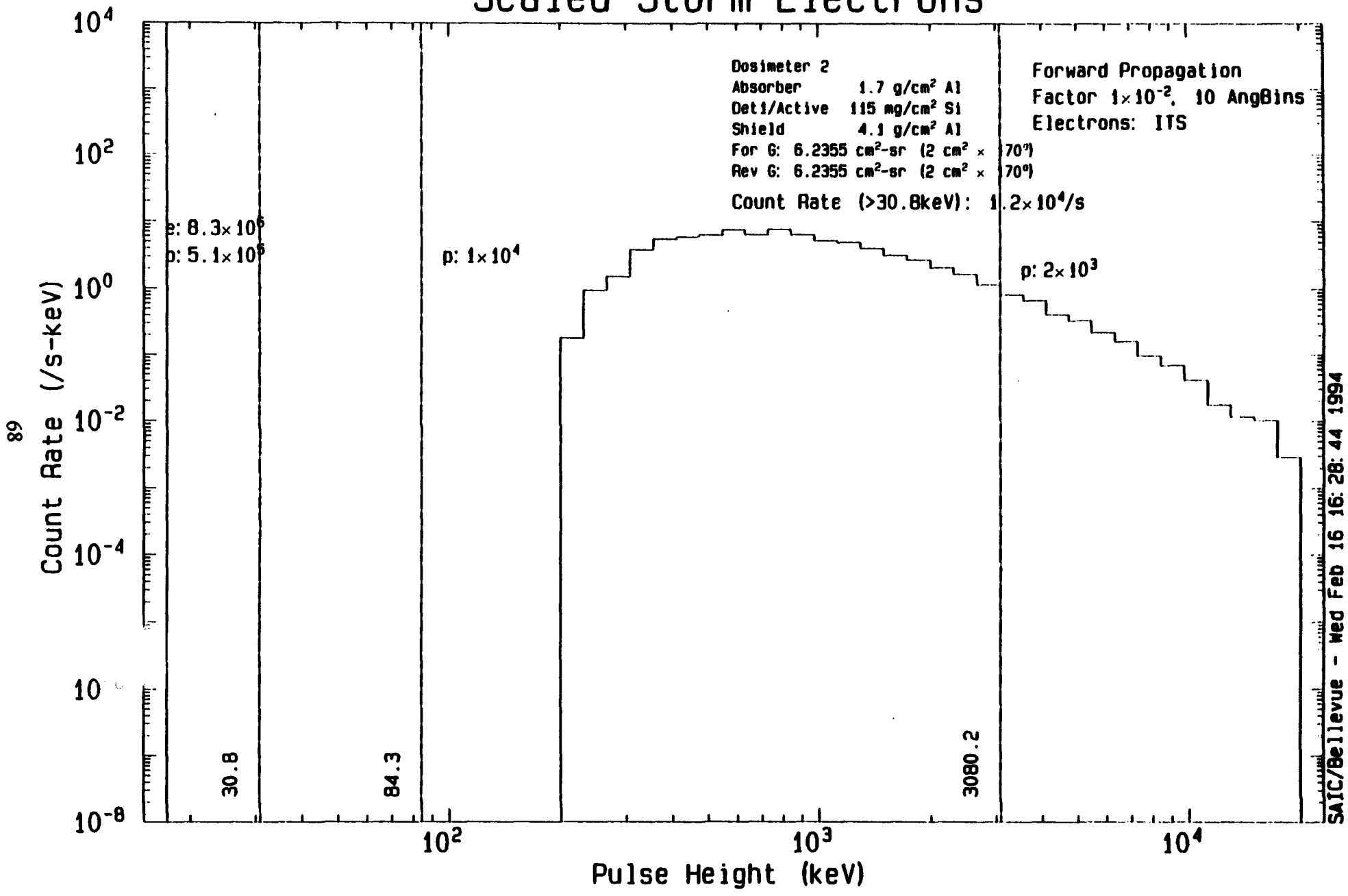
Detector 1 Response
Scaled Storm Electrons
Dosimeter 2
Absorber 1.7 g/cm² Al
Det1/Active 115 mg/cm² Si
Shield 4.1 g/cm² Al
For G: 6.2355 cm²-sr (2 cm² × 70°)
Rev G: 6.2355 cm²-sr (2 cm² × 70°)
Count Rate (>30.8keV): 1.2×10⁴/s
Forward Propagation
Factor 1×10⁻², 10 AngBins
Electrons: ITS
e: 8.3×10⁶
p: 5.1×10⁶
p: 1×10⁴
p: 2×10³
30.8
84.3
3080.2
Count Rate (/s-keV)
Pulse Height (keV)
SAIC/Bellevue - Wed Feb 16 16:28:44 1994

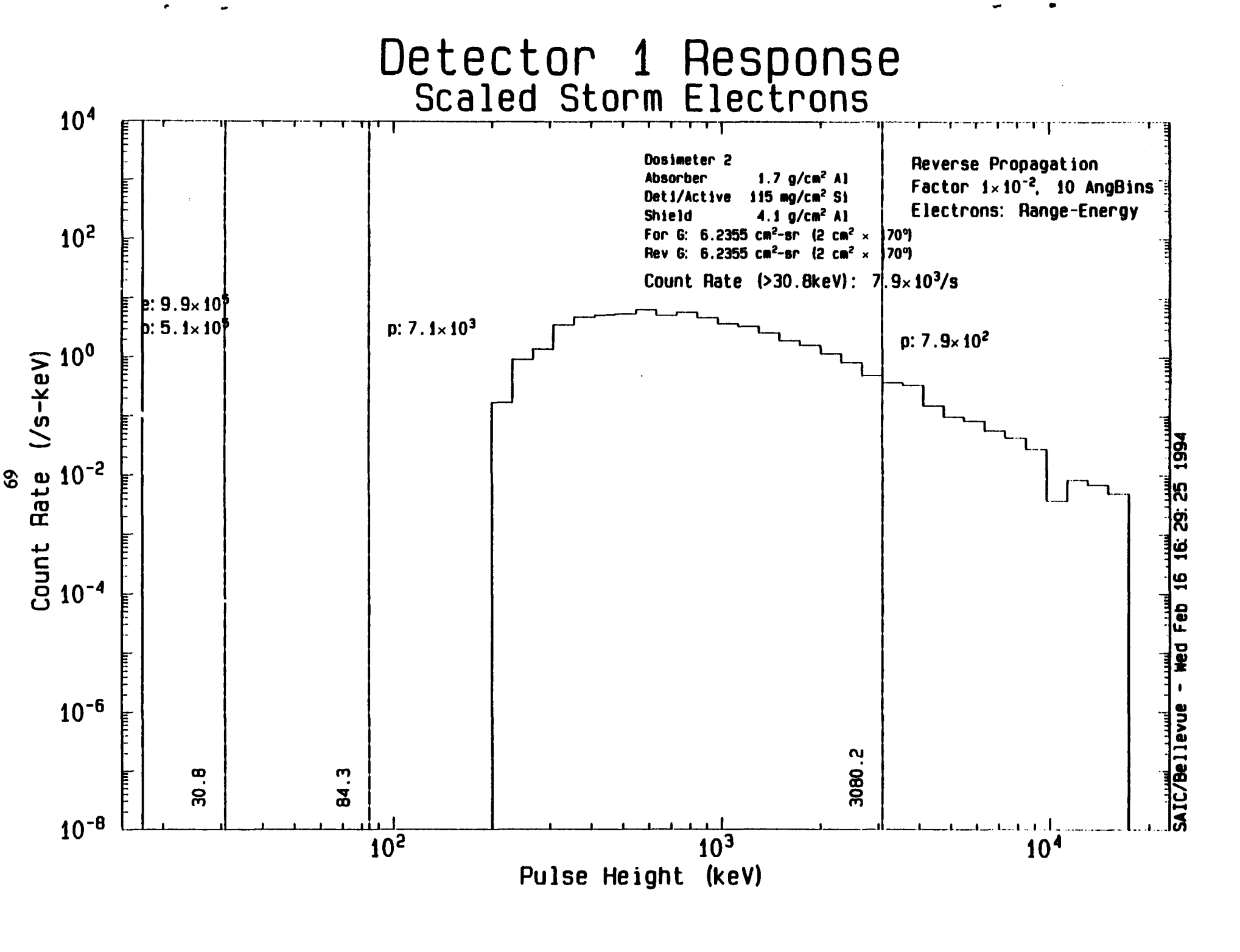
Detector 1 Response
Scaled Storm Electrons
Dosimeter 2
Absorber 1.7 g/cm² Al
Det1/Active 115 mg/cm² Si
Shield 4.1 g/cm² Al
For G: 6.2355 cm²-sr (2 cm² × 170°)
Rev G: 6.2355 cm²-sr (2 cm² × 170°)
Count Rate (>30.8keV): 7.9×10³/s
Reverse Propagation
Factor 1×10⁻², 10 AngBins
Electrons: Range-Energy
e: 9.9×10⁵
p: 5.1×10⁵
p: 7.1×10³
p: 7.9×10²
30.8
84.3
3080.2
Count Rate (/s-keV)
Pulse Height (keV)
SAIC/Bellevue - Wed Feb 16 16:29:25 1994